Parks Victoria Technical Series

Number 117

An integrated monitoring program for Port Phillip Heads Marine National Park

April 2022

Parks Victoria

Healthy Parks Healthy People

Victoria State Government

Level 10, 535 Bourke St, Melbourne Vic 3000

Authors

Daniel Ierodiaconou, Mary Young, Sam Wines, Paul Carnell, Paul Tinkler, Blake Allan, Sasha Whitmarsh – Deakin University

Steffan Howe – Parks Victoria (former)

Jacqui Pocklington – Deakin University and Parks Victoria (former)

National Library of Australia

Cataloguing-in-publication data

Includes bibliography

ISSN 1448-4935

Citation

Ierodiaconou D. Young M, Wines S, Carnell P, Tinkler P, Allan B, Whitmarsh S, Howe S, Pocklington J 2022. *An integrated monitoring program for Port Phillip Heads Marine National Park*. Parks Victoria Technical Series 117.

Front cover: Senator Wrasse (*Pictilabrus laticlavius*). Photo: Parks Victoria

Executive summary

Parks Victoria has established extensive marine research and monitoring programs for its marine protected areas (MPAs) with the aim of addressing significant management challenges. Such challenges focus on both improving baseline knowledge of Victoria's MPAs and addressing applied management questions. The Signs of Healthy Parks (SHP) monitoring program aims to ensure systematic, robust and integrated ecological monitoring across the MPA network. Building on Parks Victoria's Conservation Action Planning process, the SHP program aims to monitor the health of protected areas using a range of environmental indicators that in turn provide information about the natural values and ecological processes within the parks, as well as potential threats and other drivers. The SHP does this by fostering partnerships and collaborative projects to design, implement and evaluate monitoring programs. The collection of data is based on focused monitoring questions that address specific management needs. Parks Victoria has implemented subtidal and intertidal reef monitoring programs in a large number of MPAs from as far back as 1998; however, they only cover a small proportion of the key habitats in the parks. The monitoring program for Victoria's MPAs is now being expanded to address key management questions linked to draft conservation plans for the marine national parks and sanctuaries.

Deakin University, as part of the Research Partners program, were approached by Parks Victoria to trial an updated SHP program, currently being implemented in Point Addis Marine National Park (MNP), that is now being expanded to include Port Phillip Heads (PPH) MNP. The results from this study provide considerable new knowledge of the distribution and functioning of intertidal, subtidal and mesophotic habitats ((low-light habitats in the transition zone between well-lit shallower waters and dark deep water) within Port Phillip Heads MNP and further consolidates Parks Victoria's framework for expanded monitoring across its entire MPA estate. It provides new insights into the fish diversity of the park and in particular the high value of deeper reefs where 71 species were observed using baited remote underwater video systems. Continuing the underwater water visual census at key subtidal monitoring sites has enabled the continuation of time series data collection by adopting the Reef Life Survey approach. Benefits of protection were observed for some species, including for Greenlip Abalone inside the marine national park and at reference sites. Unfortunately, Blacklip Abalone has seen a steady decrease through time and its biomass has been below the lower control limit since 2015. This study also provides the first insights into Southern Rock Lobster abundance: fisheries-independent surveys within and adjacent to Port Phillip Heads MNP captured only a limited number of individuals and showed no trends with respect to protection.

Contents

Index of figures

Index of tables

1 Introduction

Parks Victoria manages a system of 13 marine national parks and 11 marine sanctuaries, making up approximately 5.3% of Victoria's state waters. Established in 2002, the network of marine national parks and sanctuaries was designed to represent the diversity of Victoria's marine environment, its habitats, and associated flora and fauna (Victorian Environmental Assessment Council, 2014). In order to reliably manage these areas, an understanding of the natural values that occur within the parks, sanctuaries and reserves is essential (Devillers et al., 2015). Parks Victoria has established extensive marine research and monitoring programs that address significant management challenges for its marine protected areas (MPAs). Such challenges include improving baseline knowledge of the MPAs and addressing new applied management questions. Parks Victoria's research program is guided by the research themes outlined in Parks Victoria's Environmental Research Strategy 2012–2025, and their monitoring program is guided by a draft statewide marine monitoring framework based on priorities identified through the conservation planning process for the marine national parks and sanctuaries.

1.1 Previous long-term monitoring programs

Parks Victoria's long-term Subtidal Reef Monitoring Program (SRMP) was designed using best scientific practices in the early 1990s and initiated in (what is now) the system of marine national parks and sanctuaries in 1998. These surveys were conducted from 1998 to 2015 in 13 marine national parks and sanctuaries across the state (Power and Boxshall, 2007). This program used diver underwater visual census methods, which record descriptions of macroalgae, fish and macroinvertebrate communities at each monitoring site as well as indications of change through time. In addition, the Intertidal Reef Monitoring Program (IRMP) began in late 2002 with sampling at some sites beginning in the summer of 2002–03 (Power and Boxshall, 2007); it finished in 2013. This program involved monitoring the invertebrates and macroalgae present in the intertidal zone on reefs within 9 targeted MPAs and at 9 matched reference sites outside the MPAs (see Hart and Edmunds (2005) for full methodological details). The results of these surveys are published in Parks Victoria Technical Series reports.

1.2 New marine protected area monitoring framework

Following the earlier long-term monitoring programs, Parks Victoria adopted an adaptive management framework and conservation planning process that more clearly defines the goals and objectives for managing key natural assets and threats. A draft statewide monitoring plan has been developed based on conservation, management and monitoring priorities identified for each park through the conservation planning process. The monitoring plan outlines potential indicators for subtidal and intertidal reef communities and other key habitats and ecosystems, and it identifies key threats to these priority natural assets. The process for identifying monitoring priorities at the statewide level was endorsed

by Parks Victoria and involved 3 consecutive assessments, namely, identifying high-priority parks (e.g. those identified as representative or that meet the Category II criteria in the IUCN protected area categories system), their high-priority key ecological attributes and the high-priority threats to those attributes.

The new monitoring program will focus on key ecological attributes and threats in at least one of the large marine national parks within each bioregion, currently identified as Discovery Bay Marine National Park (MNP) (Otway bioregion), Point Addis MNP (Central Victoria bioregion), Port Phillip Heads MNP (Victorian Embayments bioregion), Wilsons Promontory MNP (Flinders bioregion) and Cape Howe MNP (Twofold Shelf bioregion). It will also address monitoring priorities identified for other parks using a range of delivery models as resources permit.

1.3 Port Phillip Heads Marine National Park

This study assessed the area within and adjacent to the no-take Port Phillip Heads MNP by integrating historical data collections dating from the late 1990s with new collections in 2018 and 2019 that were funded as part of this project. This MPA differs from other Victorian MPAs in being split into 6 sections (Swan Bay, Popes Eye, Mud Islands, Point Nepean, Point Lonsdale and Portsea Hole); they cover a total of 3,475 hectares (ha). This study focused on 3 of these sections: Point Lonsdale (377 ha), Point Nepean (377 ha) and Popes Eye (The Annulus; 3.1 ha). Most of the areas of this park (all except Portsea Hole) have been marine reserves since 1979. Port Phillip Heads MNP encompasses a large variety of habitat types due to its location: half of the park is located on open coast and experiences wave heights averaging about 1.7 m while the other areas are sheltered inside Port Phillip Bay. The park has a large depth range, spanning from the intertidal zone to approximately 100 m deep in the Port Phillip Bay entrance canyon. Large variation is also observed here in exposure to tidal currents. On each diurnal tide, the whole of Port Phillip Bay (approximately 1,930 km^2 surface area) drains through a narrow gap 3.2 kilometres (km) wide between Point Lonsdale and Point Nepean, resulting in strong tidal flows. Here, tidal flows run at up to 15 kilometres per hour (km/h), compared with areas of the park that are relatively sheltered, causing large differences in currents across the marine park estate.

The subtidal reefs within Port Phillips Heads MNP provide habitat for a diverse and colourful community of sessile invertebrates, mobile invertebrates and algae. Invertebrates observed on these reefs include a variety of sponges, hydroid species, gorgonians, soft corals, jewel anemones, yellow zoanthids, hard corals, encrusting and bushy bryozoans and ascidians. Mobile invertebrates, including abalone, urchins, nudibranchs, sea stars, feather stars and rock lobsters, can also be found inhabiting these reefs. The colourful assemblages are further enhanced by a diversity of macroalgae species, including assemblages of brown, red and green algae that can experience dramatic composition changes due to disturbance in the exposed regions, overgrazing of urchins or establishment of invasive species such as *Undaria*, the Japanese Kelp.

These reefs also attract a variety of fish with the Lonsdale Wall hosting a very diverse assemblage – over 40 species have been observed (Plummer et al., 2003). A similar community of fish is distributed across the other areas of hard substrate. The species commonly found include Herring Cale (*Olisthops cyanomelas*), Horseshoe Leatherjacket (*Meuschenia hippocrepis*), Six-Spine Leatherjacket (*Meuschenia freycineti*), Scalyfin (*Parma* spp.), Sweep (*Scorpis* spp.), wrasses (Labridae spp.) and the Weedy Seadragon (*Phyllopteryx taeniolatus).*

Sediment communities are also found throughout the individual parks. Variation in sediment grain size changes the composition of the communities, but meiofauna, including nematodes and copepods, can be found inhabiting the sediments of the park. Bivalves, gastropods, amphipods and polychaetes are more visible and can be found in the upper layer of sediments. In addition, more mobile species, including fish, crabs and sea stars, can often be observed foraging within these areas.

1.4 Long-term monitoring priorities of Port Phillip Heads Marine National Park

A number of monitoring priorities have been identified for Port Phillip Heads MNP. These priorities are outlined below.

Subtidal reefs (including shallow and deep reefs)

Greater Port Phillip Heads

- Large mobile fish (including sharks and rays), especially those that are 'site attached' rather than transitory
- Mobile macroinvertebrates, especially abalone and rock lobsters as these are keystone species and illegal fishing has been identified as a major threat to these invertebrates in the park
- Beds dominated by brown macroalgae (such as Golden Kelp (*Ecklonia radiata*) and Crayweed (*Phyllospora comosa*))
- Giant Kelp (*Macrocystis pyrifera*) ecological community (where present)

Popes Eye

- Large mobile fish (including sharks and rays)
- Mobile macroinvertebrates

Portsea Hole

- Sessile invertebrate communities

Intertidal reefs

Point Lonsdale

- Communities dominated by the brown alga Neptune's Necklace (*Hormosira banksii*) (in low-mid littoral zone)
- Characteristic invertebrate communities (Point Lonsdale has the highest diversity of any Victorian calcarenite reef)

1.5 Objectives

The overarching objective for this project is to design a targeted monitoring program for Port Phillip Heads MNP based on the key conservation, management and monitoring objectives established for the park. Other related objectives include to:

- implement a baited remote underwater video stations (BRUVS) survey of demersal fish assemblages within and adjacent to the MPA
    - initiate time-series monitoring of demersal fish assemblages across the entire depth range of the park (excluding the canyon region due to sampling constraints)
    - understand the effect of seafloor structure on abundance and diversity of fish using spatially explicit distribution modelling techniques
- implement unmanned aerial vehicle (UAV) surveys for intertidal reef platforms inside the park using the methods previously tested by Deakin University (Murfitt et al., 2017)
    - implement visual census surveys for habitat-forming species and mobile invertebrates at IRMP sites inside the park at Point Lonsdale
    - extend time-series SRMP monitoring of *H. banksii* canopy cover using virtual quadrats extracted from UAV survey data
    - use image classification approaches to create estimates of *H. banksii* coverage and fragmentation statistics across the intertidal platform
    - test metrics to evaluate *H. banksii* distribution and fragmentation

- develop and implement robust survey designs for brown macroalgal–dominated communities on deeper reefs (>10 m depth) and key ecological attributes (sessile invertebrate communities in Portsea Hole) on deeper reefs using towed video and downward-facing still images
- add data collected as part of this project and related programs (e.g. data collected by Reef Life Survey volunteers) to control charts developed for the Port Phillip Heads MNP report card where available and suitable for integration at the time of reporting
- conduct multibeam surveys and ground truth video to produce habitat maps for Portsea Hole and Popes Eye and identify Japanese Kelp (*Undaria pinnatifida*) habitat extents
- use standardised fishery stock assessment methods to assess the effect of this MPA on the local population of Southern Rock Lobster (*Jasus edwardsii*)
    - determine whether protection is associated with increased biomass or size of individuals
    - determine the effect of seafloor structure and distance from MPA on lobster count, biomass and sex ratios.

2 Methods

2.1 Environmental variables

2.1.1 Bathymetry (seafloor maps)

High-resolution multibeam echosounder (MBES) data were collected as part of this study for both Popes Eye and Portsea Hole, for which no seabed mapping data existed. Surveys in January 2018 mapped the seafloor of both sites at 25 centimetre (cm) resolution. MBES surveys were conducted using a Kongsberg Maritime EM2040C MBES integrated with an Applanix POS MV WaveMaster motion reference unit. The MBES was operated at a constant frequency of 300 kilohertz (kHz) with a varying ping rate and pulse length (up to 50 Hz and down to 0.025 milliseconds (ms), respectively) automatically adjusting to water depth, in high-density equidistant mode (400 soundings per ping) and with a constant sector coverage of ±60 athwartships. One sound speed profile was captured at the start of each day of survey with a Valeport Monitor Sound Velocity Profiler and imported in Kongsberg Maritime's acoustic data acquisition software SIS to correct soundings for variation of sound velocity in the water column. The POS MV WaveMaster also measured precise vessel motion data (roll, pitch, yaw, heave). A post-processed kinematic (PPK) solution was later obtained from these position and motion data using Applanix software POSPac Mobile Mapping Suite (MMS). This solution was then integrated with the bathymetry data in CARIS software HIPS and SIPS 10.3. The soundings were manually cleaned in HIPS and SIPS and gridded at a resolution of 0.25 metres (m).

Bathymetric coverage for the greater Port Phillip Heads region was obtained from the 2017 Victorian Coastal Digital Elevation Model (VCDEM) project (Allemand et al., 2017). This project was carried out by the Cooperative Research Centre for Spatial Information (CRCSI) at the request of the Department of Environment, Land, Water and Planning (DELWP, Victorian Government, Australia) to update and extend the seaward extent of the pre-existing 2010 VCDEM. The data in the region of interest is predominantly bathymetry LiDAR data with multibeam data from the Port of Melbourne for areas such as the deep canyons depicted on the imagery in this report. While gaps remain in this high-resolution dataset along areas of the coast, full bathymetric coverage was obtained for the entire Port Phillip Heads region at a horizontal resolution of 2.5 m.

For all sites, derivatives characterising the seabed terrain were extracted using the 'raster' and 'spatialEco' packages from the programming language R. Derivatives used included bathymetry, standard deviation of depth, slope, aspect (northness and eastness), vector ruggedness measure (VRM) and complexity (Table 2.1).

Table 2.1: Descriptive bathymetry statistics tested in this study

Derivatives	Description
Depth	Elevation of a plane passed through its closest grid point.
Standard deviation of depth	Standard deviation of depth provides a measure of topographic complexity.
Slope	Maximum change in elevation between each cell and cells in a specified surrounding neighbourhood.
Vector ruggedness measure (VRM)	Incorporates the heterogeneity of both slope and aspect using 3-dimensional (3D) dispersion of vectors, calculated using 3, 5 and 9 m window sizes. See Sappington et al. (2007) for more details.
Aspect (northness and eastness)	Azimuthal direction of the steepest slope through points in an analysis window. Northness relates to the sine component of the azimuthal direction, and eastness relates to the cosine.
Complexity	Second derivative of slope (or rate of change of slope).

2.1.2 Sea-surface temperature

Sea-surface temperature (SST) data were sourced from the Integrated Marine Observing System (IMOS, 2018). IMOS is a national collaborative research infrastructure supported by the Australian Government. These data were downloaded in NetCDF format at monthly intervals and converted into individual ArcGIS rasters for analysis. Annual and summer SST means were computed from 1992 to 2018 from the monthly SST datasets. To assess patterns in SSTs within Port Phillip Heads MNP, the mean and standard deviation of annual and summer SSTs were calculated for each year and plotted through time.

2.1.3 Hydrodynamics

Wave and current information were derived from a coupled hydrodynamic and spectral wave model (DHI, 2016). More detailed information on the development of these hydrodynamic models can be found in Ierodiaconou et al. (2018). Currents along the Victorian coastline were quantified using a variable-resolution, depth-averaged approach including tides, winds, bottom rugosity (surface roughness) and regional forces such as wind, tides, currents and waves that predict currents along the coastline. Spectral wave conditions were developed from the input wind conditions. The hydrodynamic models were run as annual simulations from 1990 to 2015, starting in July of one year and ending in June of the next. The annual outputs included files describing ocean currents at 5-minute time-steps with a spatial resolution of ~500 m at the shoreline to ~30 km in the open ocean. For inclusion in the models, averaged rasters for each of the model attributes (mean and maximum current speed, mean and maximum wave orbital velocities, mean and maximum significant wave height, mean and maximum wave power, current direction, wave direction) were exported and converted to 500 m resolution rasters to retain the higher resolution in

the nearshore. These rasters were further summarised into annual and seasonal (summer and winter) averages.

2.2 Unmanned aerial vehicle surveys

To update previous visual census methods and take advantage of scientific advances using unmanned aerial vehicles (UAVs), this study implemented an updated methodology for monitoring that had been previously tested by Deakin University (Murfitt et al., 2017). Deakin University is certified by the Civil Aviation Safety Authority (CASA) as a commercial remotely piloted aircraft (RPA) operator (certificate number CASA.ReOC.6496). UAV surveys were conducted using a small (<2 kilogram (kg)) multirotor airframe (DJI Phantom 4 Pro) with varying payload multispectral sensors.

The Point Lonsdale intertidal platform was flown over on 2 different dates: 7 April 2018 and 27 March 2019. Flying height, overlap, speed and flight time per battery were all set based on previous research of intertidal platforms, which concluded that higher altitude allows for faster speed and more area captured in each image, ultimately allowing capture of a larger area (Figure 2.1). However, higher altitude is a compromise resulting in lower resolution imagery (Figure 2.2). For the proposed purpose of identifying *Hormosira banksii*, the UAV was flown at 20 m above the platform on east–west lines, capturing 70% front overlap and 80% side overlap between images and flying at 3 metres per second (m/s), running the autonomous software Pix4D Capture. All flights were planned for a maximum of 12 minutes of flight time.

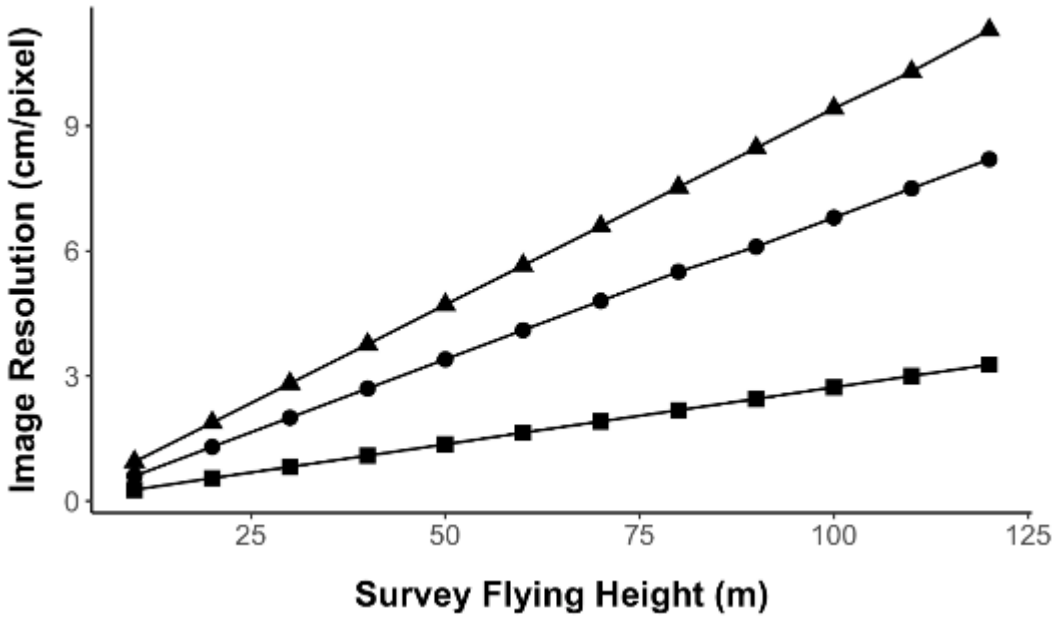

Figure 2.1: Resolution compared to survey height for each image sensor: Phantom 4 RGB (square), Red Edge M Multispectral (circle), Sequoia Multispectral (triangle). Sensors used were the DJI Phantom 4 onboard RGB camera (20 effective MP, field of view (FOV) 94°, 20 mm of 35 mm format equivalent, f/2.8, focus at ∞), Parrot Sequoia multispectral camera (1.2 effective MP, 10-bit colour depth, 4.0 mm focal length, 4.8 mm × 3.6 mm imager size, 61.9° horizontal FOV) and Micasense Red Edge M multispectral camera (1.2 effective MP, 16-bit colour depth, 5.4 mm focal length, 4.8 mm × 3.6 mm imager size, 47.9° horizontal FOV). Flight heights are expressed in metres above ground level (AGL).

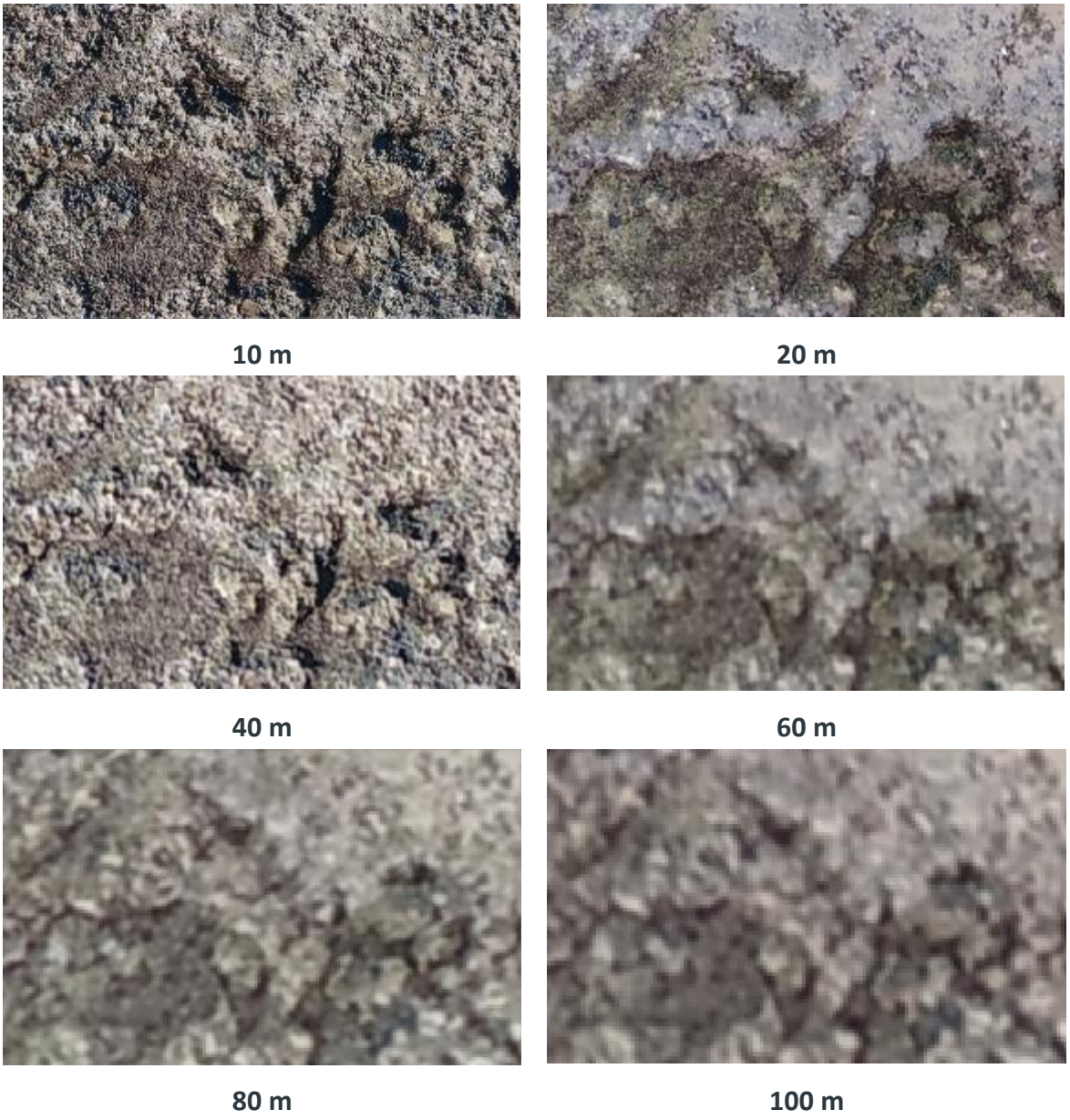

Figure 2.2: Comparative image resolution of processed images from DJI Phantom 4 onboard RGB camera at survey heights from 10 to 100 m with field of view approximately 4 m × 2 m. Superior image quality can be observed in the surveys at 10 and 40 m due to better ambient lighting conditions and absence of water on shore platform

In 2018, the flights were conducted with the DJI Phantom 4 Advanced UAV with in-built 20 MP camera and carrying a Parrot Sequoia multispectral camera (1,280 × 960 resolution, 10-bit colour depth, 4.0 mm focal length, 4.8 mm × 3.6 mm imager size and 61.9° horizontal field of view (FOV)) provided by Parks Victoria. The Parrot Sequoia multispectral camera required much more data processing than anticipated to generate usable results. Therefore, the 2019 flights were with the same UAV (DJI Phantom 4 Advanced with in-built 20 MP camera) but carrying a Red Edge M multispectral camera (1,280 × 960 resolution, 16-bit colour depth, 5.4 mm focal length, 4.8 mm × 3.6 mm imager size and 47.9° horizontal FOV).

The resultant area captured was approximately 40,375 square metres (m^2) at 20 m, requiring 7 flights. Ground control points were placed within the mapping area and marked with a real-time kinematic (RTK) GPS. In 2018, 18 ground control points were placed within the mapping area. The average error of the marked points was 10.086 (± 0.31) millimetres (mm) horizontal and 5.86 (± 0.91) mm vertical error. In 2019, 20 ground control points were placed within the mapping area, marked either with an RTK GPS or using Propeller AeroPoints. The average error of the marked points was 7.69 (± 1.44) mm horizontal and 12.31 (± 1.86) mm vertical error. The accuracy of the final models was less than 5 cm horizontal and less than 10 cm vertical, which are the literature standards for UAV operations.

The data were processed in Pix4D version 4.3.33. The outputs generated from the RGB imagery were an RGB orthomosaic and a digital surface model (DSM) of the entire platform. The outputs generated from the multispectral imagery included individual spectral reflectance layers for each spectral band captured and a Normalised Difference Vegetation Index (NDVI) calculated from the reflectance bands. The resolution of each output is recorded in Table 2.2.

Table 2.2: Outputs generated in 2018 and 2019 from the UAV aerial imagery in Pix4D, and their respective resolutions

2018		
Output	**Camera**	**Resolution (centimetres per pixel)**
RGB orthomosaic	DJI 20 MP camera with 1-inch CMOS sensor	0.52
DSM	DJI 20 MP camera with 1-inch CMOS sensor	0.52
Individual spectra (green, red, red-edge, near-infrared)	Parrot Sequoia	1.97
NDVI	Parrot Sequoia	1.97

Table 2.2 (continued): Outputs generated in 2018 and 2019 from the UAV aerial imagery in Pix4D, and their respective resolutions

2019		
Output	**Camera**	**Resolution (centimetres per pixel)**
RGB orthomosaic	DJI 20 MP camera with 1-inch CMOS sensor	0.51
DSM	DJI 20 MP camera with 1-inch CMOS sensor	0.51
Individual spectra (blue green, red, red-edge, near-infrared)	Micasense Red Edge M	1.33
NDVI	Micasense Red Edge M	1.33

A machine learning approach was taken to automate the classification of *H. banksii* across the intertidal platform. For this, RGB and DSM TIFFs were first upscaled to match the resolution of the multispectral sensor TIFFs (0.0198 metres per pixel for 2018, 0.0133 metres per pixel for 2019). A terrain ruggedness index (TRI) and topographic position index (TPI) were computed using QGIS (QGIS.org, 2019) and the DSM TIFFs. TRI is the mean of the absolute differences between the value of a cell and the value of its 8 surrounding cells. TPI is the difference between the value of a cell and the mean value of its 8 surrounding cells.

ENVI (Exelis Visual Information Solutions, n.d.) was then used to delineate quadrats of 50 cm × 50 cm in different sub-habitats on the rocky platform to try to capture different elevations and textures. Each pixel in each quadrat was manually classified as being *H. banksii* or background using the 'region of interest' tool. Red, blue, green, NDVI, near-red, red-edge, raw DSM values, terrain ruggedness index and topographic variation index values for each pixel of the training dataset were then extracted, and these 9 features were used to train a random forest algorithm. There was no blue spectral reflectance for 2018 data collected with the Parrot Sequoia multispectral camera, so it was excluded.

Random forest models are sensitive to class imbalance, so the number of pixels in each class was balanced before training the algorithm. Of the annotated pixels, 75% were assigned for model training and 25% were set aside for model validation. The R package ModelMap (Freeman et al., 2018) was used to tune the hyperparameters of the random forest algorithm and to determine the optimal number of trees, the importance of each feature and the number of features used to construct each tree. This package uses an estimation procedure to find the appropriate hyperparameters using the training dataset. In addition, the package uses the validation dataset to check the accuracy of predictions on the

remaining 25% of the data. Considering the small number of predictor variables used, all variables were retained in the final models.

The ModelMap package was then used to predict the random forest model across the entire rocky platform, allowing a prediction of the probability of *H. banksii* at a pixel level. This process was conducted separately for the 2018 and 2019 datasets as the quality of the data varied between years due to the different multispectral sensors used. For the 2018 data, the machine learning algorithms struggled with the data from the Parrot Sequoia multispectral camera, producing no obvious spike in the histogram data. Therefore, we used a probability of 0.5 (50%) to set the threshold for the 2018 *H. banksii* data, determined visually. The data from the Red Edge M multispectral camera in 2019 were much more consistent and had a clear spike in probability detection at 0.785. Therefore, we used the probability of 0.785 (78.5%) to set the threshold for the 2019 *H. banksii* data. The resulting layers were representative of *H. banksii* coverage on the Point Lonsdale intertidal platform for 2018 and 2019. We visually determined that polygons below 20 cm^2 were unlikely to be *H. banksii* and more likely to be artefacts of the classification process, so we removed those polygons from the coverage maps. Finally, the *H. banksii* cover for the Point Lonsdale intertidal platform was calculated for 2018 and 2019.

Virtual quadrats were then generated that corresponded to the on-ground quadrats scored for *H. banksii* percentage cover during the UAV operations. No on-ground quadrats were recorded in 2018, but 30 on-ground quadrats were scored in 2019. On-ground quadrats were measured using a 50 cm × 50 cm square; however, the outside corner of the quadrat was marked with the RTK GPS, resulting in virtual quadrats measuring an average of 58 cm × 58 cm, 34% larger than the on-ground quadrats. To scale for the difference, percentage cover within the quadrat was used instead of area.

Nine patch-analysis windows measuring 25 m × 25 m were allocated across the Point Lonsdale intertidal platform, visually broken into 3 broad densities: low *H. banksii* coverage (3 windows), moderate *H. banksii* coverage (3 windows) and dense *H. banksii* coverage (3 windows). The percentage of *H. banksii* coverage within the patch-analysis windows was calculated for 2018 and 2019. The *H. banksii* coverage in each of the patch-analysis windows was quantified against landscape pattern indices (*H. banksii* cover (%), number of patches, maximum patch area (m^2), mean patch area (m^2), total perimeter (m), mean patch perimeter (m) and edge density). The percentage cover of *H. banksii* and the number of patches provide a general index of spatial heterogeneity across an entire landscape. The maximum patch area indicates whether the window was dominated by a single patch. Minimum patch size was not included as it was always at the single pixel scale from clipping the window edge. The mean patch size provides an indication of coverage, while the standard deviation is a measure of absolute variation that is a function of the mean patch size and the difference in patch size among patches. The perimeter measures provide an indication of connectivity, while edge distance standardises patch edges to a per unit area

basis. The patch-analysis windows create false patch edges on the perimeter of the windows, but these were uniform across all windows, and minimal compared to total edge length, so were included in the analysis.

2.3 Reef Life Survey

Using the methods developed by the Reef Life Survey (RLS) citizen science program, surveys were completed at all historical Subtidal Reef Monitoring Program sites within the Port Phillip Heads MNP (10 sites within the MPA and 8 reference sites) in the years 2016 to 2019 to continue the time series following cessation of SRMP in 2015. In recent years, Reef Life Survey methods have become common for completing underwater visual census surveys of shallow subtidal reefs. Globally, the RLS technique has allowed approximately 2,000 sites to be surveyed using a standard set of survey methods, which are described in detail in an online methods manual (Reef Life Survey, 2015).

RLS surveys encompass an underwater visual census (UVC) technique in which scuba divers swim along a 50 m transect line laid on hard substrate, along the depth contour of the site being surveyed (depths of Port Phillip Heads sites were <11 m). All fish species observed within 5 m of the transect line are recorded on a waterproof datasheet as the diver swims slowly along the line (at approximately 2 metres per minute). On the same transect, all macroinvertebrates and cryptic fish larger than 2.5 cm and within 1 m of the transect tape are recorded. At each site, divers complete two 50 m transects in opposite directions along the same depth contour. This means that an area of 1,000 m^2 is surveyed for fish and 200 m^2 for invertebrates at each location.

In addition, a series of 20 digital photo quadrats were collected at 2.5 m intervals along each transect. Photo quadrats are taken from approximately 50 cm above the seabed (usually sufficient to encompass an area of approximately 0.3 m × 0.3 m). These photo quadrats are later annotated using TransectMeasure software (SeaGIS) with 25 evenly distributed points on a 5 × 5 grid. Each point is classified to the lowest taxonomic level possible using an adapted Collaborative and Annotation Tools for Analysis of Marine Imagery and video (CATAMI) classification scheme (Althaus et al., 2015). This classification allows data on algae, sessile invertebrates and substratum type to be recorded and stored for later analysis. The main difference of this survey approach compared with previous SRMP methods is the replacement of in situ quadrat surveys with photo quadrats. To account for the differences in quadrat scoring, this study only compares canopy-forming species to previous SRMP observations, as understorey communities are likely to be obscured in photo quadrats.

RLS surveys were conducted at the same sites that had been surveyed in the SRMP after that program stopped in 2015. However, surveys from 2016 to 2018 only completed a 100 m transect at each site. In 2019, RLS survey effort was doubled at each site (Figure 2.4). Data were normalised to account for differences in area covered by the 2 techniques and results were compared.

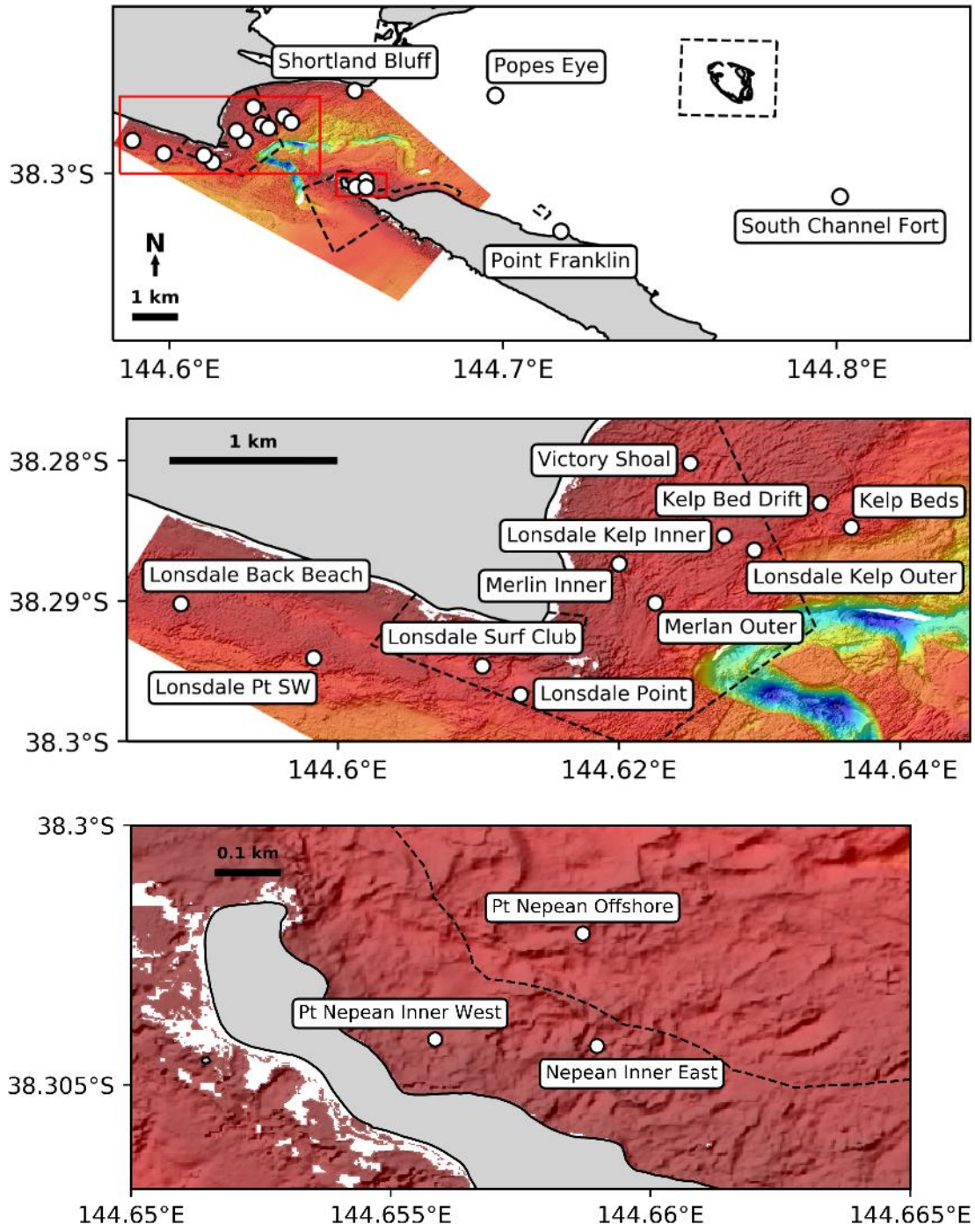

Figure 2.3: Port Phillip Heads region showing the locations of all SRMP/RLS monitoring sites. Red boxes in the top map show the extents of the middle and bottom maps

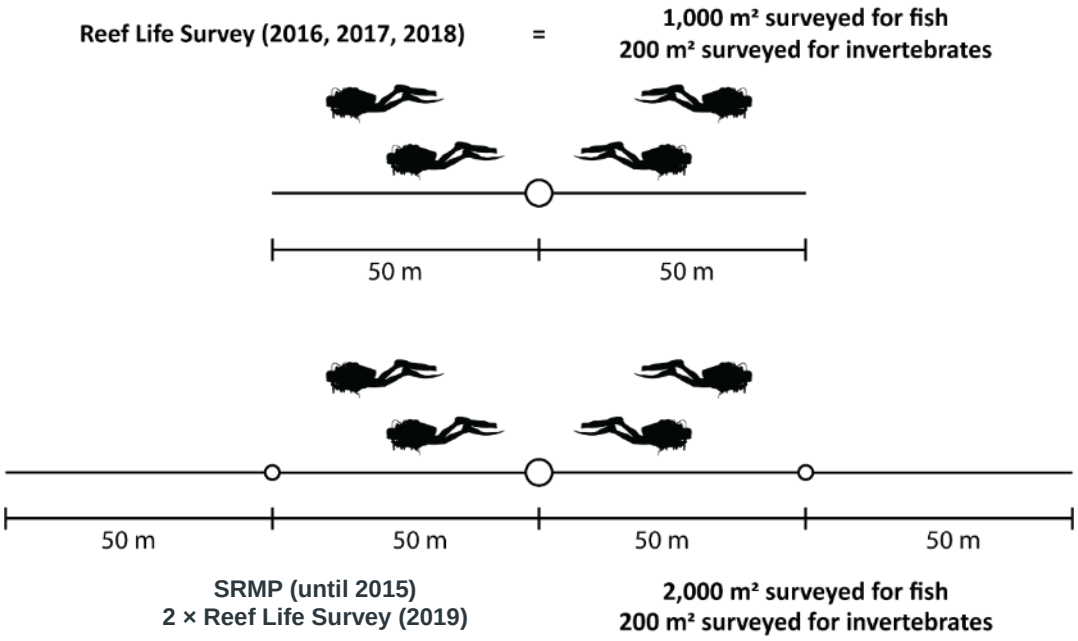

Figure 2.4: Differences in underwater visual census sampling methodologies for each year of sampling

2.4 Baited remote underwater video stations

Fish assemblages in this project were sampled using baited remote underwater video stations (BRUVS) at 2 time points. Sample sites were stratified using existing seafloor bathymetry data and habitat maps to ensure habitat variability was captured across each site. Surveys took place in April and May 2018 and February 2019. The sample sites surveyed in 2018 were repeated in 2019 to allow direct comparison between years. BRUVS surveys aimed to target fish communities on deeper (>10 m depth) algal-dominated reefs and complement fish data collected using RLS methods on shallow subtidal reefs inside and outside the MPA.

For both surveys, 2 high-definition video cameras (Sony Legria HF G10 or M300 cameras) were fitted on each of 6 BRUVS frames. The pairs of cameras were mounted 0.7 m apart and angled in at 8° to allow for stereo imaging. This stereo imaging allows for the lengths and distance from the camera of fish to be determined (Langlois et al., 2018). A synchronising diode was placed in the field of view so the camera frames could be synced for size measurements. Each BRUVS frame was calibrated in a pool before undertaking fieldwork. A bait bag made up of 1 kg of Pilchards (*Sardinops sagax*) was suspended 1.2 m in front of the cameras. The BRUVS were located at least 250 m apart to minimise potential movement of fish between sites. Sixty minutes of footage on the seafloor was analysed for each drop location. Post-processing of BRUVS footage was completed using the program EventMeasure (SeaGIS). For each video, the *MaxN* (maximum number of individuals of a particular species in the frame at any given time) was recorded, providing a conservative

measure of relative abundance. Measuring *MaxN* is a widely recognised way of obtaining fish population data from BRUVS and means that no individual is double-counted (Cappo et al., 2004). The total length of each individual fish at the *MaxN* for each species, in each video, was then measured using 5 mm as the maximum uncertainty accepted for each measurement. Relative species richness, relative family richness, total relative abundance, total relative biomass and relative abundance of 10 predominant species were then evaluated for each drop location. Predominant species selected included Snapper (*Chrysophrys auratus*), Dusky Morwong (*Dactylophora nigricans*), Smooth Stingray (*Bathytoshia brevicaudata*), *Meuschenia freycineti*, *Meuschenia hippocrepis*, Eagle Ray (*Myliobatis tenuicaudatus*), Blue-Throat Wrasse (*Notolabrus tetricus*), Senator Wrasse (*Pictilabrus laticlavius*), Sand Flathead (*Platycephalus bassensis*) and Southern Fiddler Ray (*Trygonorrhina dumerilii*).

To associate fish species and communities with the structure of the seafloor, a number of bathymetric derivatives were compiled. Derivatives of the seabed terrain were extracted using the R packages 'raster' and 'spatialEco'. Derivatives used included bathymetry (depth), standard deviation of depth, vector ruggedness measure, slope, complexity and aspect (northness and eastness) (Table 2.1). Because species vary in their response to habitat characteristics at a variety of scales, we calculated the mean of all variables at circular radius scales of 5, 10, 25, 50, 100, 150 and 300 m using the 'focal statistics' geoprocessing function in ArcGIS's Spatial Analyst toolbox. This tool calculates the mean of each cell in an input raster using a roving window that varies in size depending on the scale being tested. The 'extract multi values to points' tool in ArcGIS was then used to extract the underlying seafloor variables of all spatial scales at each BRUVS deployment location. The 'findCorrelation' function from the R package 'caret' (Kuhn, 2008) was used to remove highly correlated variables (>0.7) (Dormann et al., 2013). Variance inflation factors were calculated following analysis, but values were all below 2.5, indicating no multicollinearity was present (James et al. 2013).

Generalised additive models (GAMs) were used to investigate and model the effect of environmental variables on various subsets of the fish assemblages captured using BRUVS. GAMs were selected for use in this study because of their ability to allow for nonlinear relationships (Austin, 1998; Yee and Mitchell, 1991), as well as being a conventional and well-developed method for modelling fish–habitat relationships (Galaiduk et al. 2017; Valavanis et al., 2008). Before running GAMs, spatial autocorrelation of the response variables were tested using a spline correlogram generated in the R package 'ncf' (Bjørnstad, 2009). The R package 'mgcv' (Wood, 2015) was then used to run GAMs. In GAMs, the number of predictor variables able to be included is limited by the ability of the sample size to capture the variability across the study region. Bolker et al. (2009) recommends using a rule of thumb of more than 10–20 samples per experimental unit. Of the 85 successful BRUVS deployments (excluding Popes Eye, Portsea Hole and South Channel Fort), 63 (75%) were used for training the models while the remaining 22 (25%)

were used for evaluating the model performance. Therefore, a maximum of 4 predictor variables could be used per model. All combinations of the 7 predictor variables selected (*n* = 98 combinations) were modelled to obtain the highest possible model performance. Model selection was conducted using the 'MuMIn' package in R (Barton, 2018), in which a confidence set of models was made. Because the ratio of Akaike weights for 2 candidate models can be used to assess the preference for one model over another (Anderson et al., 2000), the confidence set of models included only those candidate models with Akaike weights within 5% of the largest weight (Thompson and Lee, 2000). These were selected after passing the general rule of thumb (i.e. 1/8 or 12%) suggested by Royall (1997) for evaluating whether strength of evidence was met. To be included in the confidence set, models also had to have a difference in Akaike information criterion (AIC) value from the best model (ΔAIC) of less than 5. From the confidence set, the model with the lowest second-order AIC (AIC_C) was deemed the best model. To account for variations in the scale of habitat relationships between different groups of demersal fish, modelling in this study was completed using environmental derivatives extracted at multiple spatial scales (5, 10, 25, 50, 100, 150 and 300 m) around the BRUVS deployment location. This allowed models to consider the individual spatial ecology of species interactions with the surrounding environment. Pearson's correlations were used to assess the accuracy of the predicted data compared with observed data. Individual contributions were then summed, and a percentage of relative importance in the model was derived. The R package 'raster' (Hijmans and van Etten, 2014) was used to create predictive maps extrapolating model predictions over the entire study area for those models that performed relatively well (e.g. higher relative deviance explained and higher relative prediction accuracy).

2.5 Towed video

Towed video surveys were used to obtain transect data on benthic habitats extending beyond diving depths within the marine national park. Two towed video surveys were conducted as part of this study. The first took place between January and April 2018, and the second took place in February 2019. These surveys used a VideoRay remotely operated vehicle (ROV) modified to function as a towed camera by inserting it into a stainless steel frame and adding a micro-wing attachment to assist with stability during deployment. Forward-facing, high-definition, stereo video footage was obtained from 2 GoPro Hero 3+ cameras fastened to the top of the frame in a custom-built stereo housing with a 40 cm base bar positioned at a 45° angle to the seabed. This angle allowed the seabed, as well as the water column, to be captured in the camera's field of view. Similar angles have been used in other studies assessing fish communities (Spencer et al., 2005). To reduce the distorting effect of the fish-eye lens in the cameras, footage was recorded with medium field of view, at a resolution of 1920 × 1,080 pixels and 60 frames per second (FPS). A Ricoh Caplio GX100 downward-facing stills camera with an attached strobe light was additionally used to create photo quadrats of the seafloor every 10 seconds. These detailed images make it possible to obtain high-resolution classifications of benthos. Two lasers, of a fixed

separation, were further added for the 2019 surveys, allowing for increased scaling of benthos. The position of the unit in the water column was tracked at one-second intervals using a Tracklink 1500MA ultra-short baseline (USBL) acoustic tracking system. The unit was towed approximately 1 m above the seafloor using a winch system while observing a live-feed video obtained via an umbilical cable from the ROV unit. During both surveys, the boat speed was kept between 0.5 and 1.0 knots (0.26–0.5 m/s) for the majority of the transect. Time synchronisation between the live towed video, stereo GoPro HD footage, downward-facing still images and the USBL system enabled measurement of the geographical location of benthic habitat observations along transects.

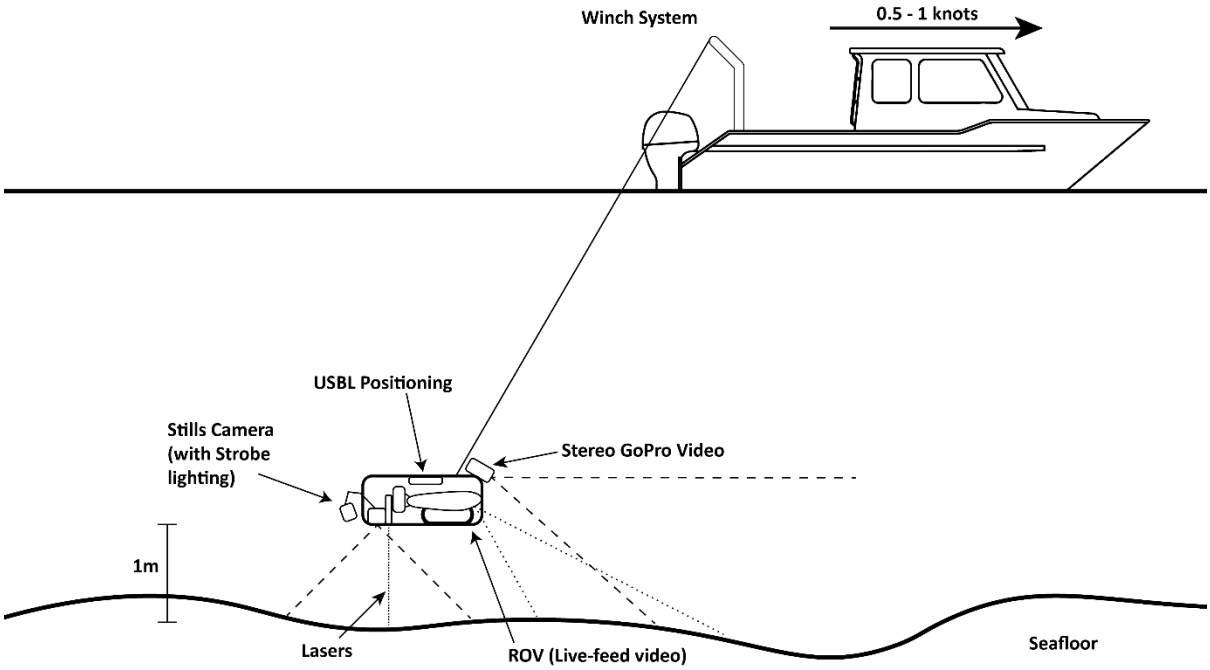

Figure 2.5: Typical arrangement of equipment in a towed video survey

Post-processing of photo quadrats was conducted using the program TransectMeasure (SeaGIS). The georeferenced images were overlaid on previously mentioned bathymetric variables (Section 2.1.1), allowing depth to be extracted for each image. From these data, 40 georeferenced still images (or the maximum number of images available) were extracted and classified for each 5 m depth stratum for the greater Port Phillip Heads MNP. A higher density of images was classified for the Popes Eye and Portsea Hole sites to ensure all habitat types were covered in habitat maps. Using TransectMeasure, each image was scored with 25 randomly distributed points and classified using an adapted CATAMI classification scheme (Althaus et al., 2015). Thus, differences in the contribution of each biotic component could be identified at the lowest taxonomic resolution for each depth stratum.

Habitat maps were additionally created for Popes Eye and Portsea Hole. These maps were developed using classes derived from the new Combined Biotope Classification Scheme

(CBiCS) developed by Australian Marine Ecology and Fathom Pacific (Edmunds and Flynn, 2015). Habitat maps were developed using the previously mentioned environmental variables from multibeam sonar (Section 2.1) and ground truthing of biotopes using towed video surveys. CATAMI scoring from the downward-facing stills and oblique view were also used to inform CBiCS biotopes.

CBiCS, which has been adopted by DELWP (Edmunds and Flynn, 2015), was used to classify video observations. CBiCS delineates habitat classes, based on observations of biota from the video data, into multiple categories for each of the CBiCS hierarchies (Edmunds and Flynn, 2015). There are 6 hierarchical levels within CBiCS (Eigenraam et al., 2016). Of the 2 sites mapped, only Popes Eye was able to be predicted to the biotope complex (BC4) level. The high diversity of biotopes on the wall of Portsea Hole resulted in too few classifications being obtained for each class to inform the classification process, hence these classes could not be included in the models. When these observations were grouped into their respective habitat complex (BC3) levels, however, sufficient sample sizes were present. It is envisaged that with a higher density of classifications, future studies may be able to achieve BC4-level classifications for habitat prediction.

Using a method similar to that described in Section 2.2, a machine learning approach was used to map the biota of these sites. Random forest (RF) machine learning models were used from the 'randomForest' package in R (Liaw and Wiener, 2002). Prior to modelling, Pearson product-moment correlation was used to assess correlation of predictor variables. Where there was a strong correlation (>0.7) between covariates, the variable with highest importance was retained and the remaining variables in the correlated subset were excluded from analyses. Variable importance was calculated by assessing out-of-bag (OOB) errors and percentage increase in misclassification. OOB errors and percentage increase in misclassification were calculated by randomly removing each predictor variable and measuring their respective changes. From both OOB errors and percentage increase in misclassification, mean decrease accuracy was computed and used as a representation of variable importance. The lower the mean decrease accuracy value, the smaller the impact of the variable on model accuracy. Once models were made, classified maps of both Popes Eye and Portsea Hole were predicted from these models using the R package 'ModelMap' (Freeman et al., 2018).

2.6 Fisheries-independent Southern Rock Lobster survey

Lobster have previously been identified as an essential indicator of the health of subtidal reefs, as well as a proxy for the effect of poaching in marine national parks and sanctuaries. Rock lobster surveys offer valuable information about 'secondary' ecosystem services provided by the park to the rock lobster fishery and can also inform ecosystem-based management of the fishery. Southern Rock Lobster (SRL) (*Jasus edwardsii*) have previously been surveyed as part of the Subtidal Reef Monitoring Program; however, it has been difficult to accurately sample SRL populations as monitoring sites rarely overlapped with

prime rock lobster habitat. As an alternative, this study used standardised fishery assessment trapping methods to provide fine-scale SRL population information within and adjacent to the Port Phillip Heads MNP.

For this survey the sampling design was created in conjunction with local commercial lobster fisherman who provided a wealth of knowledge (>20 years experience) in the local area. Lobster pots were baited with 1 kg of locally available bait and escape gaps were wired shut (Ierodiaconou et al., 2018; Woods and Edmunds, 2013; Young et al., 2016). A total of 116 pots were deployed during this survey: 60 were placed inside the park and 56 outside. For each day's sampling, pots outside the park were deployed in areas of similar habitat to those deployed inside the park to help test the effect the park has on the local SRL population while controlling for habitat. All captured SRL were counted and sexed, females were assessed for reproductive condition, and all SRL were measured for carapace length (CL). T-bar tags were applied to all lobsters caught as part of the Victorian Fisheries Authority's tag and recapture program, in which between 2,500 and 7,000 lobsters are tagged each year. Genetic fin clip samples were taken from all lobsters caught. Bycatch was recorded for each pot location before being promptly returned to the water. To calculate SRL biomass, we used the length–weight relationship provided in Punt (2003): $W = a\ CL^b$, where W is the weight in kilograms and a and b are coefficients related to sex and size class (females: a = 0.000271, b = 3.135; males: a = 0.000285, b = 3.114).

2.7 Control charts

Parks Victoria, in collaboration with the University of Melbourne and Deakin University, has developed a series of control charts to provide timely, accurate and reliable information on the condition of natural assets, level of threats and management effectiveness. These charts form part of Parks Victoria's State of the Parks evaluation. They depict a simple line graph tracking an indicator through time, identifying a zone of acceptable change and upper and/or lower control limits to flag values where a management response should be considered.

Control limits around the zone of acceptable change are calculated to reflect the statistical properties of the chart (Montgomery, 2007) as follows:

$$UCL = ULAC + \frac{Z_\alpha \sigma}{\sqrt{n}}$$

$$LCL = LLAC + \frac{Z_\alpha \sigma}{\sqrt{n}}$$

where *UCL* = upper control limit, *LCL* = lower control limit, *ULAC* = upper limit of acceptable change, *LLAC* = lower limit of acceptable change, Z_α = multiplier for number of standard deviations to correspond with desired Type I error rate α, σ = weighted average standard deviation, and n = modal sample size to allow for possibly unequal sample sizes.

In the Port Phillip Heads MNP dataset, the lower limit of acceptable change (LLAC) was initially identified as the minimum value inside the MPA from SRMP surveys before the marine national park was declared (1998–2002). For some indicators, modification of this LLAC was needed to ensure the lower control limit remained above zero. Each chart was then plotted over the entire survey period including SRMP surveys (1998–2011 and 2014–15) and RLS surveys (2012–13 and 2016–19). The lower control limit (LCL) was then calculated from the LLAC, taking into account the variation in the data (standard deviation) and number of sites surveyed (*n*) over the entire survey period. For ease of interpretation, zones of acceptable change on charts were shaded green, control limits were indicated by dashed horizontal lines, and areas outside the control limits were shaded red.

One of the current limitations of the control chart approach is how we choose to define the LLAC. Ideally, these limits relate to different management scenarios and actions. However, this often requires a sound understanding of threats to the ecosystem and the resilience of the ecosystem to disturbance and change. We are probably in the strongest position to do this with existing information for *Hormosira banksii* on intertidal reefs. Here, we chose an LLAC of 48% cover, which was based on the minimum value from the reference site. However, LLAC can be chosen in other ways. Another way would be to use the value within 3 standard deviations (42%), which represents the limit of natural mean variation of *H. banksii* in the area. If we use 42%, the LCL would then be 30% cover of *H. banksii*. Fortunately, previous experimental studies on *H. banksii* have investigated the resilience of this ecosystem to disturbance. Experimental research has shown that disturbance that reduces cover of *H. banksii* to 30% can then take multiple (e.g. 1–3) years to recover (Keough and Quinn, 1998; Povey and Keough, 1991; Schiel and Taylor, 1999). This is important to consider, as different levels of *H. banksii* affect diversity and abundance of associated intertidal communities (Pocklington et al., 2018; Pocklington et al., 2019). Establishing an LCL of 30% means Parks Victoria should act if the *H. banksii* cover went below 30% and this decline was linked to a threat that could be managed (e.g. by reducing human access and trampling disturbance). While we have made our best efforts in this report to choose LLACs, ultimately this is a process that requires further thought and consideration on a case-by-case basis.

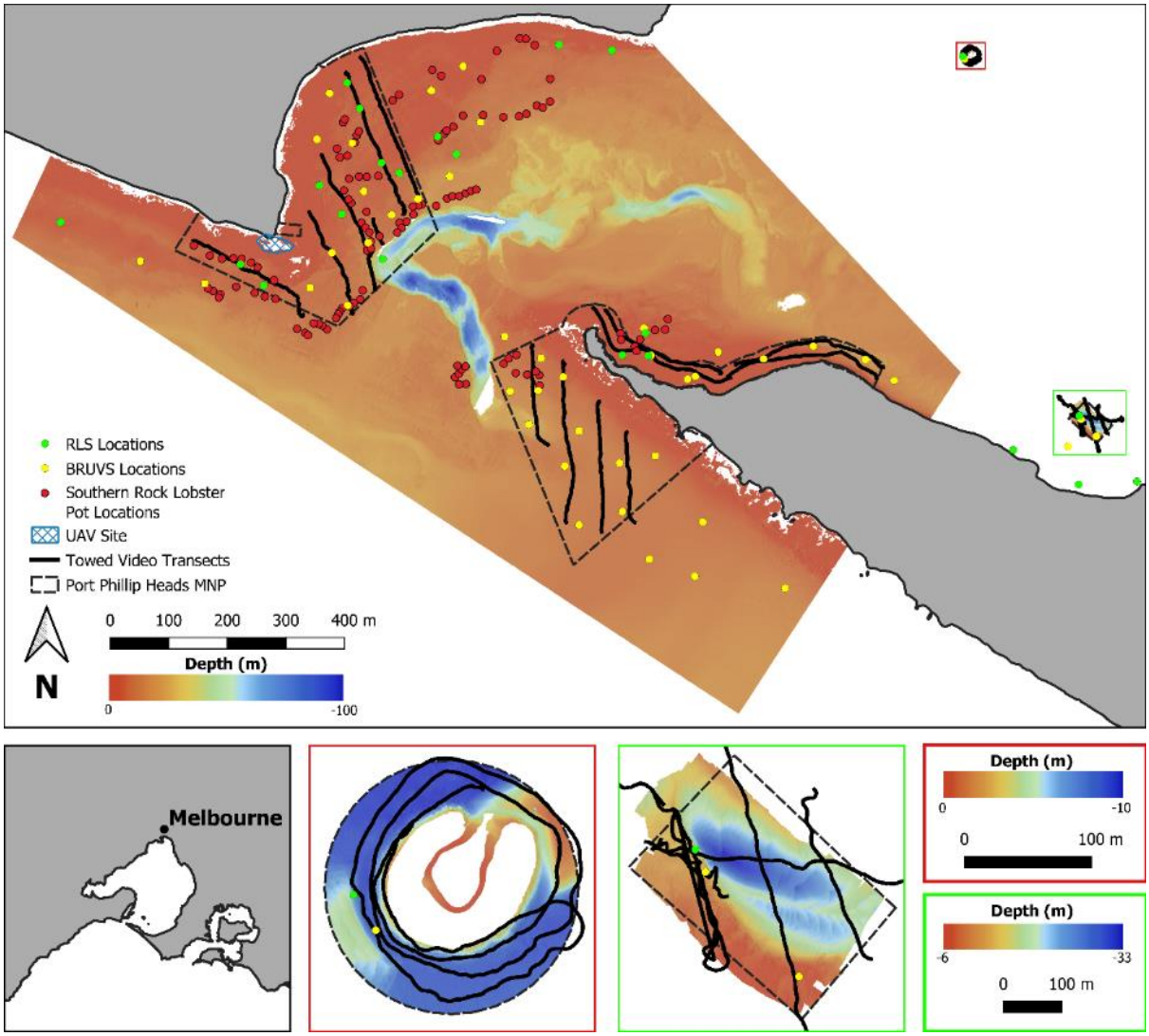

Figure 2.6: Locations of Reef Life Survey transects (green points), Southern Rock Lobster pots (red points), baited remote underwater video station (BRUVS) deployments (yellow points), unmanned aerial vehicle (UAV) survey extent (blue shape), and towed video transects (black full line) across the entire study site. The dashed line indicates the boundaries of the Port Phillip Heads MNP. Sites are overlaid on high-resolution hillshaded (shading to show 3D relief) bathymetry of the area coloured by depth. Note: All Reef Life Survey locations also had BRUVS deployments.

3 Results

3.1 Bathymetry (seafloor maps)

High-resolution multibeam echosounder (MBES) data were collected as part of this study for both Popes Eye and Portsea Hole within Port Phillip Heads MNP. This resulted in 122,000 m^2 of the marine national park being mapped at 25 cm horizontal resolution (Figure 3.1). Full bathymetric coverage was obtained for the greater Port Phillip Heads region at a horizontal resolution of 2.5 m from the 2017 Victorian Coastal Digital Elevation Model project (Allemand et al., 2017). From these surfaces, 8 derivatives of bathymetry were calculated to further our understanding of seafloor features. Derivatives created included bathymetry, standard deviation of bathymetry, vector ruggedness measure, slope, complexity, and aspect (northness and eastness) (Table 2.1, Figure 3.2). In addition to the bathymetric products and derivatives, information on wave energy and current speeds were also extracted for each location using the rasters from the statewide downscaled hydrodynamics.

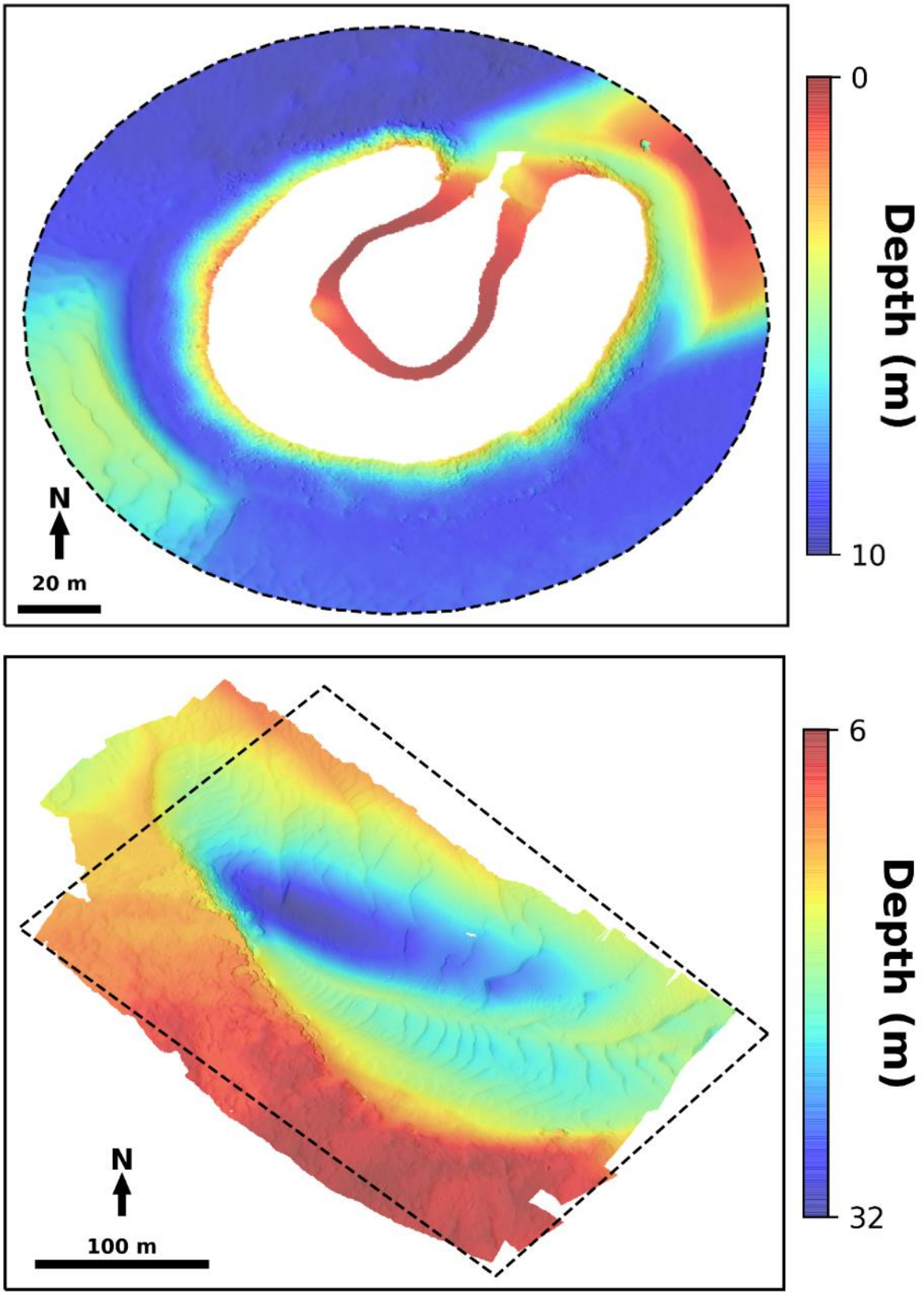

Figure 3.1: Hillshaded bathymetric coverage of Popes Eye (top) and Portsea Hole (bottom) from the Port Phillip Heads MNP. Dashed lines indicate the boundaries of the marine national park

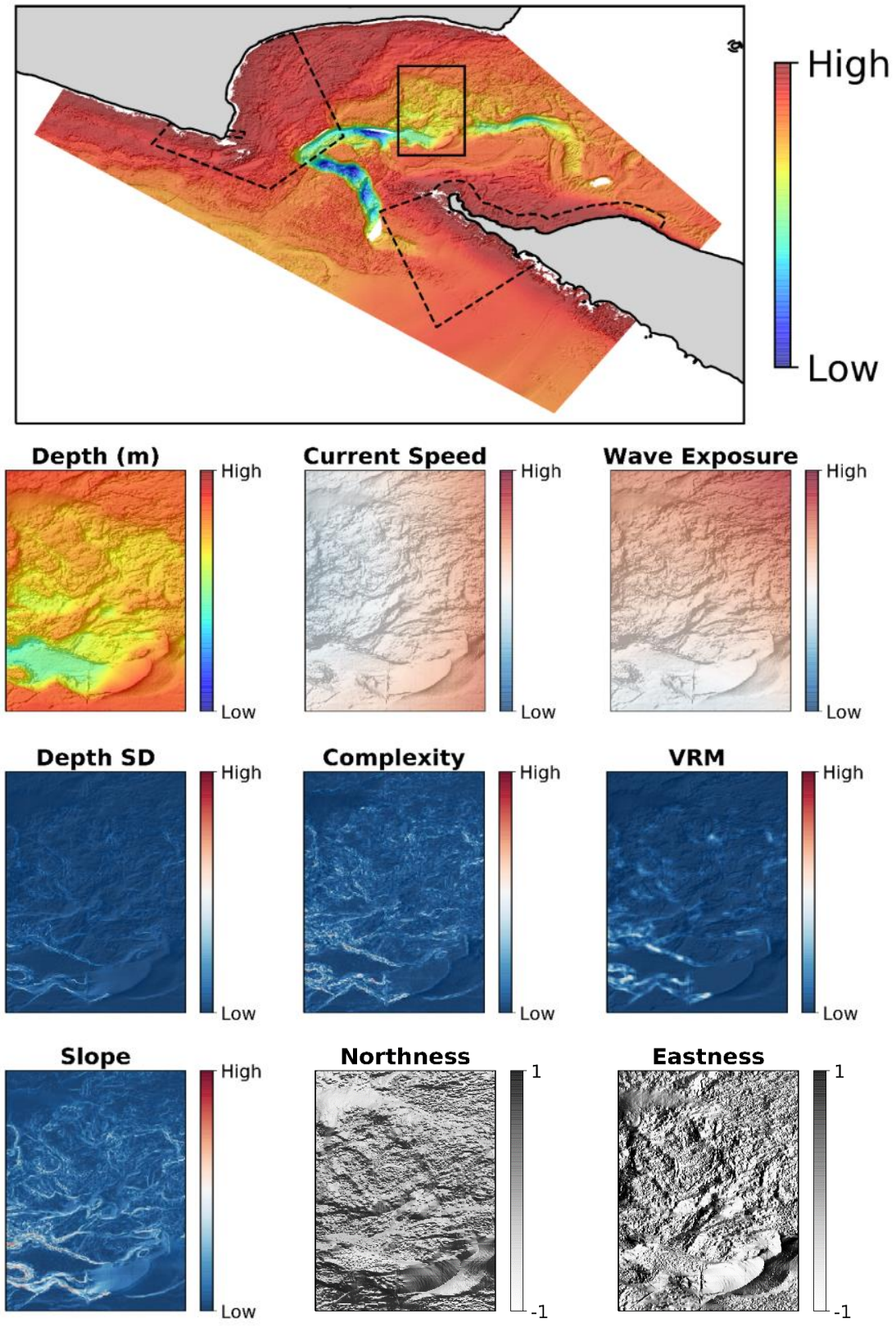

Figure 3.2: Overall map of bathymetry data available for this study with subset images of example derivatives used to characterise seafloor structure. Dashed lines indicate the boundaries of the marine national park and the solid lines show the extent of the zoomed-in region used to display the derivatives

3.2 Sea-surface temperature

Mean sea-surface temperature (SST) varies seasonally and temporally in the Port Phillip Heads MNP with higher mean temperatures in summer. The SST has experienced an overall mean increase since 1992 in both annual and summer time series, but this trend is not linear. Temperatures oscillations over time, and variability tends to be higher in summer (Figure 3.3). Also, summer temperatures have increased in recent years while annual temperatures have experienced a slight decrease following a spike in 2004.

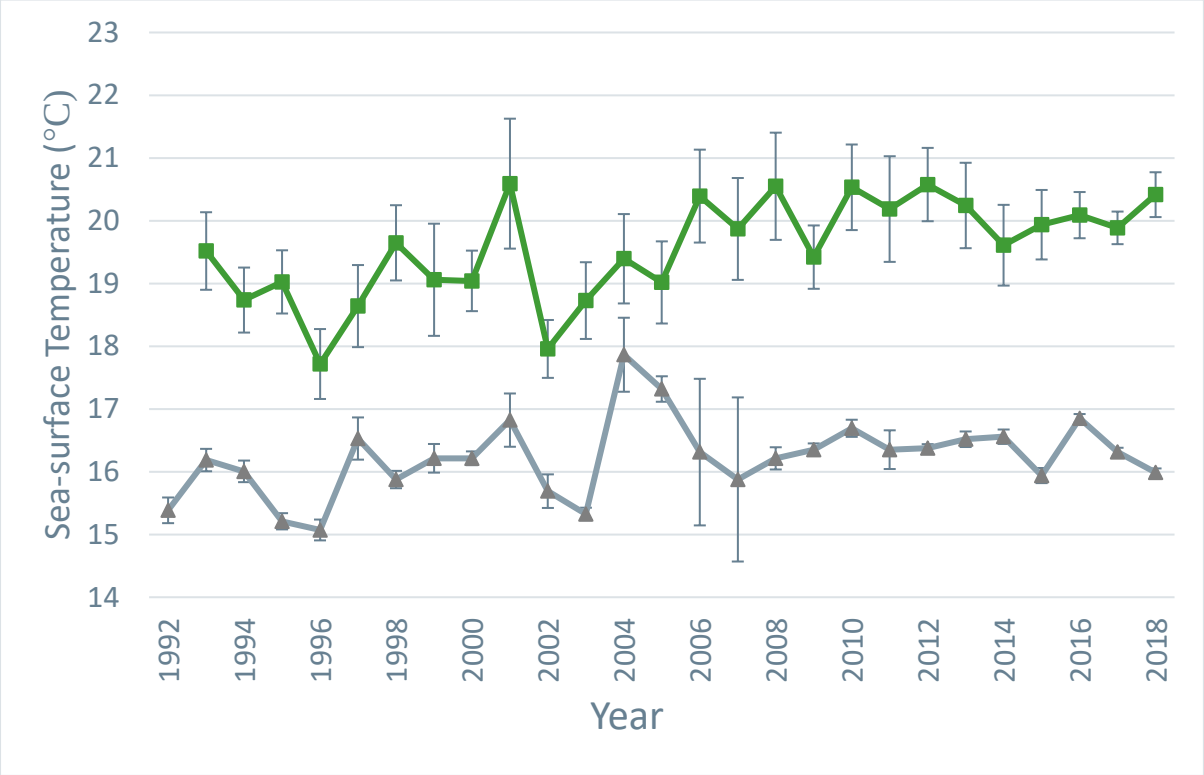

Figure 3.3: Sea-surface temperature (SST) trends through time for annual (grey line) and summer (green line) means in the Port Phillip Heads MNP. Error bars show the standard deviations of the means across the park

3.3 Intertidal reefs

Hormosira banksii cover was maintained well above the LLAC of 48% (minimum value from reference site). Indeed, cover increased from 62% in 2013 to an all-time high of 87% in 2018 and 2019. No surveys were conducted at the reference site (Cheviot Beach) in 2018 or 2019, so it is difficult to know if this is representative of a broader pattern (e.g. relating to environmental conditions) or a result of park management.

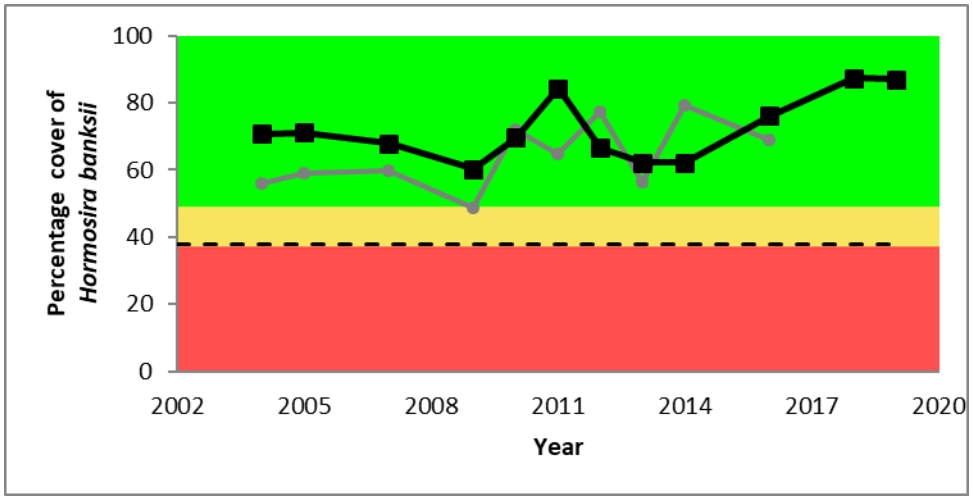

Figure 3.4: Control chart showing change in percentage cover of *Hormosira banksii* at Point Lonsdale in Port Phillip Heads National Park (black line) and reference site (grey line). Observations for these charts were sourced from the IRMP program. These charts have a lower limit of acceptable change (set as the minimum value from the reference site) and lower control limit indicating the level at which conditions are sufficiently poor that some management response is required

3.3.1 Unmanned aerial vehicle surveys

UAV operations were successfully conducted on 7 April 2018 and 27 March 2019. Saturday 7 April 2018 was a sunny day with a low tide of 0.3 m and winds less than 10 knots. However, low tide was at 1015h, so multispectral mapping was conducted earlier than recommended (recommended flight time is within 2.5 hours of solar noon). Wednesday 27 March 2019 was a sunny day with a low tide of 0.2 m and winds less than 10 knots. Low tide was at 1112h, so multispectral mapping was conducted closer to solar noon than on the earlier survey. These differences in lighting conditions, based on the time of capture, likely drove differences in data capture rate between surveys (Figures 3.5 and 3.6). There was also a difference in the resolution captured by the Parrot Sequoia and the higher resolution Micasense Red Edge M multispectral cameras. Furthermore, there is a difference in image clarity. Image clarity refers to attributes such as image detail, colour depth, and image distortion (Figure 3.6). Intermittent GPS functionality in the Parrot Sequoia also created complications in the processing, and greater time and manual processing were required to generate the final spectral maps.

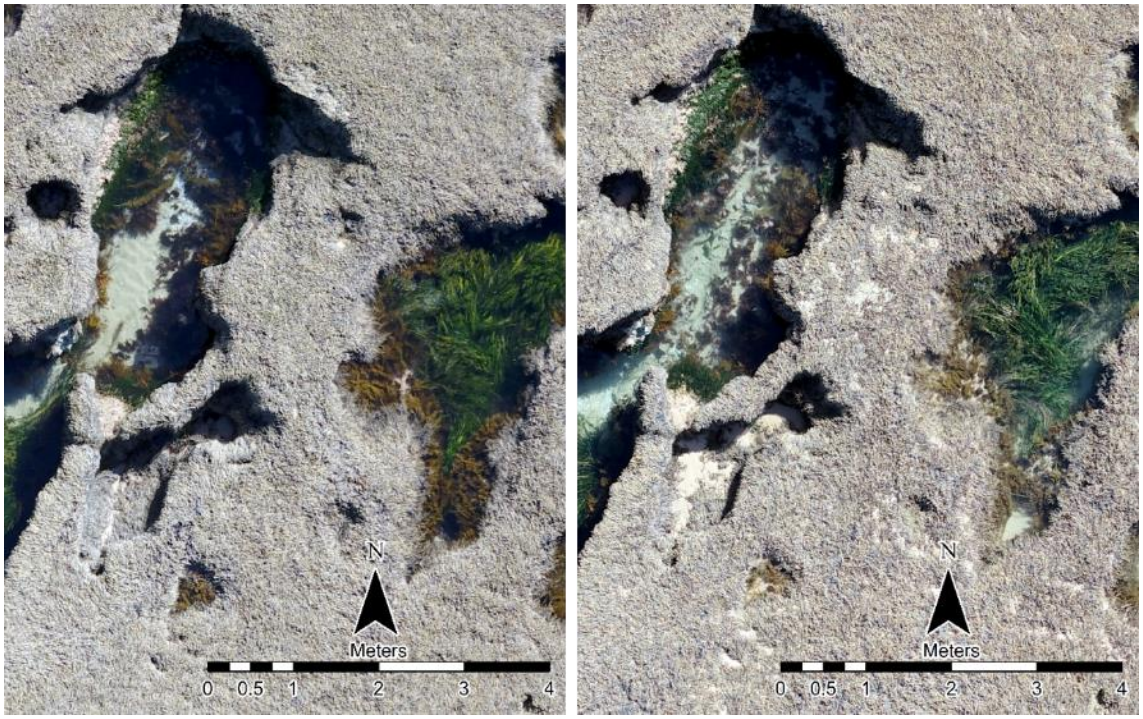

Figure 3.5: Comparison of image quality based on weather conditions and tide. Both images were captured at 20 m. The image on the left was captured on 7 April 2018. The image on the right was captured on 27 March 2019

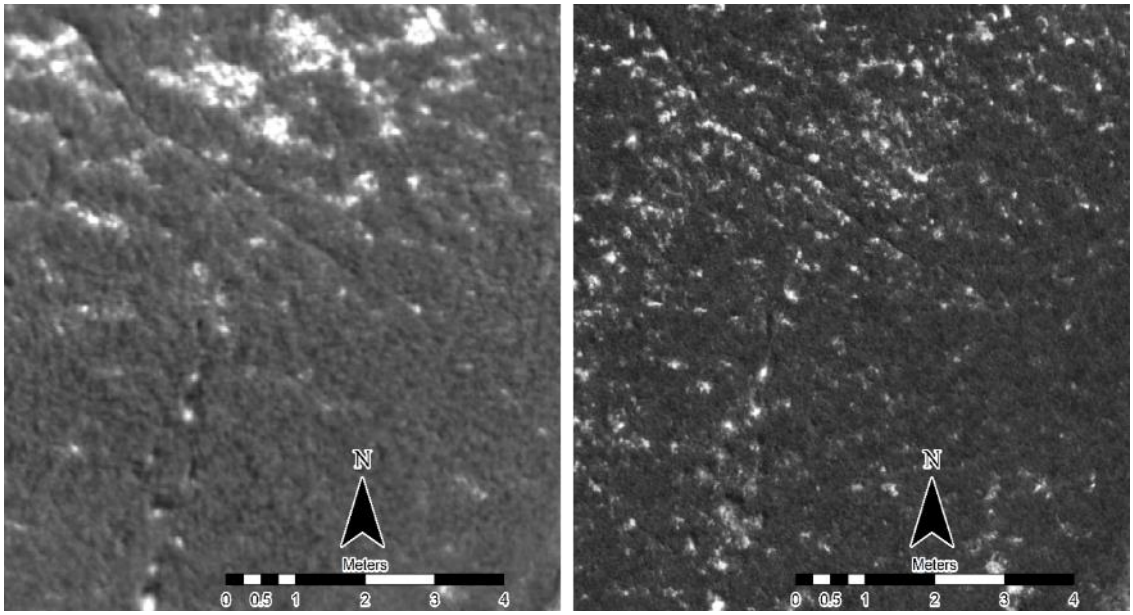

Figure 3.6: Comparison of the same section of the Point Lonsdale intertidal platform represented in the NDVI reflectance band of the Parrot Sequoia spectral camera (left) and the Micasense Red Edge M spectral camera (right). They have the same resolution but different clarity

Spatially accurate orthomosaic and spectral maps were generated for the Point Lonsdale intertidal platform (Figures 3.7 and 3.8). The coverage extent varied between the years for surrounding rocky outcrops and tidal levels, so an area of 27,706 m^2 was determined as the main Point Lonsdale intertidal platform (Table 3.1). Multispectral analysis generated calibrated reflectance indices which were used in random forest models to calculate the coverage of *H. banksii* in 2018 and 2019. The resultant *H. banksii* coverage maps are shown in Figure 3.9. The coverage classification was effective at defining extents of *H. banksii* where it appeared on reef pavement but was susceptible to misclassifying similarly shaped and coloured objects on the reef platform such as other algae and seagrasses, or areas in shadow caused by overhangs. Over-classification was also evident at habitat boundaries where areas beyond the extents of the coverage as *H. banksii* were classified. The recorded *H. banksii* coverage increased by 2.33 percentage points on the main Point Lonsdale intertidal platform between 2018 and 2019 (Table 3.1).

Table 3.1: The area of the main Point Lonsdale intertidal platform and the percentage cover of *H. banksii* recorded on 7 April 2018 and 27 March 2019

Year	*Hormosira banksii* coverage (m^2)	Total platform area (m^2)	*Hormosira banksii* percentage cover
2018	17,270.49	27,705.58	62.34%
2019	17,916.48	27,705.58	64.67%

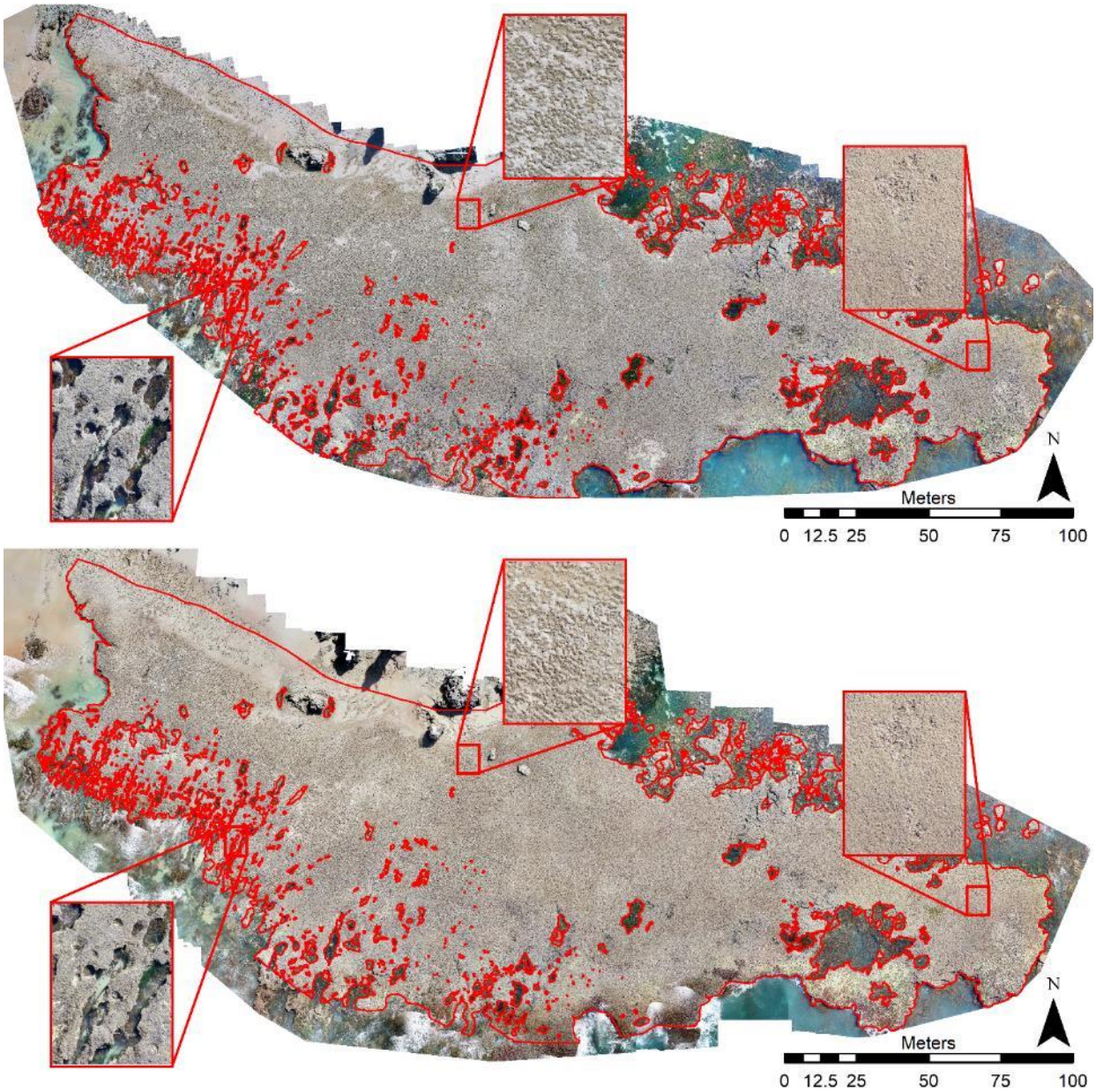

Figure 3.7: Georeferenced orthomosaic maps of the Point Lonsdale intertidal platform for 7 April 2018 (top) and 27 March 2019 (bottom)

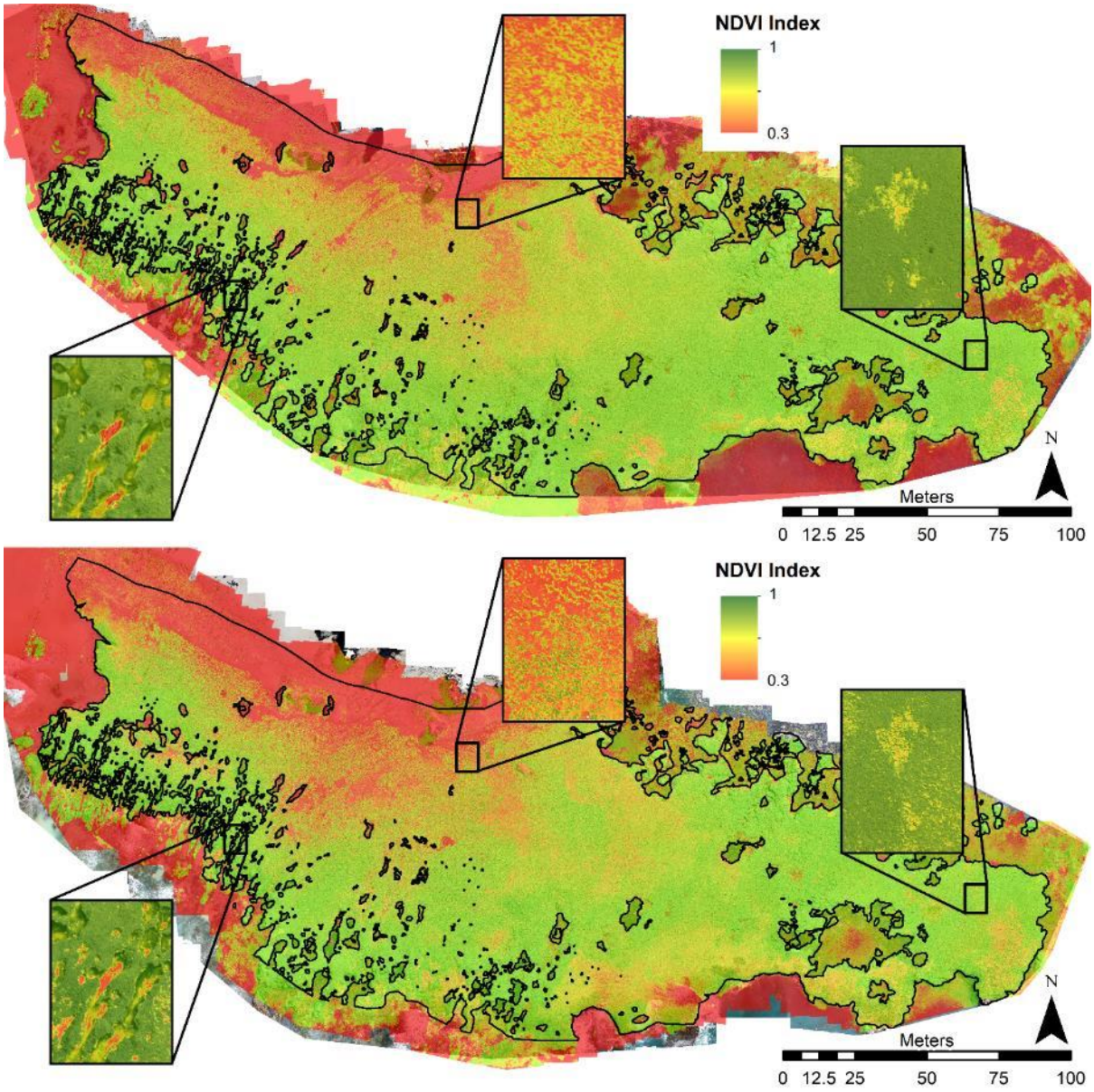

Figure 3.8: Georeferenced NDVI maps of the Point Lonsdale intertidal platform for 7 April 2018 (top) and 27 March 2019 (bottom)

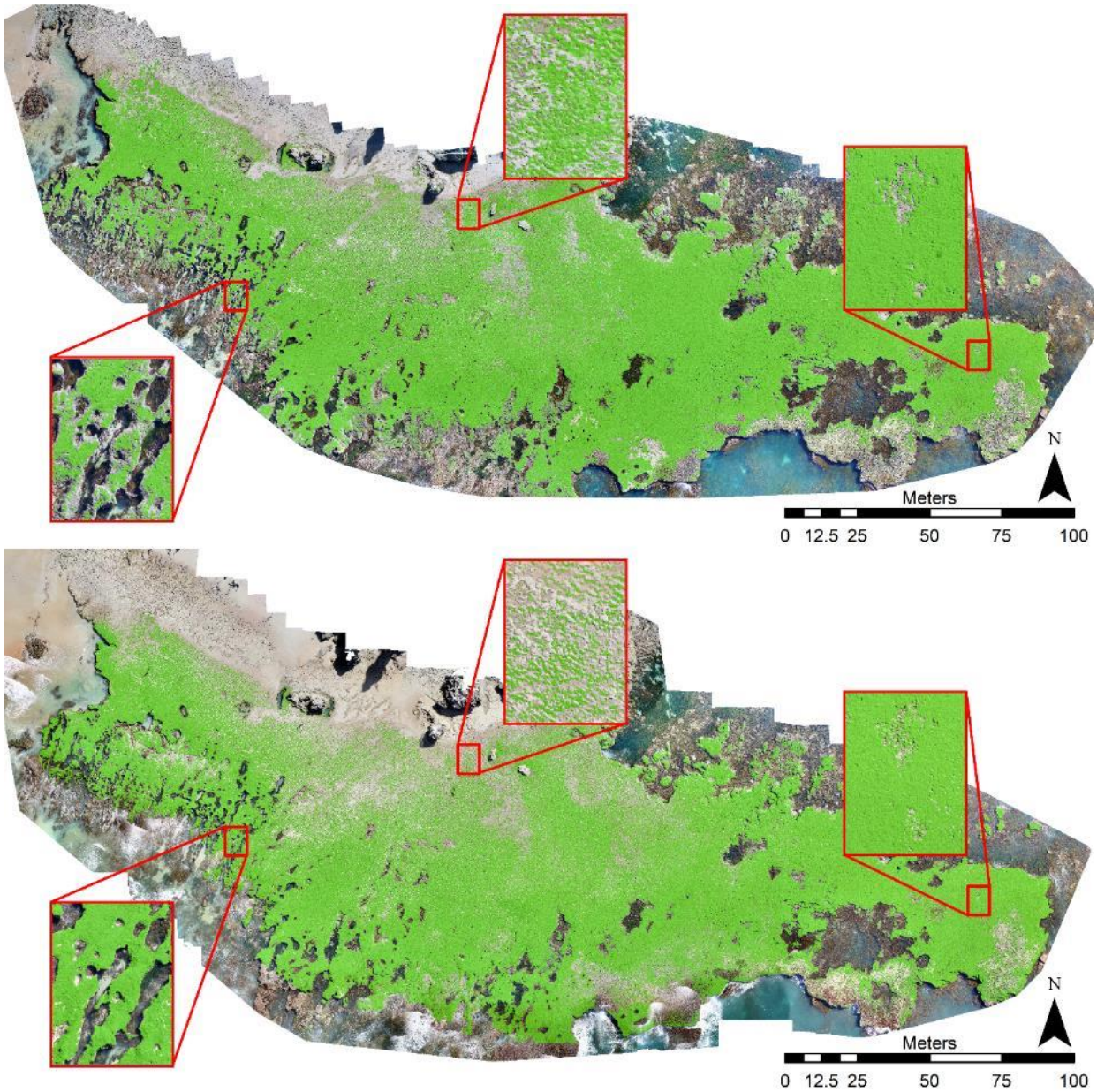

Figure 3.9: Georeferenced maps depicting the classification of *H. banksii* (green) from the random forest models for the Point Lonsdale intertidal platform for 7 April 2018 (top) and 27 March 2019 (bottom)

Figure 3.10: Comparison of an on-ground photograph (top), virtual quadrat (red outline, bottom left), and virtual quadrat with *H. banksii* coverage identification indicated in green (bottom right) for Quadrat 29

Table 3.2: Comparison of the percentage cover of *H. banksii* recorded via on-ground quadrat sampling and the same quadrats recreated virtually for real-time kinematic GPS points of the quadrat corners for the main Point Lonsdale intertidal platform recorded on 27 March 2019

Quadrat	Virtual quadrat *H. banksii* coverage (%)	On-ground *H. banksii* coverage (%)	Difference (percentage points)
Q01	47.37	69.00	21.63
Q02	99.00	100.00	1.00
Q03	100.00	100.00	0.00
Q04	96.52	88.00	8.52
Q05	99.48	71.00	28.48
Q06	75.94	96.00	20.06
Q07	97.98	92.00	5.98
Q08	97.18	96.00	1.18
Q09	99.68	92.00	7.68
Q10	69.55	0.00	69.55
Q11	98.40	100.00	1.60
Q12	15.57	29.00	13.43
Q13	100.00	98.00	2.00
Q14	46.46	69.00	22.54
Q15	0.00	0.00	0.00
Q16	68.96	84.00	15.04
Q17	99.93	100.00	0.07
Q18	77.45	90.00	12.55
Q19	11.09	16.00	4.91
Q20	100.00	100.00	0.00
Q21	85.68	96.00	10.32
Q22	96.25	98.00	1.75
Q23	99.95	100.00	0.05
Q24	100.00	100.00	0.00
Q25	55.16	47.00	8.16
Q26	32.96	67.00	34.04
Q27	66.60	80.00	13.40
Q28	76.19	80.00	3.81
Q29	84.44	82.00	2.44
Q30	93.51	96.00	2.49

Hormosira banksii coverage comparisons between the virtual quadrats and the on-ground quadrats showed some variation, with an average 10.42% (± 14.23%) difference (Table 3.2). Quadrat 10 recorded 69.55% *H. banksii* coverage in the virtual quadrat, but 0% *H. banksii* coverage in the on-ground quadrat. Photographs of the on-ground quadrats were collected during the 2019 data collection, and a comparison to the virtual quadrat found this difference to be a misclassification by the machine learning algorithm of a green alga.

The landscape pattern indices measured across the 9 patch-analysis windows (low *H. banksii* coverage (3 windows), moderate *H. banksii* coverage (3 windows) and dense *H. banksii* coverage (3 windows)) showed a general trend of higher coverage, fewer patches and lower edge density in 2018 than 2019 (Table 3.3). Much of this may be due to the lower-quality data collected by the Parrot Sequoia multispectral camera. The lower-clarity images provided by the lower-quality Parrot Sequoia multispectral camera offered less detail in the coverage maps, which resulted in fewer but larger patches being recorded (Figure 3.6).

Table 3.3: Landscape pattern indices of the 9 patch-analysis windows for the main Point Lonsdale intertidal platform recorded on 7 April 2018 and 27 March 2019

	H. banksii cover (%)		Number of patches		Maximum patch area (m^2)		Mean patch area (m^2)		Total perimeter (m)		Mean patch perimeter (m)		Edge density	
	2018	***2019***	***2018***	***2019***	***2018***	***2019***	***2018***	***2019***	***2018***	***2019***	***2018***	***2019***	***2018***	***2019***
Low cover 01	48.17	38.79	1,198	1,319	238.81	179.12	0.251 (± 6.938)	0.184 (± 4.942)	3,758.87	3,798.36	3.14 (± 73.48)	2.88 (± 56.3)	12.49	15.67
Low cover 02	30.25	21.77	1,654	1,987	48.97	9.39	0.114 (± 1.587)	0.068 (± 0.276)	4,636.38	3,249.73	2.8 (± 34.2)	1.64 (± 4.68)	24.52	23.88
Low cover 03	53.66	39.70	893	1,894	315.79	121.70	0.376 (± 10.567)	0.131 (± 3.039)	4,264.05	5,640.76	4.77 (± 121.12)	2.98 (± 55.13)	12.71	22.73
Moderate cover 01	76.90	78.33	1,238	1,242	446.25	451.68	0.388 (± 12.683)	0.394 (± 12.817)	2,287.05	4,330.86	1.85 (± 33.52)	3.49 (± 84.78)	4.76	8.85
Moderate cover 02	83.83	68.99	268	938	518.71	399.22	1.955 (± 31.685)	0.46 (± 13.035)	5,418.44	6,588.97	20.22 (± 320.06)	7.02 (± 177.51)	10.34	15.28
Moderate cover 03	61.73	50.33	1,881	2,211	341.08	251.84	0.205 (± 7.865)	0.142 (± 5.357)	7,198.88	5,428.59	3.83 (± 129.96)	2.46 (± 73.62)	18.66	17.26
Dense cover 01	94.62	94.34	34	84	590.54	588.64	17.393 (± 101.272)	7.019 (± 64.224)	909.84	1,384.27	26.76 (± 152.26)	16.48 (± 146.03)	1.54	2.35
Dense cover 02	92.47	86.24	92	74	577.44	537.75	6.282 (± 60.202)	7.284 (± 62.51)	1,762.00	2,907.72	19.15 (± 180.36)	39.29 (± 332.94)	3.05	5.39
Dense cover 03	93.57	89.00	59	126	584.37	555.11	9.913 (± 76.077)	4.415 (± 49.453)	2,243.88	3,066.65	38.03 (± 288.97)	24.34 (± 267.67)	3.84	5.51

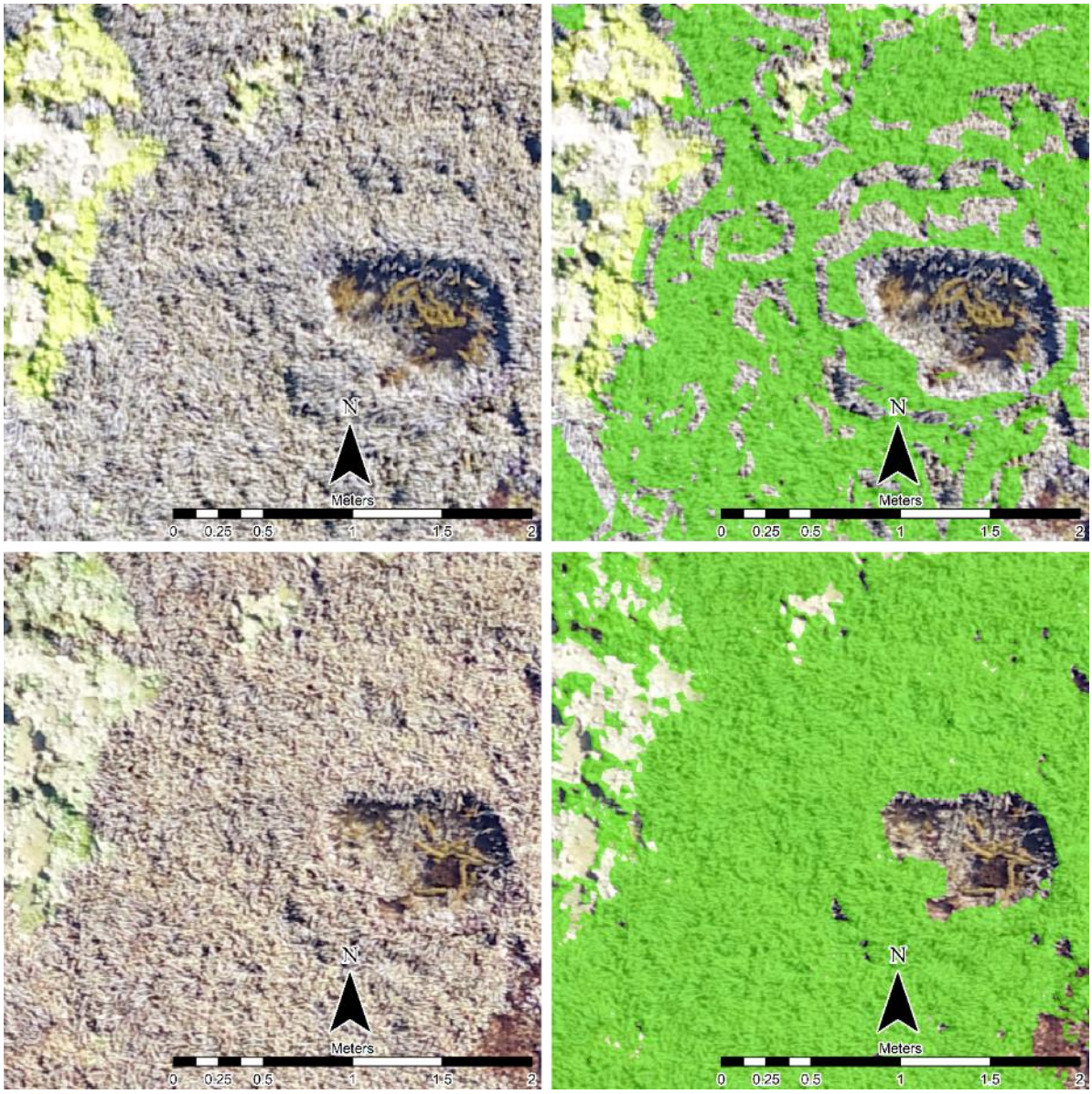

Figure 3.11: Comparison of photographs showing *H. banksii* (left) with images created from RGB imagery showing areas classified as *H. banksii* in green (right). RGB imagery was collected on 7 April 2018 (top) and 27 March 2019 (bottom). There is minor misclassification due to similar spectral and textural characteristics of other vegetation and changes in sensor characteristics

3.4 Reef Life Survey

When combined with the previous SRMP program, data from shallow subtidal reefs at Port Phillip Heads MNP now spans over 20 years. However, SRMP surveys were not restricted to a particular season and thus show seasonal variation within the dataset. This is mostly an issue for fish communities, which previous research has shown can exhibit substantial differences in diversity and abundance between seasons (particularly summer and autumn compared to winter) (Jung et al., 2010). While macroalgal communities also show seasonal changes in Port Phillip Bay, this is less pronounced than with fish (Carnell and Keough, 2016). Fortunately, RLS surveys are now all carried out in February each year.

As part of this study, 4 years of surveys (2016–19) were added to the time series, allowing time series at historical SRMP sites to be continued. Across these 4 years, a total of 1,570 observations of 85 individual species of fish, and 1,117 observations of 93 individual species of invertebrates and cryptic fish, were made. In addition to this, benthic habitat was classified for 66,475 points from a total of 2,659 photo quadrats, allowing canopy cover metrics to be extracted for comparison with previous SRMP data. Common species of fish observed across years included *Notolabrus tetricus*, Victorian Scalyfin (*Parma victoriae*), *Pictilabrus laticlavius* and unidentified herring (Spratelloides spp.) (Figure 3.12). Common species of invertebrates and cryptic fish observed across years included Orange Feather Star (*Cenolia trichoptera*), Greenlip Abalone (*Haliotis laevigata*), Blacklip Abalone (*Haliotis rubra*) and Purple Sea Urchin (*Heliocidaris erythrogramma*).

Table 3.4: Summary of Reef Life Survey sampling and observations across all years

	2016	2017	2018	2019	Total
No. of sites completed	11	12	15	18	18
Area surveyed for fish (m^2)	11,000	12,000	15,000	36,000	74,000
Area surveyed for invertebrates (m^2)	2,200	2,400	3,000	7,200	14,800
No. of photo quadrats classified for benthic habitat	460	414	548	1,237	2,659
No. of points classified for benthic habitat	11,500	10,350	13,700	30,925	66,475
No. of fish observations	275	293	386	616	1,570
No. of fish species observed	58	55	55	52	85
No. of invertebrates and cryptic fish observations	224	188	248	457	1,117
No. of invertebrate and cryptic fish species observed	60	50	57	58	93

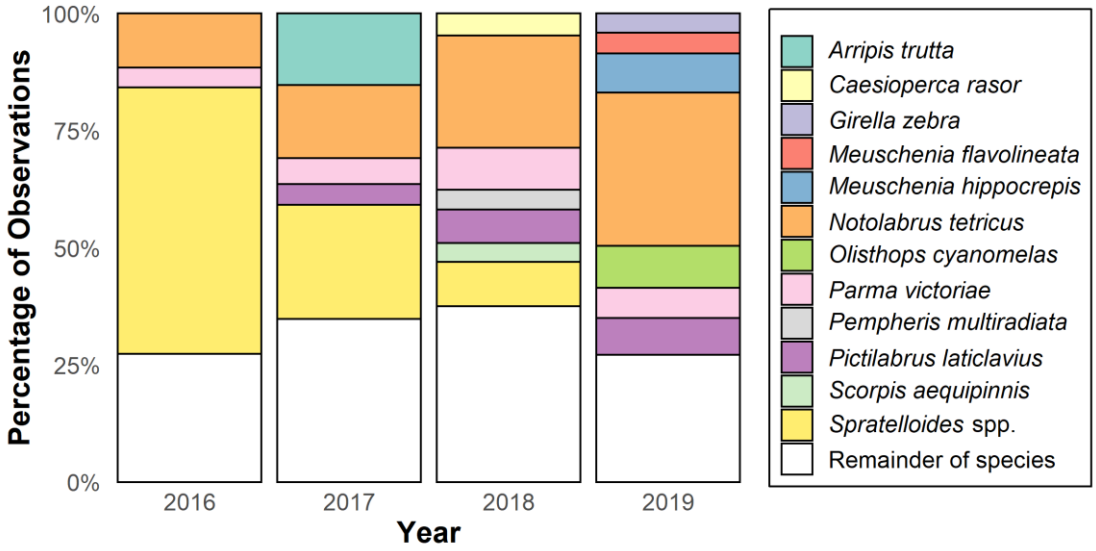

Figure 3.12: Proportions (as percentages) of the total observations of fish made in Port Phillip Heads Reef Life Surveys between 2016 and 2019. Remainder of species represents all species with a proportion of the total observations less than 4%

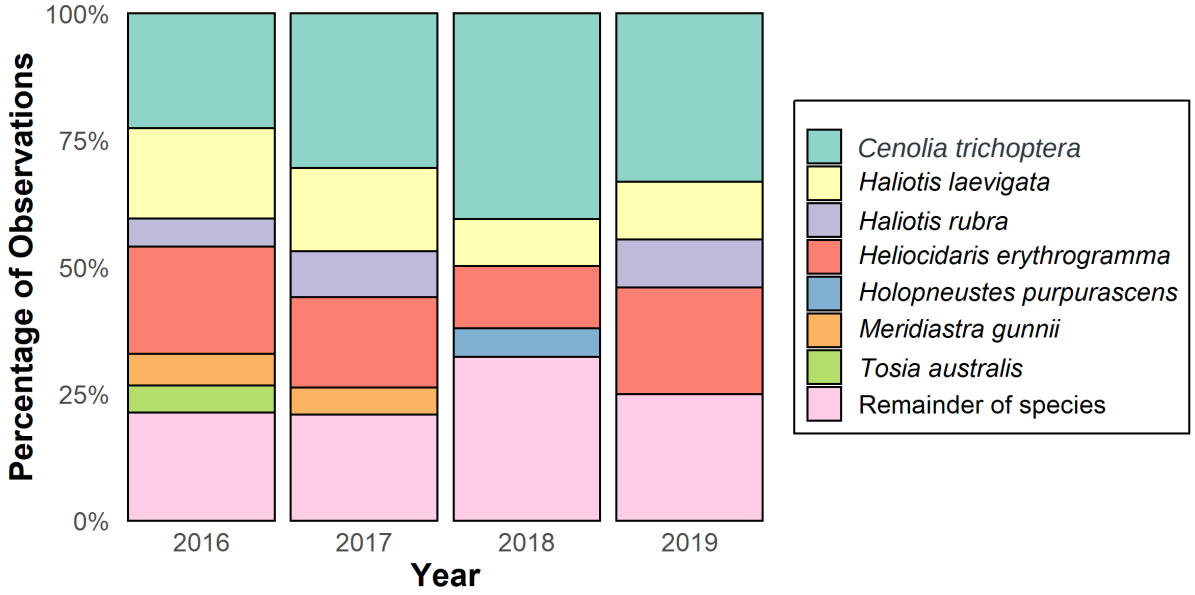

Figure 3.13: Proportions (as percentages) of the total observations of invertebrates made in Port Phillip Heads Reef Life Surveys between 2016 and 2019. Remainder of species represents all species with a proportion of the total observations less than 4%

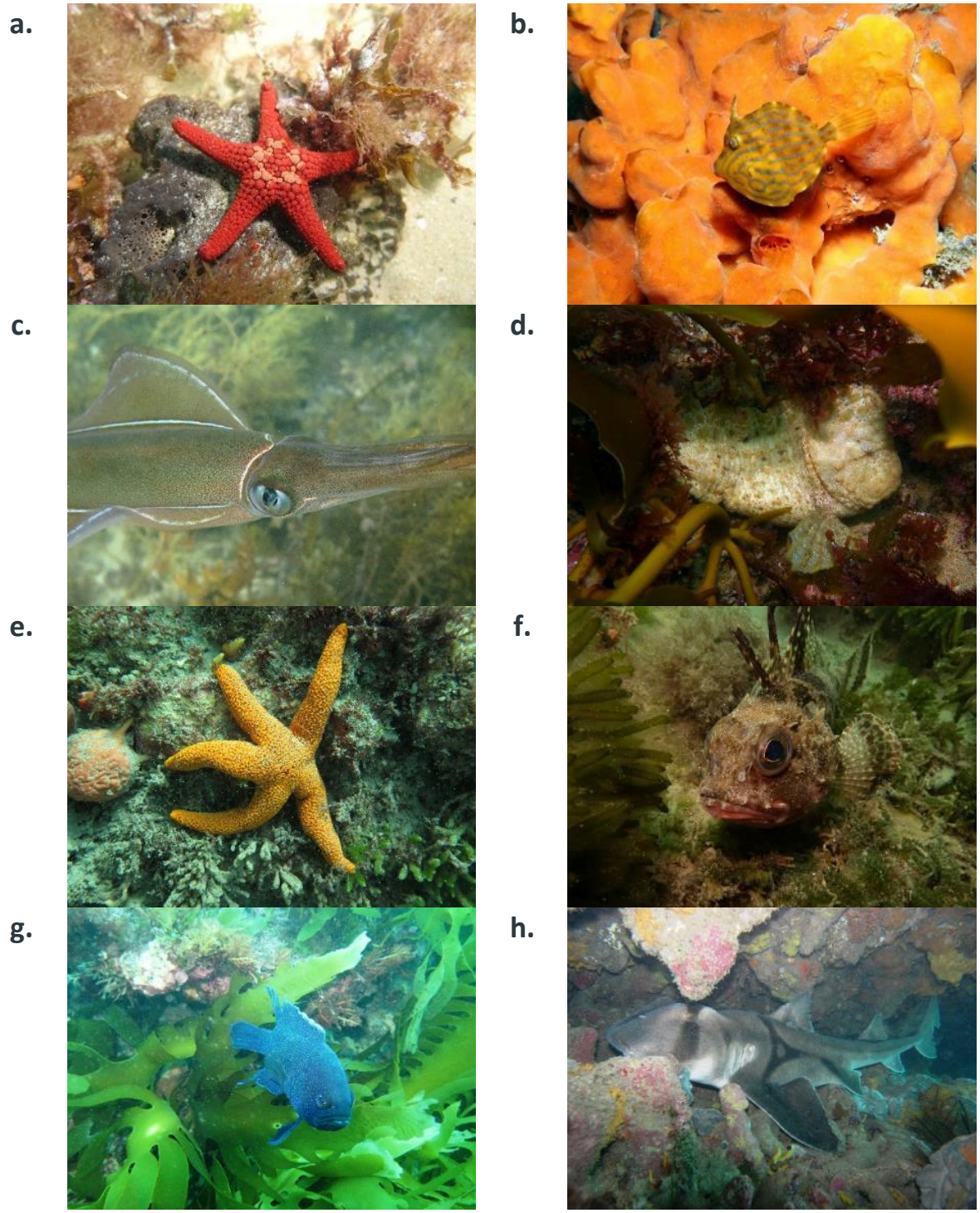

Figure 3.14: Example photos of fish and invertebrates observed in Reef Life Survey transects. These images are taken to allow for accurate identification post survey. (a) Multi-Spined Seastar (*Nectria multispina*), (b) Mosaic Leatherjacket (*Eubalichthys mosaicus*), (c) Southern Calamary (*Sepioteuthis australis*), (d) Warty Prowfish (*Aetapcus maculatus*), (e) Many-Spotted Seastar (*Fromia polypora*), (f) Common Gurnard Perch (*Neosebastes scorpaenoides*), (g) Western Blue Devil (*Paraplesiops meleagris*), (h) Port Jackson Shark (*Heterodontus portusjacksoni*)

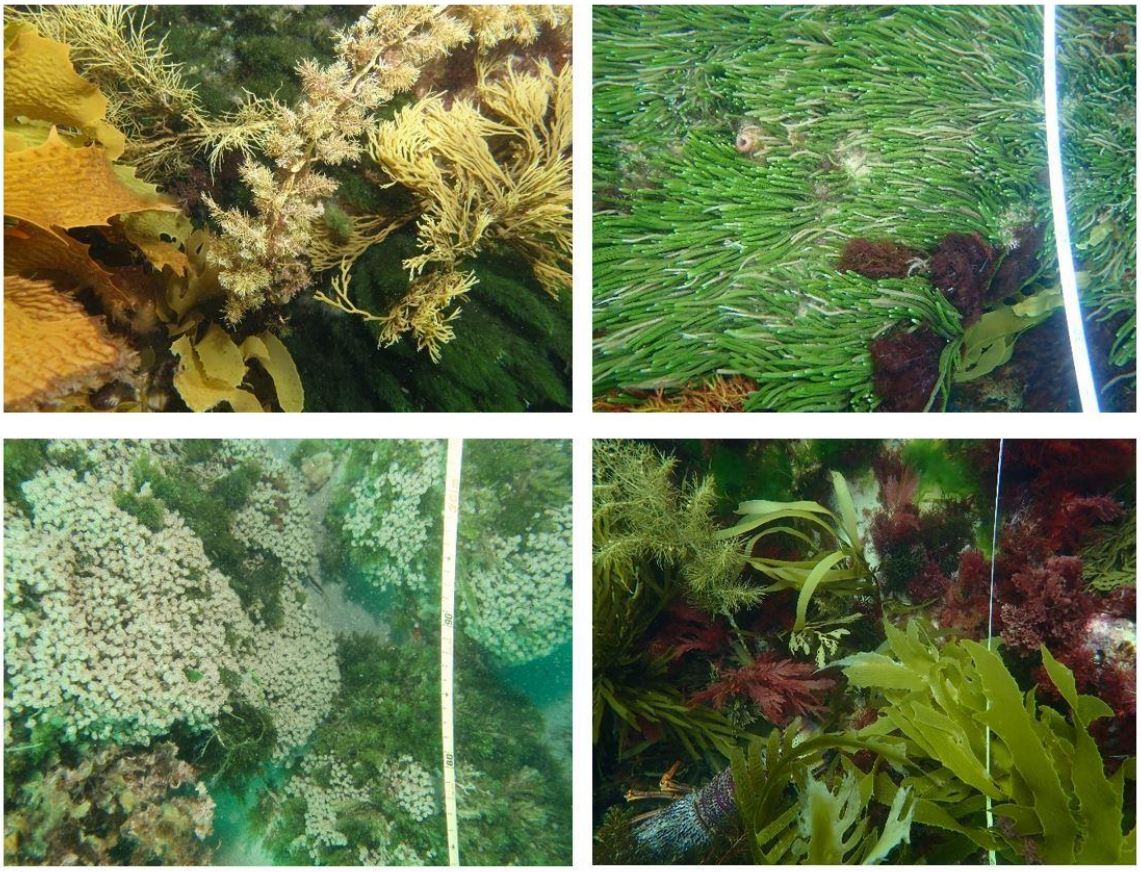

Figure 3.15: Example photo quadrats taken on Reef Life Survey transects. Photo quadrats are subsequently classified using 25 gridded points, which allows for detailed habitat classifications to be made and continuation of metrics for control charts

3.4.1 Key mobile fish species

Control charts indicate that the current status of all key mobile fish species is healthy (above the lower control limit) with all species analysed currently being within the zone of 'good' condition (Figure 3.16). While the control charts do not specifically test for the effect of the marine national park on increasing abundance relative to before declaration or reference sites, results for some species do show promising trends. In particular, *N. tetricus* and *M. hippocrepis* showed increases in the mean number present in MPA sites after declaration of the marine national park (after 2002) compared to before.

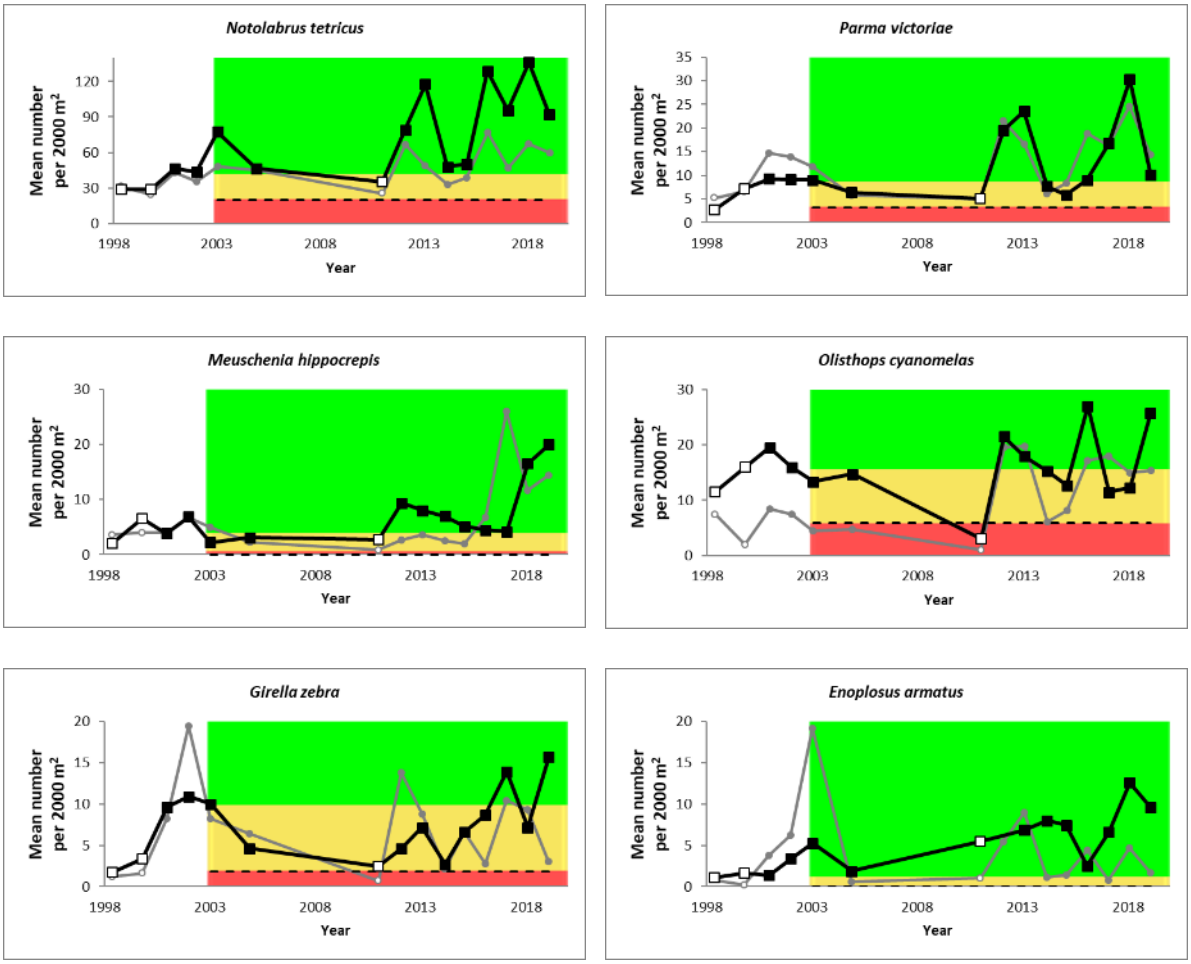

Figure 3.16: Control charts showing change in abundance of key mobile fish species within the Port Phillip Heads MNP (black line) and reference sites outside the park (grey line). Observations for these charts were sourced from SRMP and Reef Life Survey diver transects. These charts have a lower limit of acceptable change (LLAC, top of the yellow band – set as the minimum value inside the MPA from SRMP surveys from 1998 to 2002) and lower control limit (LCL, dashed line at top of red band) based on the variation from surveys, which indicate the level at which conditions are sufficiently poor that some management response is required

Average fish biomass varied markedly between seasons and over the past 20 years of surveys (Figure 3.17). Herring Cale (*Olisthops cyanomelas*) has been mostly below its lower control limit since 2003, the exception being 2014–16 after which it declined back below its lower control limit in the surveys between 2017 and 2019. The Victorian Scalyfin (*Parma victoriae*) and the Zebra Fish (*Girella zebra*) are both currently below their lower limit of acceptable change and should be closely monitored in future surveys. The Blue-Throat Wrasse (*Notolabrus tetricus*), Horseshoe Leatherjacket (*Meuschenia hippocrepis*) and the Old Wife (*Enoplosus armatus*), while variable over time, are currently well above their lower limit of acceptable change.

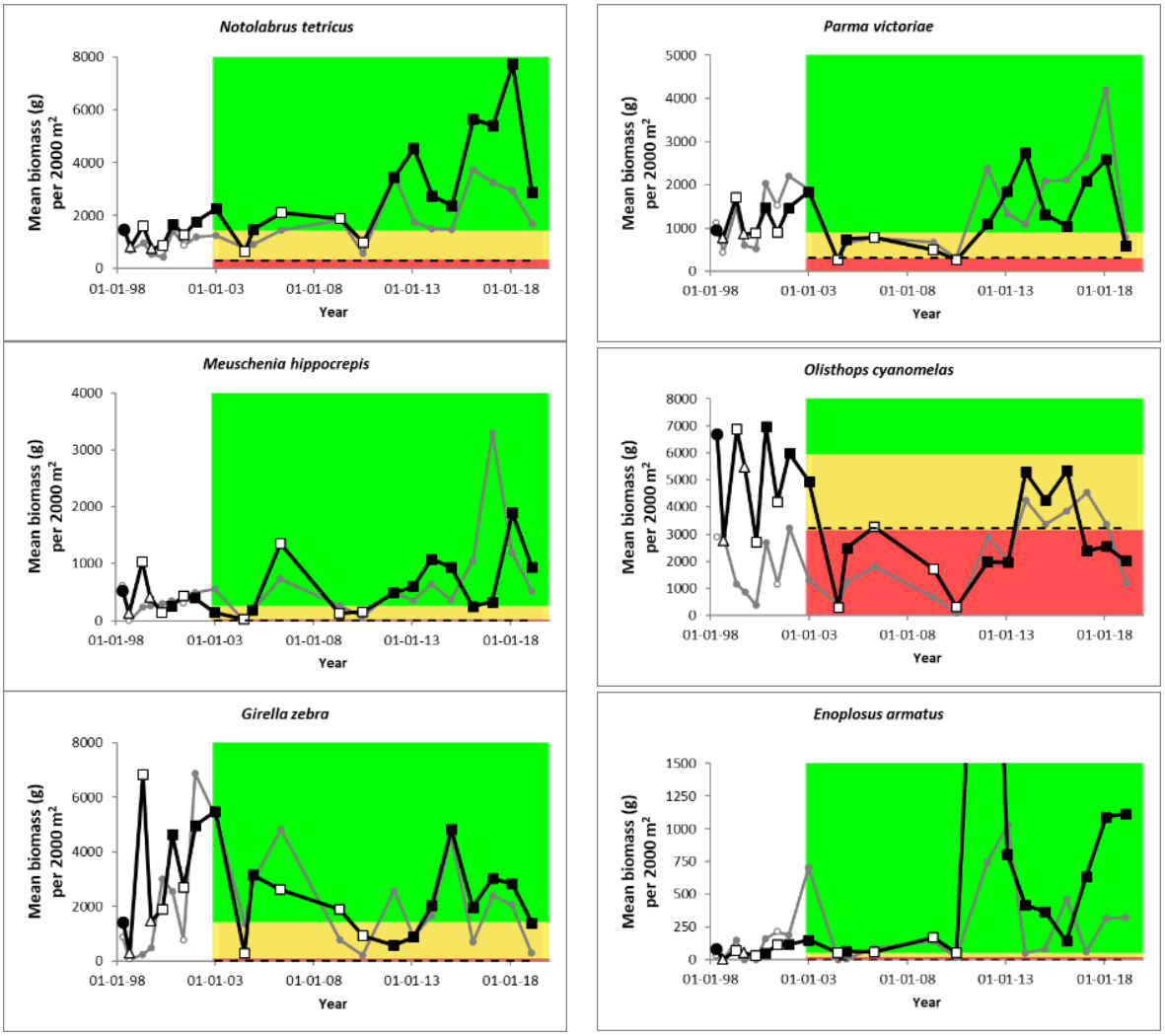

Figure 3.17: Control charts showing change in biomass of key mobile fish species within the Port Phillip Heads MNP (black line) and reference sites outside the park (grey line). Observations for these charts were sourced from SRMP and Reef Life Survey diver transects. These charts have a lower limit of acceptable change (LLAC, top of the yellow band – set as the minimum value inside the MPA from SRMP surveys from 1998 to 2002) and lower control limit (LCL, dashed line at top of red band) based on the variation from surveys, which indicate the level at which conditions are sufficiently poor that some management response is required

Across the Port Phillip Heads region, species richness (averaged across the 2016–19 surveys) was found to be highest at Popes Eye and South Channel Fort, where an average of 18.4 and 15.8 species of fish, respectively, were observed in any given survey. The sites with the next highest species richness were Kelp Beds and Kelp Beds Drift, both averaging 13 species of fish. These trends were mirrored when the Shannon–Wiener diversity index was calculated for each site: Popes Eye, South Channel Fort, Kelp Beds and Kelp Beds Drift had the highest mean diversity of all sites (2.4, 1.9, 2.1 and 2.1, respectively). Highest total abundance was observed at the Point Nepean Inner West site, for which an average of 366.2 individual fish were observed. A neighbouring site, Nepean Inner East, also showed a high mean total

abundance of 173.8 individuals. Other sites with high abundances included Popes Eye and South Channel Fort with means abundances of 237.8 and 214.6 individuals, respectively.

Spatial trends of key species varied largely across the Port Phillip Heads MNP. *Notolabrus tetricus, Meuschenia hippocrepis* and *Olisthops cyanomelas* were observed consistently across the entire survey area and exhibited little variation between sites inside and outside the heads or between Point Nepean and Point Lonsdale. *N. tetricus* was also present in high abundances at Popes Eye and South Channel Fort, with average abundances of 23.6 and 15.6 individuals respectively. *M. hippocrepis* and *O. cyanomelas*, however, showed large variation in mean abundance between Popes Eye (average of 11.4 and 8.6 individuals per survey, respectively) and its SRMP reference site South Channel Fort (average of 2.1 and 0 individuals per survey, respectively). Popes Eye contained the highest average abundance of *Enoplosus armatus* by far, with an average of 14.9 individuals being observed in each survey. This compared to Nepean Inner East which contained the second-highest average abundance of 7.6 individuals per survey. *Parma victoriae* was also observed in highest abundances at Popes Eye (23.1 individuals) and South Channel Fort (19.5 individuals). After this, the next highest average abundance (10.7 individuals) was observed at Kelp Beds Drift. Highest average abundance of *Girella zebra* was found at sites inside Port Phillip Heads, the highest abundances averaging 6.9 individual per survey at Lonsdale Kelp Inner and Lonsdale Kelp Outer. In light of this, average abundances of *G. zebra* were low at Portsea Hole and South Channel Fort with an average of 0.1 individual per survey being found at both sites. A rarer species, the Western Blue Groper (*Achoerodus gouldii*), was widespread across Port Phillip Heads, being found at the furthest west site (Lonsdale Back Beach) and the furthest east site (South Channel Fort). Sightings, however, were not consistent; its highest average abundance was 0.2 individuals per survey.

3.4.2 Key macroinvertebrates

The current (2019) status of Greenlip Abalone (*Haliotis laevigata*) and Orange Feather Star (*Cenolia trichoptera*) is that they are in good condition (well above the lower limit of acceptable change) (Figure 3.18). However, consistent declines over the last 13 years were observed in Blacklip Abalone (*Haliotis rubra*) and Southern Biscuit Star (*Tosia australis*). *H. rubra* has been below its lower control limit of 14 individuals per 200 square metres since 2015; from 2009 to 2014, the average abundance inside the MPA reduced from 58 ± 15 to 19 ± 8. A similar trend was also seen for *Tosia australis*, whose highest abundance of 10 ± 5 per 200 square metres occurred in 2006. Since then, it has declined to be near or below its lower limit of acceptable change of 0.5 individuals per 200 square metres.

In contrast *Haliotis laevigata* has shown an increase in abundance since the marine national park was declared and also in the reference areas since protection. As a result, *H. laevigata* is currently classed as being in good abundance. With *H. laevigata* outside the park protected, increases in abundance were observed from 2010 in reference locations. *Cenolia*

trichoptera has maintained a stable abundance between 1998 and 2015 and shown a recent increase in numbers between 2016 and 2019. Despite approaching the lower limit of acceptable change in 2016, the 2019 mean abundances of *C. trichoptera* returned to within acceptable levels.

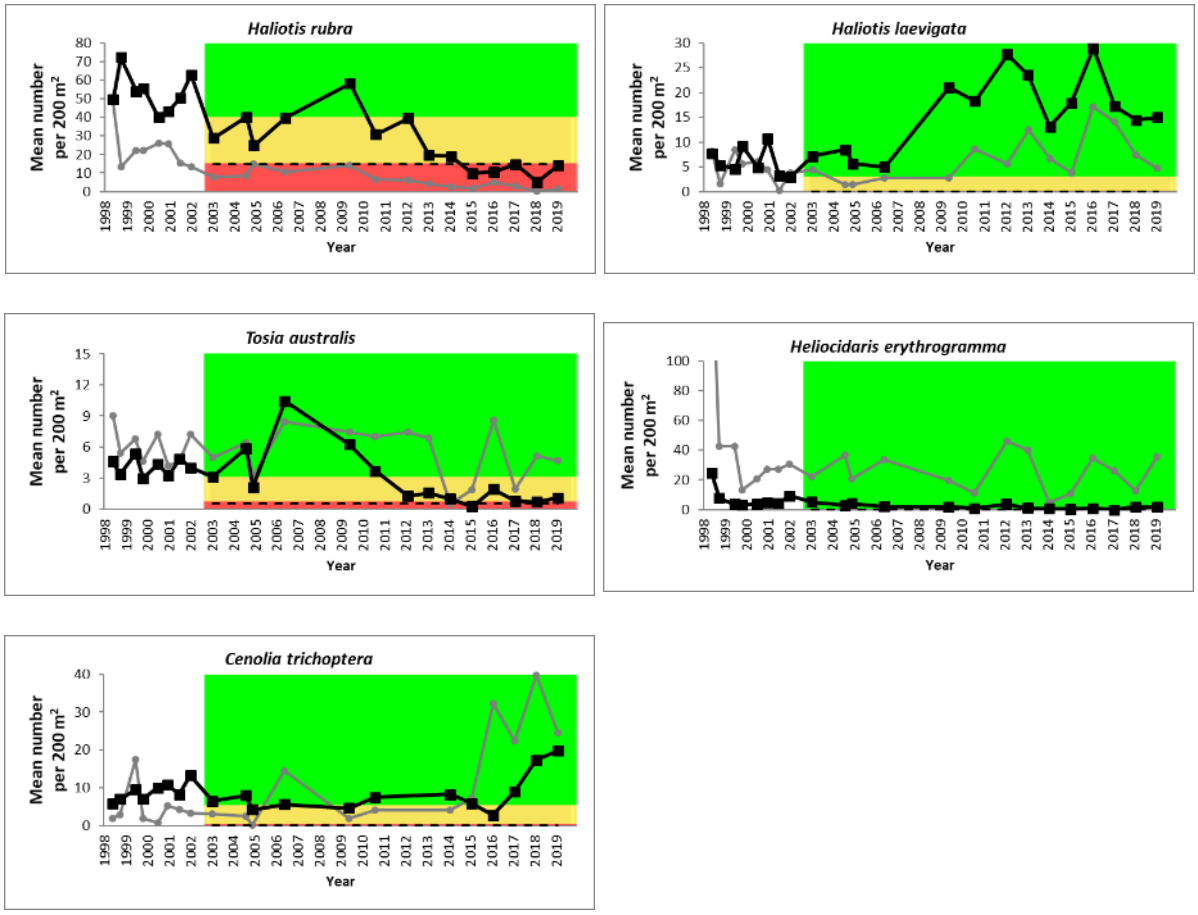

Figure 3.18: Control charts showing change in abundance of key motile macroinvertebrate species within the Port Phillip Heads MNP (black line) and reference sites outside the park (grey line). Observations for these charts were sourced from SRMP and Reef Life Survey diver transects. These charts have a lower limit of acceptable change (LLAC, top of the yellow band – set as the minimum value inside the MPA from SRMP surveys from 1998 to 2002) and lower control limit (LCL, dashed line at top of red band) based on the variation from surveys, which indicates the level when conditions are sufficiently poor that some management response is required

Across the entire Port Phillip Heads MNP, abundances of the Purple Sea Urchin (*Heliocidaris erythrogramma*) have been low since 1998. Here, the management thresholds have been set as upper control limits (UCL) rather than a lower control limit. This is due to the ability of *H. erythrogramma* in high abundance to have an impact on macroalgal canopy cover (Carnell and Keough, 2016). However, isolated sites both within the marine national park

(Lonsdale Point and Merlan Outer) and at the references sites (in particular Shortland Bluff and Point Franklin) have had higher abundances of *H. erythrogramma*. Given the abundance and impact of this species in other parts of Port Phillip Bay (Carnell and Keough, 2019), this is an important species to continue to monitor.

Unlike community metrics for fish species, mean species richness, mean total abundance and mean Shannon–Wiener diversity index of macroinvertebrates and cryptic fish were evenly spread across Port Phillip Heads. The sites with the highest species richness included Kelp Beds Drift and Point Franklin, both with an average of 9 species per survey. Lowest average species richness was observed at Lonsdale Back Beach, Lonsdale Point South-West, Kelp Beds, Point Nepean Offshore, Merlin Inner and Lonsdale Kelp Outer, all of which had an average of less than 6 species observed. Popes Eye and Kelp Beds had considerably low average Shannon–Wiener diversity indices, while all other sites had indices between 1.1 and 1.6. Popes Eye and Point Franklin had the highest mean total abundance of all groups, averaging 110.9 and 98 organisms per survey, respectively. Lonsdale Point South-West, Lonsdale Kelp Outer, Point Nepean Offshore and Lonsdale Back Beach all showed low total abundance, with an average of less than 20 organisms being found per survey.

The highest abundances of *Haliotis rubra* (up to an average of 14.7 per survey) were found inside the Port Phillip Heads MNP, on both the Point Lonsdale and Point Nepean sides. Conversely, the highest abundances of *Haliotis laevigata* were found at Victory Shoal and Shortland Bluff, where averages of 40.7 and 18.2 individuals per survey were found, respectively; these abundances were considerably higher than those of *H. rubra*. The next highest site abundance for *H. laevigata*, however, was 7.2 individuals at Lonsdale Kelp Inner. By far, the highest abundance of *Tosia australis* was at Point Franklin, where an average of 8.8 individuals per survey was found. The next highest site for *T. australis* was Shortland Bluff, where an abundance of 3.3 was found. The highest abundances of *Cenolia trichoptera* were found at Popes Eye with an average of 88.7 individuals per survey. Following this, Kelp Beds, Kelp Beds Drift and Lonsdale Surf Club had average abundances of 39.5, 33.3 and 28.25 respectively. All other sites had abundances below 15.

The invasive Northern Pacific Seastar (*Asterias amurensis*) was observed twice in surveys in 2018 at the South Channel Fort site. South Channel Fort is the reference site for Popes Eye and located approximately 7.5 km east of the nearest section of the Port Phillip Heads MNP (Portsea Hole) (−38.3069, 144.8010; SRMP Site Code: 2804).

3.4.3 Macroalgal beds

An average of 23 habitat classes per survey was observed across all SRMP survey sites between 2016 and 2019. While richness was evenly spread across the region, 2 sites scored considerably lower than the others. Kelp Beds and Merlan Outer both had low average richness (14.3 and 12.2 habitat classes, respectively) compared with all other sites, which averaged between 19.8 and 31.1 habitat classes per survey. Kelp Beds was heavily

dominated by Golden Kelp (*Ecklonia radiata*) (average cover of 80.23% across all surveys) and Merlan Outer was dominated by Crayweed (*Phyllospora comosa*) (average cover of 59.7% across all surveys). Kelp Beds had by far the highest average cover of *E. radiata* across all surveys (80.23%); it was followed by Popes Eye (48.82%). All other sites averaged less than 29% cover of *E. radiata*. The highest average cover of *P. comosa* was observed at Merlan Outer, Lonsdale Point and Lonsdale Kelp Inner, where average covers were 59.7%, 52.8% and 48.8%, respectively. In comparison, the other canopy-forming brown algae (a group that combines *Sargassum* spp., *Cystophora* spp., *Acrocarpia paniculata* and *Seirococcus axillaris*), made up a highest cover of 34.1% at Point Nepean Inner West. The seagrass Sea Nymph (*Amphibolis antarctica*) accounted for the highest percentage cover at Point Nepean Offshore (32.6%), Point Nepean Inner West (23.9%) and Shortland Bluff (19.6%). The highest densities of all green seaweed *Caulerpa* spp. were found at South Channel Fort (14.2%), Lonsdale Point South-West (7.4%), Lonsdale Back Beach (6.8%) and Popes Eye (4.8%). Also of note, while not in high quantities, Southern Bull Kelp (*Durvillaea potatorum*) was observed at Lonsdale Point where it made up 5.6% of the cover in the 2019 surveys.

The most notable change in the subtidal reef macroalgal communities of the Port Phillip Heads MNP has been the decline of the Golden Kelp (*Ecklonia radiata*, hereafter *Ecklonia*) from a high of 29% cover in 2002 down to 6% cover in 2016 and 2017 (Figure 3.19). In the most recent surveys (2018 and 2019) *Ecklonia* cover has recovered to 14% and 19% respectively, to be above the limit of acceptable change. Similarly, *Phyllospora comosa* has seen a gradual decline in cover since 2009, from 38% down to 16% in 2017. However, the 2018 and 2019 surveys recorded a recovery back up to 27% cover. Thallose red algae has also seen a decline, from a high of 23% cover in 2010 to an all-time low of 6% in 2016. While there has been some recovery in recent surveys, it currently sits right on the LAC of 10%.

In comparison, the other canopy-forming brown algae saw an increase in cover between 2015 and 2018 but a decline in the 2019 survey. This recent decline is likely due to the increase in cover of *Ecklonia* and *P. comosa*, which may obscure the other canopy-forming species. Cover of *Amphibolis antarctica* has slowly declined from a high of 12% cover in 2003 to a low of 4% in 2019. However, before the declaration of the marine park, cover was as low as 1% in the autumn of 1998, which makes both the LCL and LLAC lower than that figure.

The invasive Japanese Kelp (*Undaria pinnatifida*) was observed in 2 benthic photo quadrats at the Merlin Inner (PPH-S7) site in the 2019 surveys. Merlin Inner is a site approximately 400 m east of the township of Point Lonsdale (−38.2873, 144.6200; SRMP Site Code: 2807), within the marine national park. There were no observations of *U. pinnatifida* in photo quadrats from all other years (2016, 2017 and 2018). The species was also observed off diver transects at Portsea Hole and in towed video.

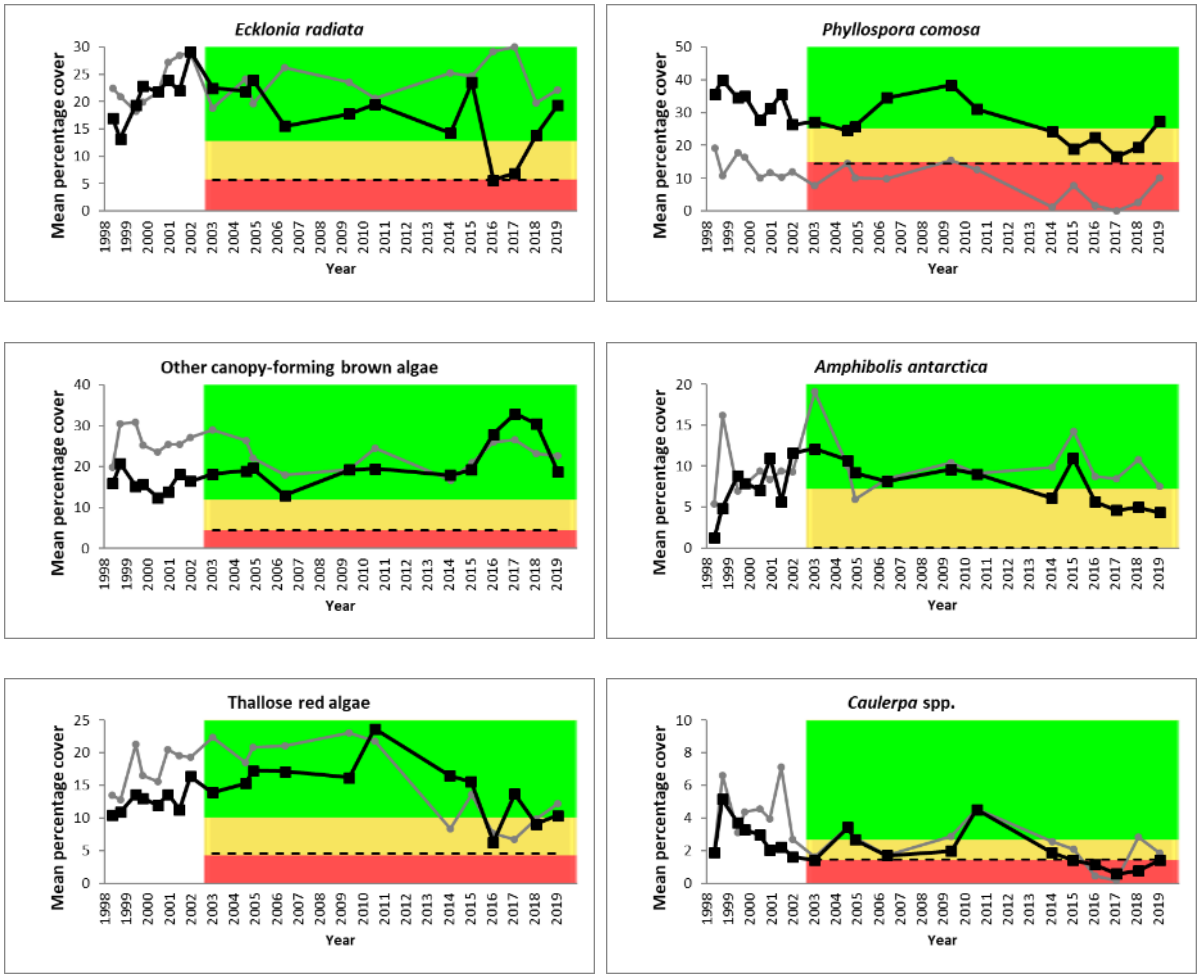

Figure 3.19: Control charts showing change in percentage cover of algal species within the Port Phillip Heads MNP (black line) and reference sites (grey line). Observations for these charts were sourced from Reef Life Survey diver photo quadrats from 2016. These charts have a lower control limit (set as the minimum value inside the MPA from SRMP surveys in 2003, 2005 and 2006) indicating the level when conditions are sufficiently poor that some management response is required. However, for *Amphibolis antarctica* and *Caulerpa* spp., the LCL was set as the average in the period 1998–2002, to ensure an LLAC above zero. 'Other canopy-forming brown algae' is a combination of *Sargassum* spp., *Cystophora* spp., *Acrocarpia paniculata* and *Seirococcus axillaris*.

3.5 Baited remote underwater video stations

A total of 2,714 observations of 71 taxa belonging to 40 families were recorded in this study (Table 3.5). Depths of sample sites ranged from 0 to 27 m (Figure 2.6). Of a total of 110 BRUVS deployments, 92 were deemed successful (Figure 3.20). Most failures were due to flipping in tidal flow. The most abundant families observed were Labridae (35.3%) and Monacanthidae (17.7%) (

Figure 3.21). The most abundant species in this study were *Notolabrus tetricus* (28.4%), *Meuschenia freycineti* (7.0%), *Girella zebra* (5.4%), *Meuschenia hippocrepis* (5.2%), *Chrysophrys auratus* (4.9%), *Pictilabrus laticlavius* (4.9%) and *Trygonorrhina dumerilii* (4.6%)

Figure 3.21). Biomass estimates at this site were largely dominated by shark and ray species, for which *Bathytoshia brevicaudata* (57.7%), *Myliobatis tenuicaudatus* (16.3%), *Trygonorrhina dumerilii* (8.2%) and *Heterodontus portusjacksoni* (2.7%) made up a combined 84.9% of the total biomass observed (Figure 3.22).

Table 3.5: Summary of successful baited remote underwater video stations (BRUVS) observations across both years

	2018	2019	Total
Total no. of individuals	1,070	1,644	2,714
Total no. of taxa	55	65	71
Total no. of deployments	54	56	110
Total no. of successful deployments	44	48	92
No. of successful deployments inside MPA	30	30	60
No. of successful deployments outside MPA	14	18	32

Figure 3.20: Screen grabs from high-definition BRUVS video exhibiting the diversity of habitat and species that can be sampled by this method

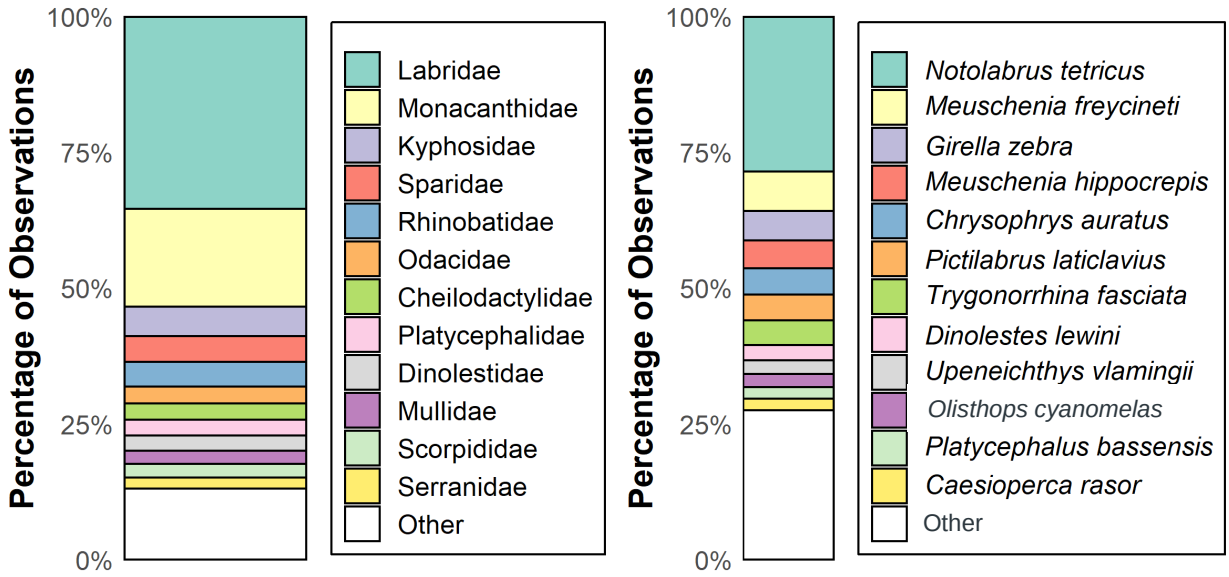

Figure 3.21: Proportions (as percentages) of abundance across the complete fish assemblage (across both years of BRUVS sampling) based on family (left) and species (right). Other represents families or species with total observation of less than 2%

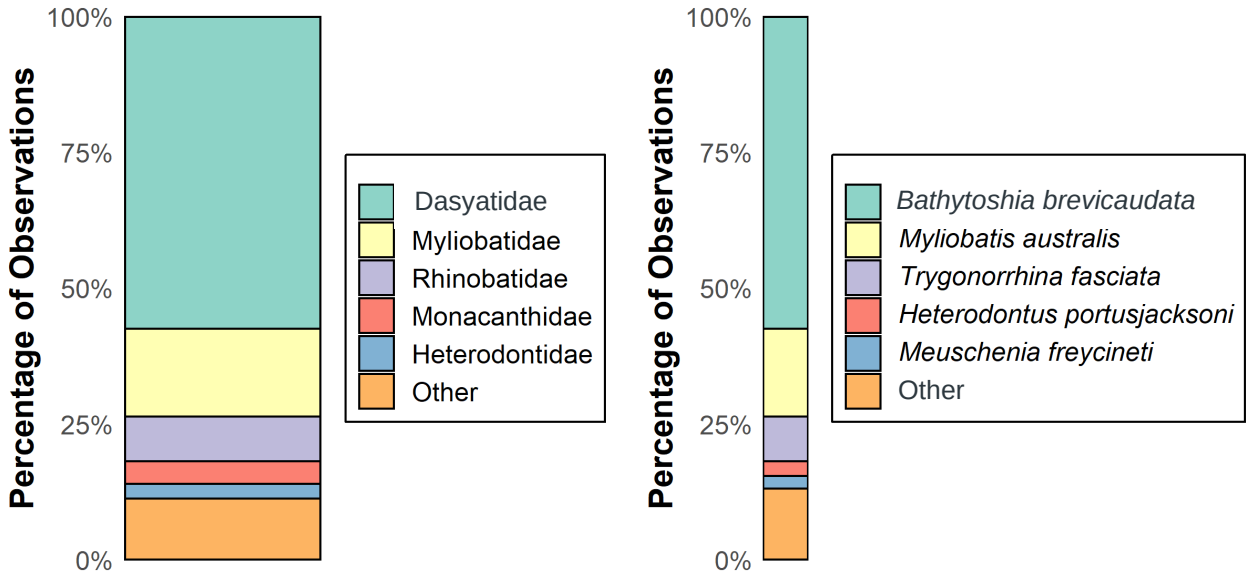

Figure 3.22: Proportions (as percentages) of biomass across the complete fish assemblage (across both years of BRUVS sampling) based on family (left) and species (right). Other represents families or species with total observation of less than 2%

Table 3.6: Proportions (as percentages) of the total abundance of fish observed in BRUVS surveys across sampling years and protection status (inside and outside the marine national park). Note: This is not a complete species list. This list only contains top contributors (greater than 1% of total)

Species	2018 inside	2018 outside	2019 inside	2019 outside	Combined inside	Combined outside
Notolabrus tetricus	36.90	28.88	25.42	20.05	30.48	23.12
Meuschenia freycineti	9.82	5.60	6.85	4.38	8.16	4.80
Pictilabrus laticlavius	3.90	6.47	3.87	7.83	3.89	7.36
Chrysophrys auratus	0.50	3.02	5.56	11.98	3.33	8.86
Meuschenia hippocrepis	4.66	8.19	5.76	3.00	5.27	4.80
Trygonorrhina dumerilii	5.29	4.31	3.18	6.45	4.11	5.71
Girella zebra	6.30	1.72	6.45	3.23	6.39	2.70
Olisthops cyanomelas	2.39	3.02	1.99	3.23	2.17	3.15
Platycephalus bassensis	2.14	3.88	1.19	3.46	1.61	3.60
Upeneichthys vlamingii	3.40	3.02	1.99	1.84	2.61	2.25
Scobinichthys granulatus	1.51	5.17	0.50	1.38	0.94	2.70
Meuschenia flavolineata	2.14	2.16	1.89	1.61	2.00	1.80
Bathytoshia brevicaudata	1.39	3.02	1.49	1.84	1.44	2.25
Heterodontus portusjacksoni	1.13	2.16	1.09	3.00	1.11	2.70
Pseudogoniistius nigripes	1.76	1.72	1.59	2.07	1.67	1.95
Parma victoriae	1.39	2.16	1.89	1.38	1.67	1.65
Scorpis aequipinnis	0.50	0.43	3.57	0.69	2.22	0.60
Enoplosus armatus	1.01	1.29	1.29	1.61	1.17	1.50
Contusus brevicaudus	0.25	1.29	0.89	2.30	0.61	1.95
Acanthaluteres vittiger	2.02	0.43	0.50	1.84	1.17	1.35
Dactylophora nigricans	1.13	0.86	1.59	1.15	1.39	1.05
Meuschenia galii	0.50	1.29	0.70	0.92	0.61	1.05

Table 3.7: Proportions (as percentages) of the total biomass of fish observed in BRUVS surveys across sampling years and protection status. Note: This is not a complete species list. This list only contains top contributors (greater than 1% of total)

Species	2018 inside	2018 outside	2019 inside	2019 outside	Combined inside	Combined outside
Bathytoshia brevicaudata	60.73	74.90	41.11	64.84	50.13	69.19
Myliobatis tenuicaudatus	7.55	6.93	31.56	11.23	20.52	9.37
Trygonorrhina dumerilii	8.98	4.82	7.14	11.37	7.98	8.54
Heterodontus portusjacksoni	3.39	2.94	1.87	2.89	2.57	2.91
Meuschenia freycineti	3.56	1.47	2.45	1.38	2.96	1.42
Girella zebra	1.60	0.47	1.37	0.73	1.48	0.61
Dactylophora nigricans	1.51	0.38	1.27	0.56	1.38	0.48
Olisthops cyanomelas	0.79	0.38	0.70	0.90	0.74	0.67
Meuschenia hippocrepis	0.97	0.55	0.61	0.48	0.77	0.51
Neosebastes scorpaenoides	0.87	0.45	0.50	0.72	0.67	0.61
Pseudogoniistius nigripes	0.84	0.40	0.60	0.60	0.71	0.51
Notolabrus tetricus	1.03	0.34	0.58	0.44	0.79	0.40
Chrysophrys auratus	0.13	0.53	0.57	0.67	0.37	0.61
Meuschenia flavolineata	0.61	0.29	0.51	0.36	0.55	0.33
Pictilabrus laticlavius	0.33	0.26	0.29	0.27	0.31	0.26
Scobinichthys granulatus	0.33	0.39	0.13	0.24	0.22	0.31
Meuschenia galii	0.24	0.21	0.27	0.34	0.25	0.28
Parma victoriae	0.28	0.20	0.39	0.18	0.34	0.19
Platycephalus bassensis	0.29	0.22	0.20	0.23	0.24	0.22
Contusus brevicaudus	0.05	0.10	0.17	0.24	0.11	0.18
Upeneichthys vlamingii	0.18	0.06	0.16	0.12	0.17	0.09
Scorpis aequipinnis	0.05	0.04	0.18	0.20	0.12	0.13
Acanthaluteres vittiger	0.16	0.06	0.07	0.07	0.11	0.06
Enoplosus armatus	0.04	0.02	0.08	0.09	0.07	0.06
Diodon nicthemerus	0.04	0.03	0.09	0.08	0.06	0.06

3.5.1 Species distribution models

Model performance varied to a large degree across community metrics and individual species (Table 3.8). Of the community metrics tested, species richness and relative total biomass were found to show a significant correlation between predictions and ground truth, indicating good predictability. Models of species richness explained 66.87% of the deviance in species richness and had a Pearson's correlation of 0.43 (P = 0.044) present between test data and predictions (Figure 3.23). Depth (bathymetry), ruggedness of terrain (VRM 3) and current speed were found to best explain trends in species richness. In particular, species richness was predicted to increase with increasing ruggedness (Figure 3.24). Variation was also observed between years of sampling. While relative total biomass had a significant Pearson's correlation of 0.52 (P = 0.012) present between test data and predictions, only 31.13% of the deviance was able to be explained by models. Models for relative family richness and relative total abundance had low performance.

Of individual species modelled, relative abundance was able to predict with a degree of confidence for *Meuschenia freycineti, Platycephalus bassensis and Trygonorrhina dumerilii* (Table 3.8). Models of *Meuschenia freycineti* explained 74.47% of the deviance in relative abundance and had a Pearson's correlation of 0.62 (P = 0.002) present between test data and predictions (Figure 3.25). These models were found to be best explained by depth (bathymetry), northness and ruggedness (VRM 3) (Figure 3.26). While models of *Platycephalus bassensis* showed very high deviance explained (90.23%), they showed low predictability (0.34, P = 0.118) (Figure 3.27). These models were linked to depth, complexity and aspect (northness and eastness) (Figure 3.28). A high deviance explained (67.54%) and correlation between test data and predictions (0.73, P < 0.0005) was further found for models of relative abundance of *Trygonorrhina dumerilii* (Figure 3.29). This model was solely driven by bathymetry, in which abundance was found to increase with depth (Figure 3.30). In a similar manner to relative total biomass, while models of *Dactylophora nigricans* showed a significant Pearson's correlation of 0.65 (P = 0.001) between test data and predictions, only 40.29% of the deviance in relative total biomass was able to be explained by models. Models of relative abundance of *Chrysophrys auratus, Bathytoshia brevicaudata, Meuschenia hippocrepis, Myliobatis tenuicaudatus, Notolabrus tetricus* and *Pictilabrus laticlavius* were unable to be strongly fit.

Table 3.8: Summary statistics of best performing generalised additive models (GAMs) completed at spatial scales of 5, 10, 25, 50, 100, 150 and 300 m. Best descriptor variables are identified by +.

Response variable	Year	Current speed	Bathymetry	VRM 3[1]	VRM 9[1]	Eastness	Northness	Optimal scale (m)	Degrees of freedom	AICc [2]	Deviance explained (%)	Test data correlation	Test data correlation (*P* value)
Chrysophrys auratus			+			+		50	10	278.8	33.25	0.58	0.58
Dactylophora nigricans		+	+	+			+	25	7	106.93	40.29	0.65	0.001
Bathytoshia brevicaudata					+		+	5	7	100.54	20.39	0.32	0.152
Meuschenia freycineti			+	+			+	150	19	272.56	74.47	0.62	0.002
Meuschenia hippocrepis	+			+		+		300	9	271.14	49.91	0.41	0.058
Myliobatis tenuicaudatus							+	25	3	17.03	7.09	0.23	0.307
Notolabrus tetricus			+	+				300	9	386.02	69.80	0.16	0.475
Pictilabrus laticlavius			+	+			+	50	14	209.08	65.46	0.19	0.388
Platycephalus bassensis			+	+		+	+	150	17	114.61	90.23	0.34	0.118
Trygonorrhina dumerilii			+					25	4	193.36	67.54	0.73	0.000
Species richness	+	+	+	+				100	12	327.06	66.87	0.43	0.044
Family richness		+		+				150	8	283.5	52.59	0.24	0.279
Total abundance	+	+		+				150	8	504.97	57.23	0.22	0.326
Total biomass	+	+	+				+	10	7	1,490.75	31.13	0.52	0.012

Notes: **1 VRM 3 = vector ruggedness measure (VRM) with 3 m window; VRM 9 = VRM with 9 m window**
2 AICc = Akaike information criterion (AIC) with correction for small sample sizes
3 Deviance explained is an indication of the model's goodness-of-fit
4 Pearson correlation between test data and corresponding predictions

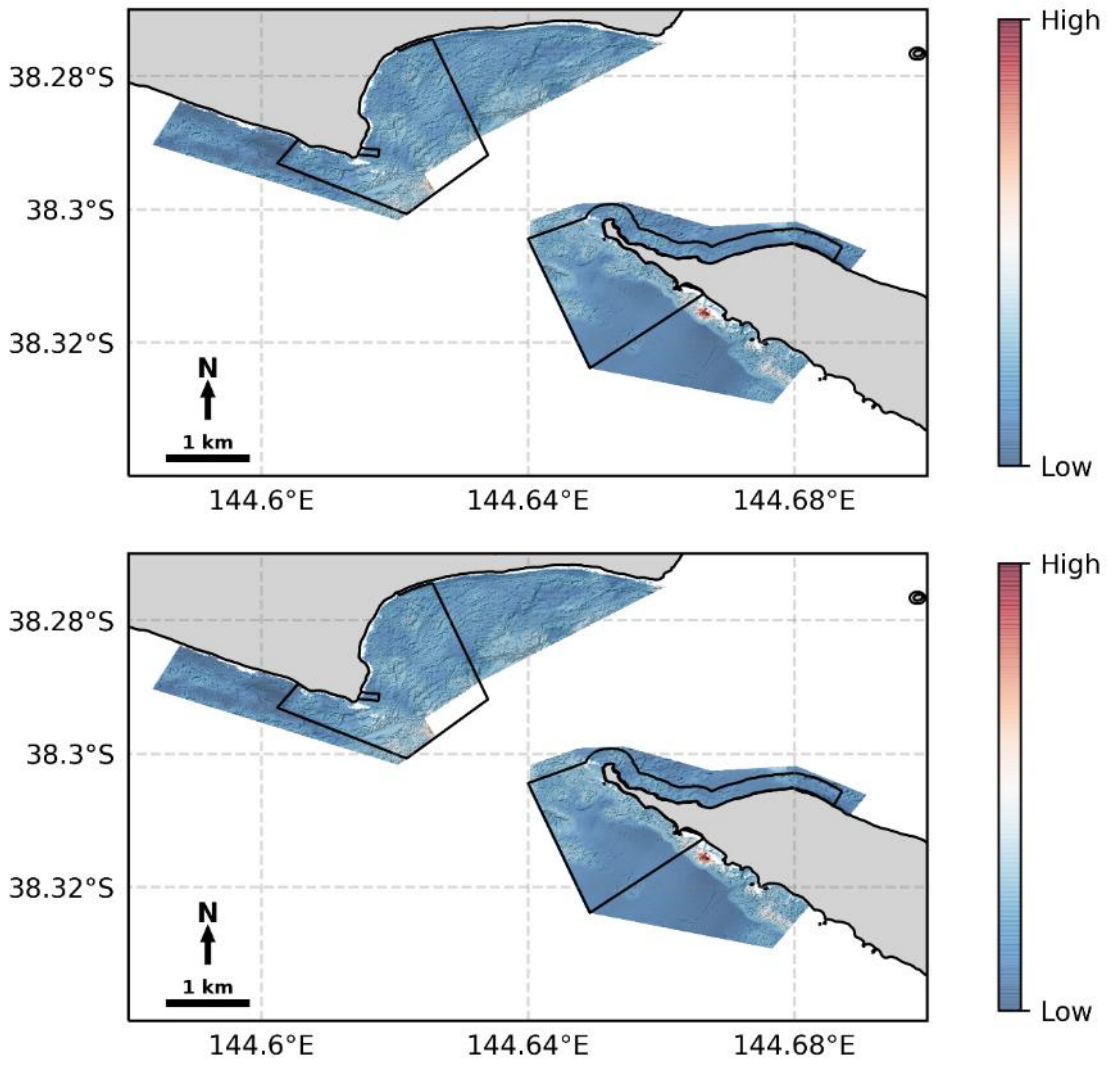

Figure 3.23: Predicted species richness in 2018 (top) and 2019 (bottom), from BRUVS sampling across the whole study site

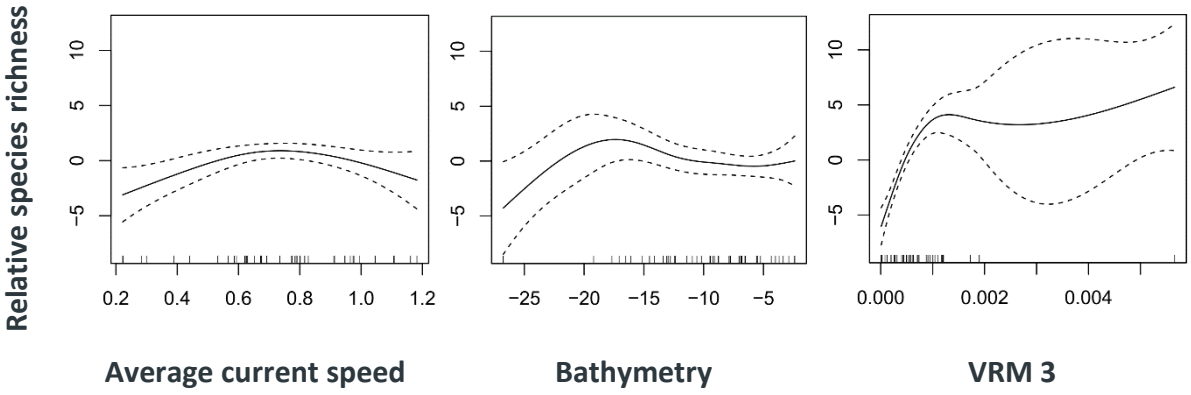

Figure 3.24: Smoother estimates for the environmental predictors as obtained from generalised additive models (GAMs) of relative species richness. Error bar lines are 95% confidence intervals

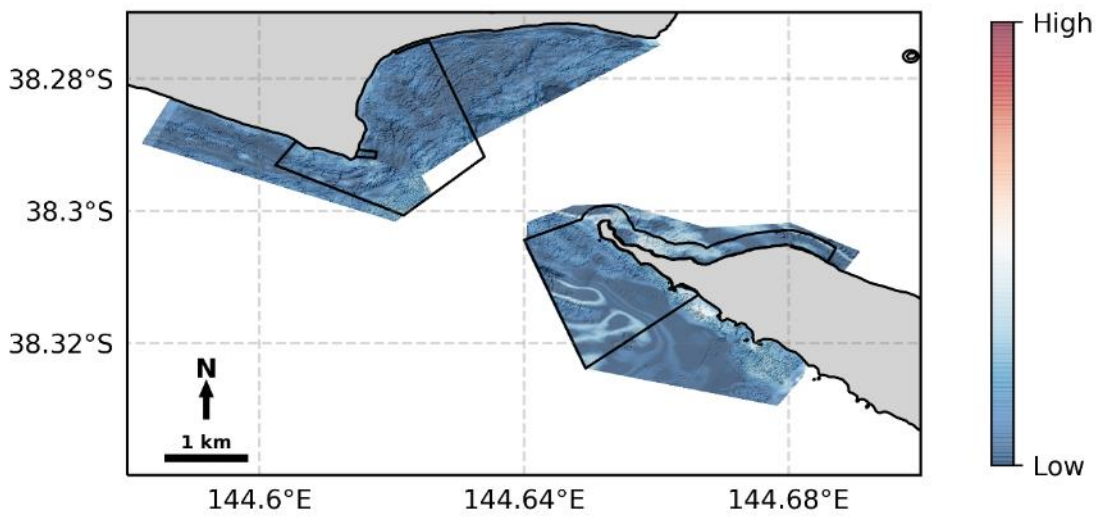

Figure 3.25: Predicted relative abundance of *Meuschenia freycineti* from BRUVS sampling across the whole study site

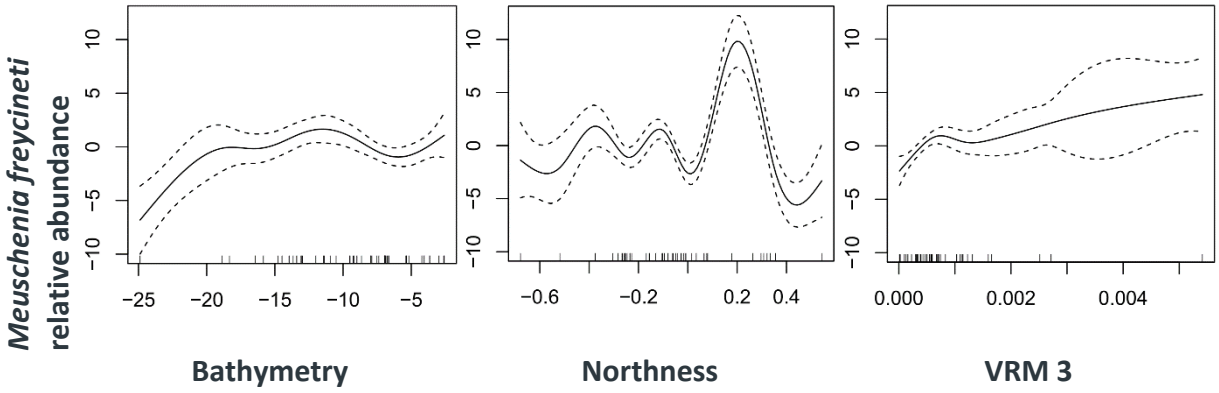

Figure 3.26: Smoother estimates for the environmental predictors as obtained from generalised additive models (GAMs) of *Meuschenia freycineti* relative abundance. Error bar lines are 95% confidence intervals

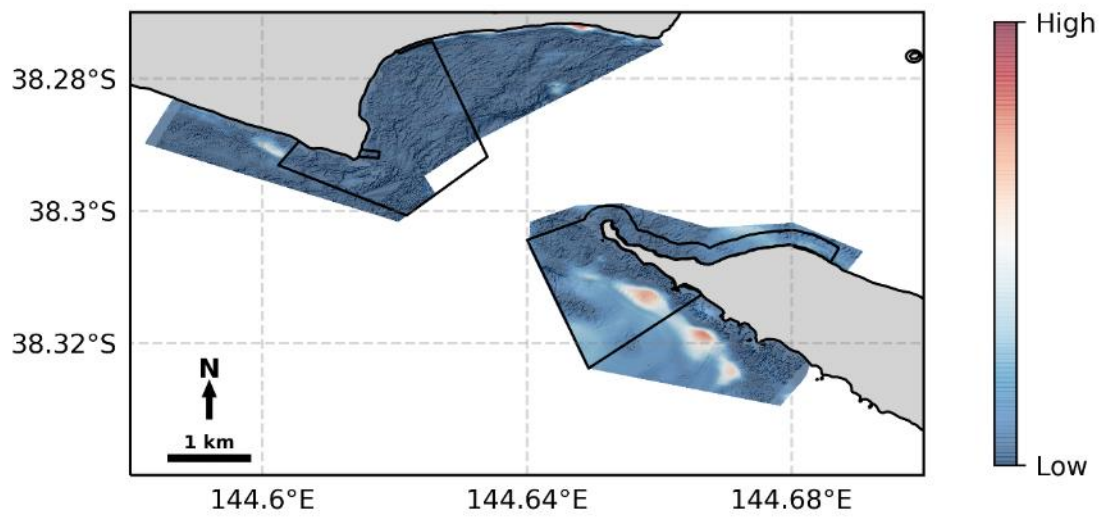

Figure 3.27: Predicted relative abundance of *Platycephalus bassensis* from BRUVS sampling across the whole study site

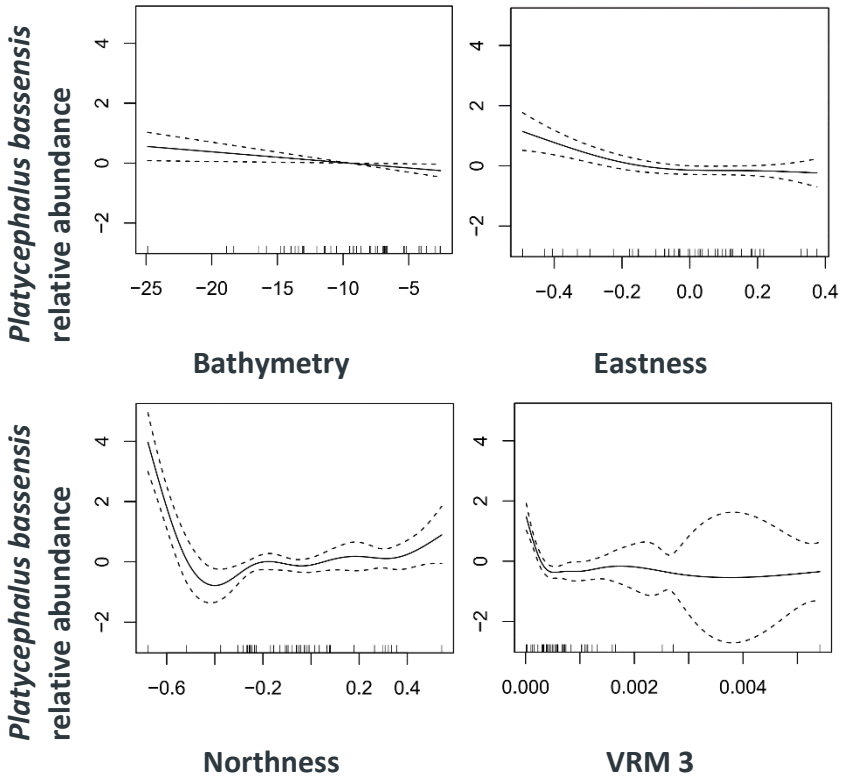

Figure 3.28: Smoother estimates for the environmental predictors as obtained from generalised additive models (GAMs) of *Platycephalus bassensis* relative abundance. Error bar lines are 95% confidence intervals

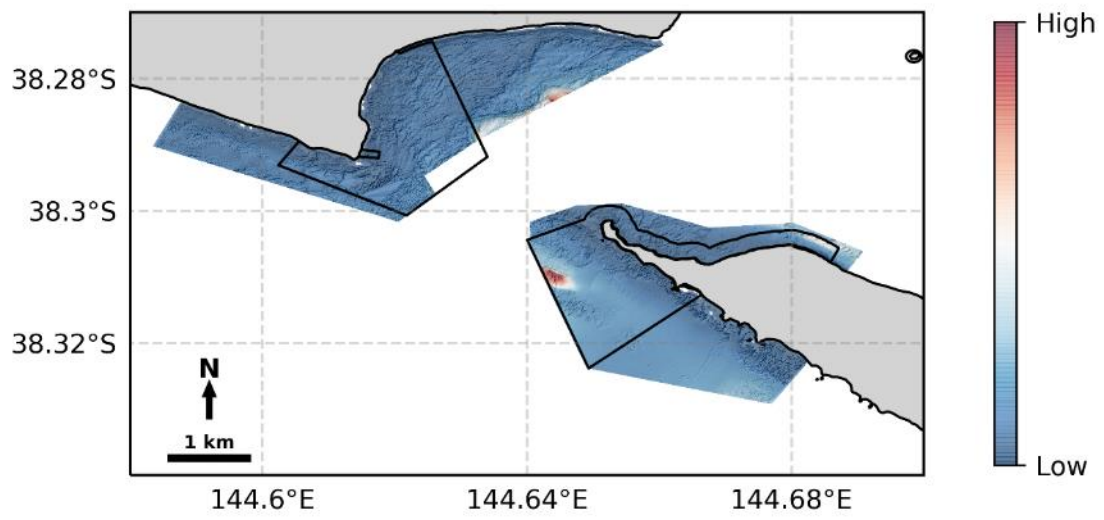

Figure 3.29: Predicted relative abundance of *Trygonorrhina dumerilii* from BRUVS sampling across the whole study site

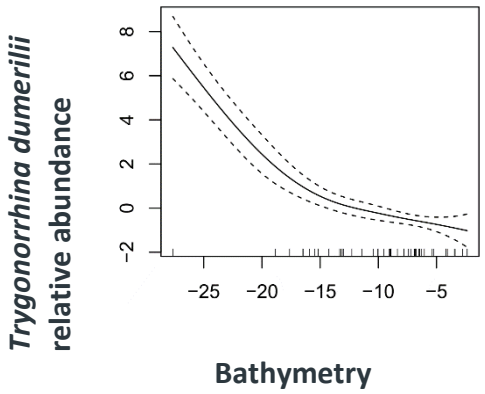

Figure 3.30: Smoother estimates for the environmental predictors as obtained from generalised additive models (GAMs) of *Trygonorrhina dumerilii* relative abundance. Error bar lines are 95% confidence intervals

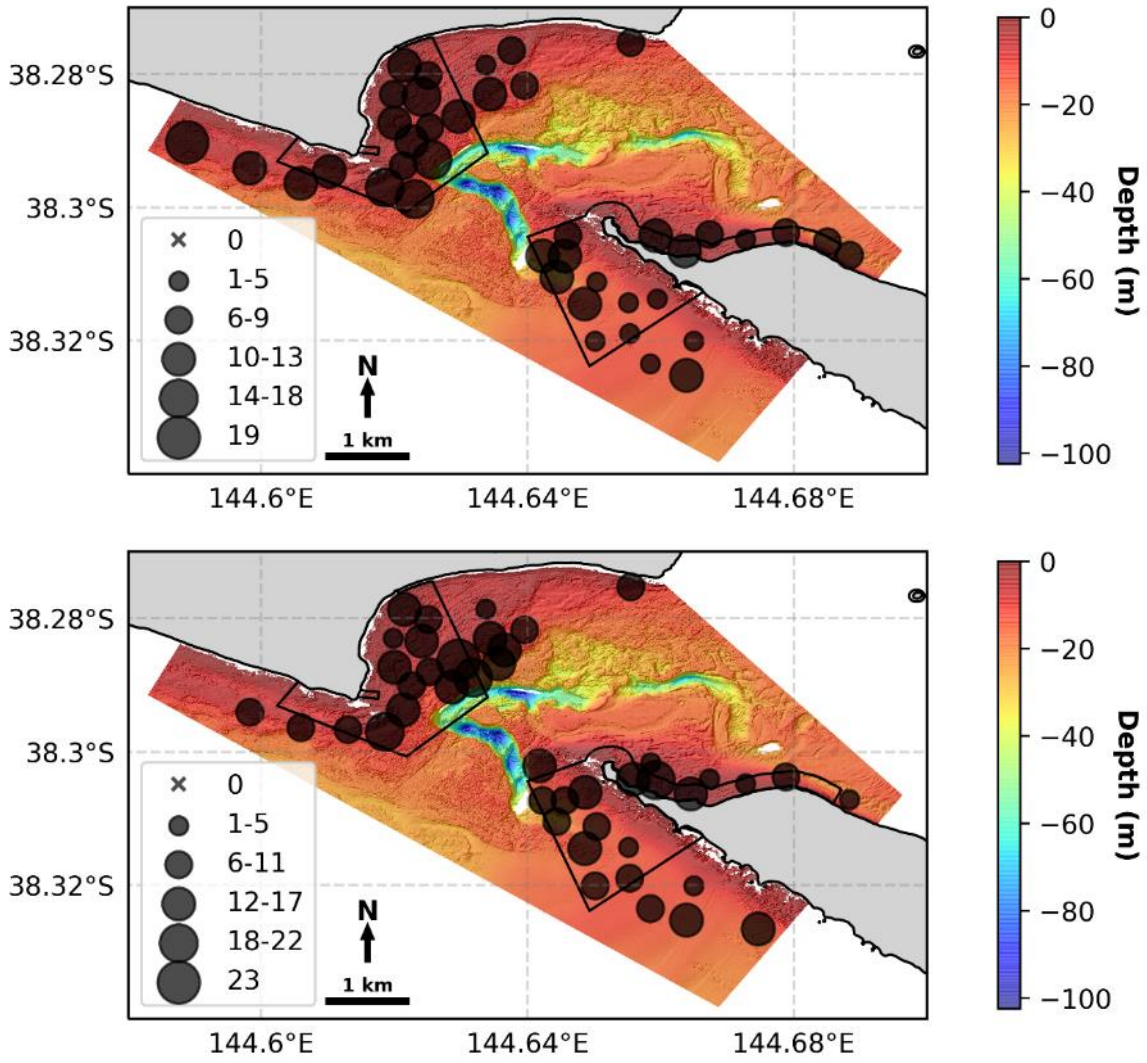

Figure 3.31: Relative species richness of fish observed for all BRUVS deployments from 2018 (top) and 2019 (bottom) sampling efforts. The size of each site marker corresponds to the relative species richness of fish observed at that site. These sites are overlaid on hillshaded bathymetry of the study area, coloured by depth. Black boxes denote Port Phillip Heads MNP boundaries

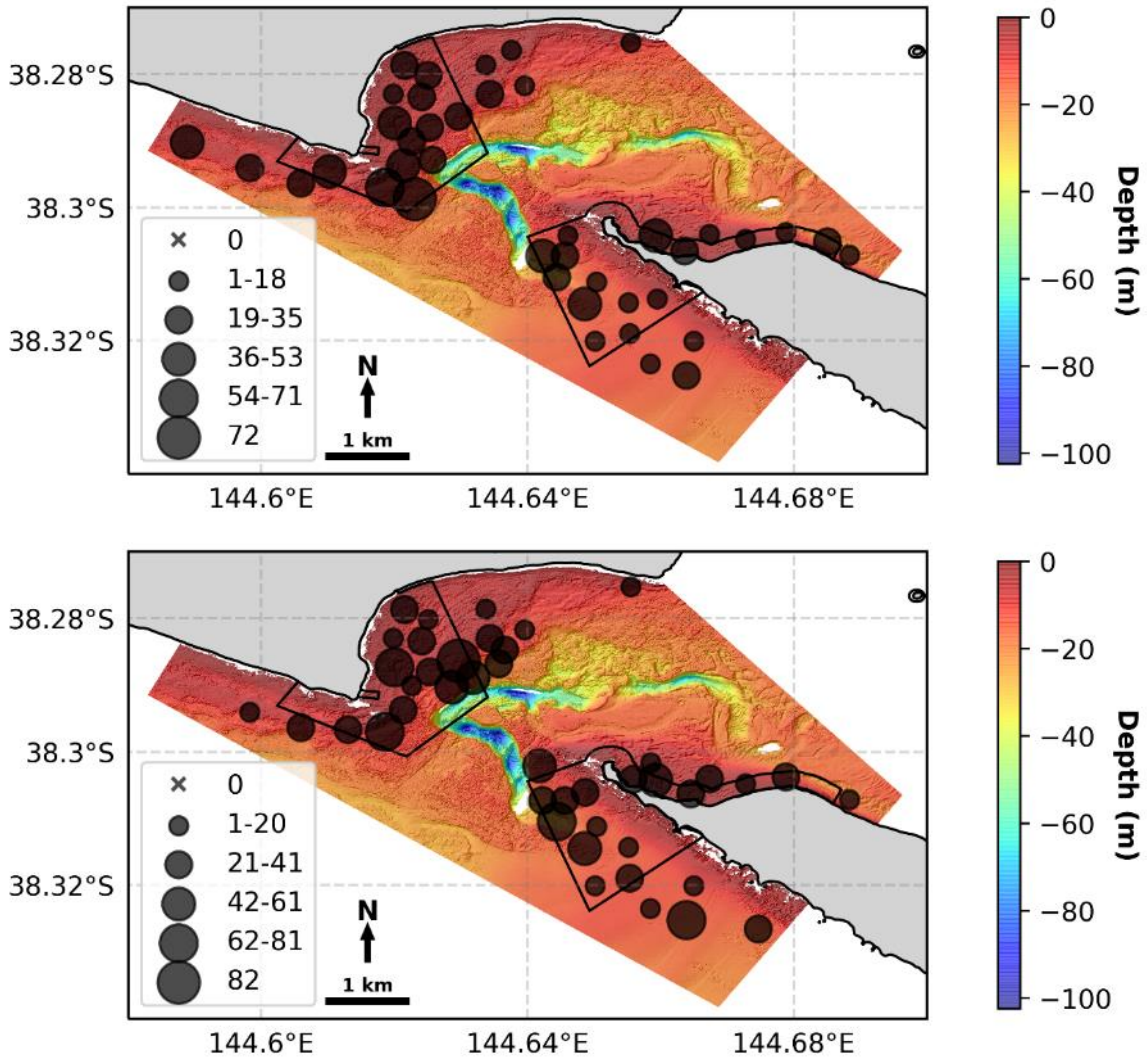

Figure 3.32: Total relative abundance of fish observed for all BRUVS deployment sites from 2018 (top) and 2019 (bottom) sampling efforts. The size of each site marker corresponds to the total relative abundance of fish observed at that site. These sites are overlaid on hillshaded bathymetry of the study area, coloured by depth. Black boxes denote Port Phillip Heads MNP boundaries

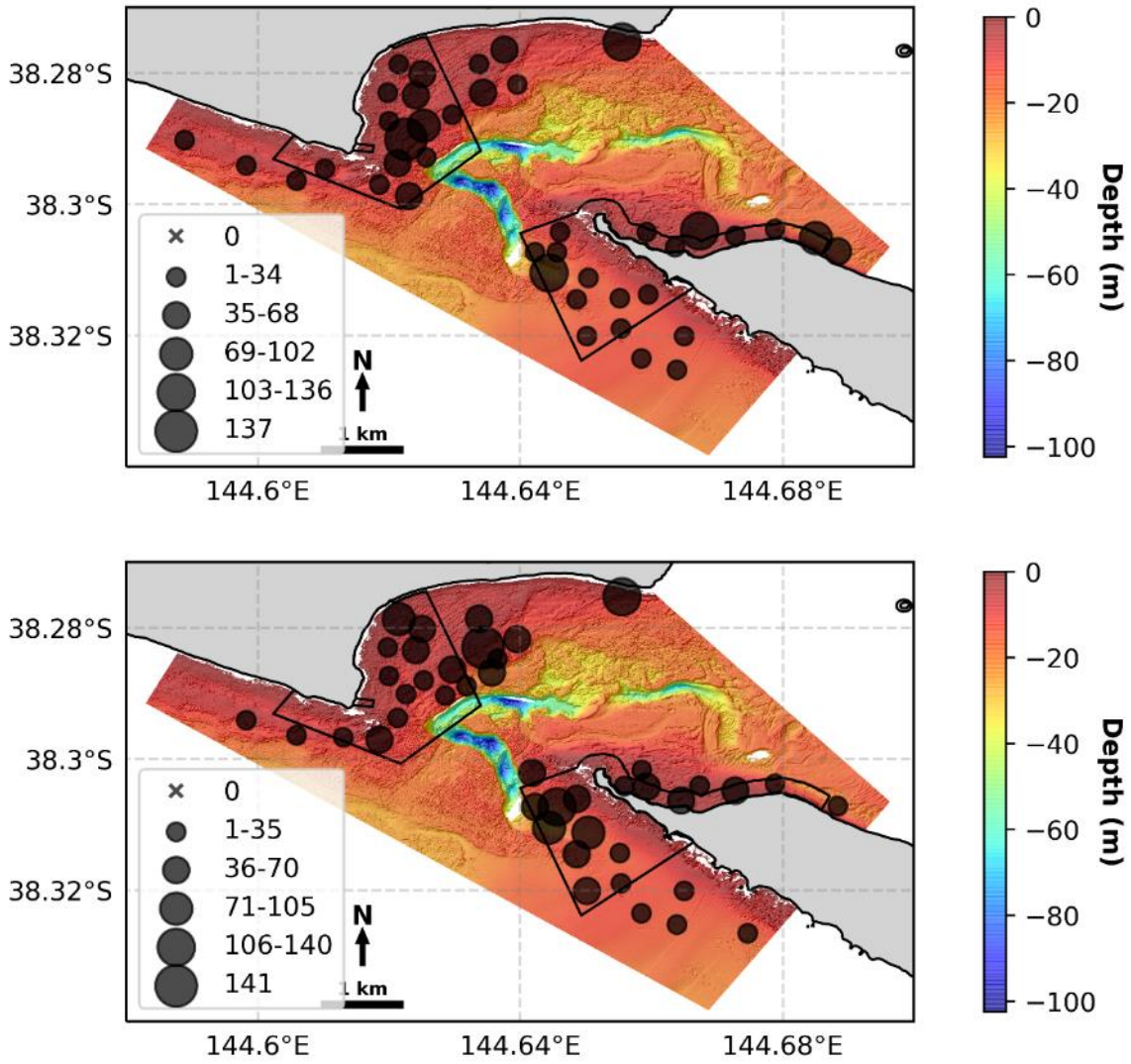

Figure 3.33: Relative total biomass (kg) of fish for all BRUVS deployments from 2018 (top) and 2019 (bottom) sampling efforts. The size of each site marker corresponds to the relative total biomass (kg) of fish observed at that site. These sites are overlaid on hillshaded bathymetry of the study area, coloured by depth. Black boxes denote Port Phillip Heads MNP boundaries

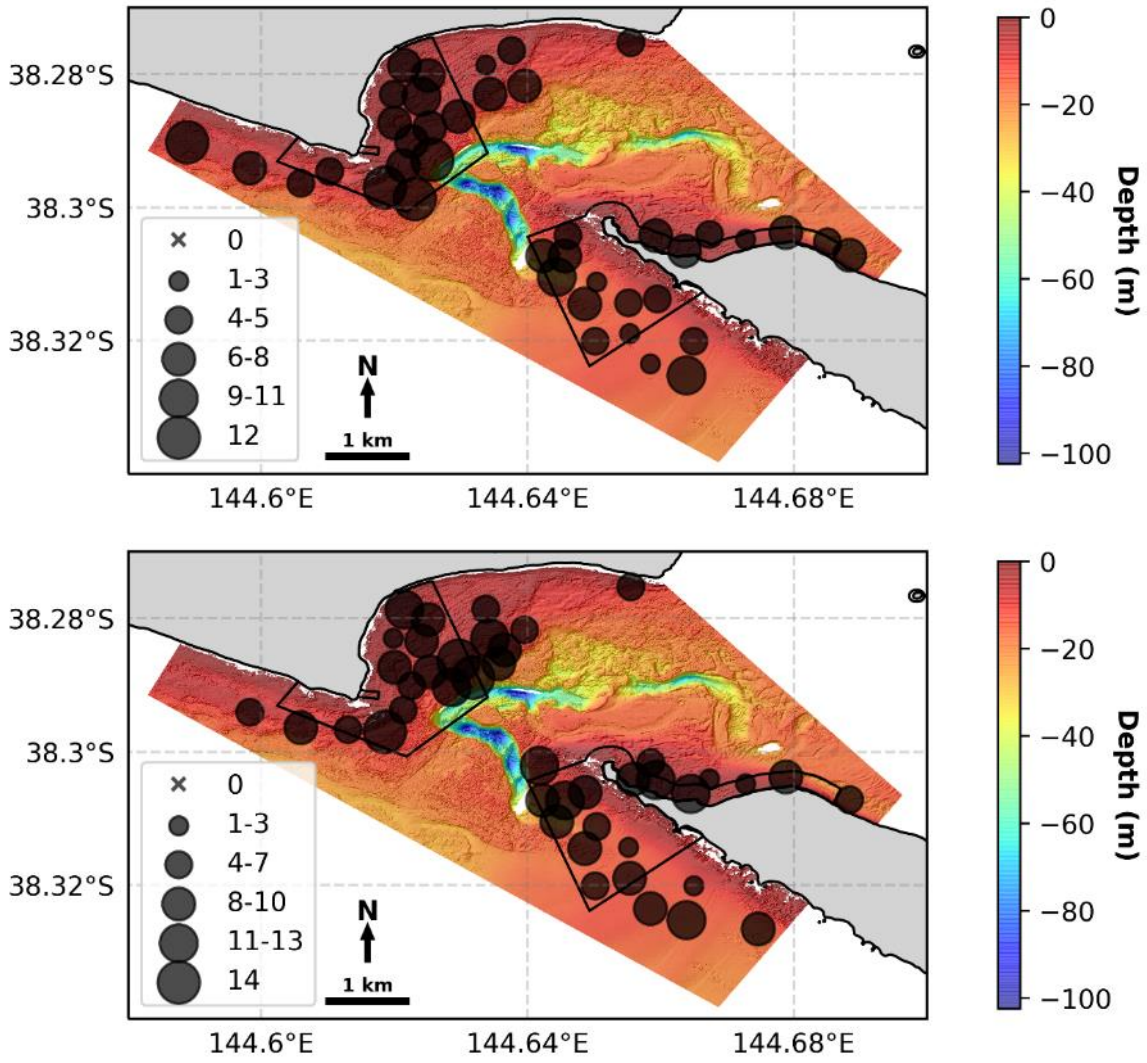

Figure 3.34: Relative family richness of fish for all BRUVS deployments from 2018 (top) and 2019 (bottom) sampling efforts. The size of each site marker corresponds to the relative family richness of fish observed at that site. These sites are overlaid on hillshaded bathymetry of the study area, coloured by depth. Black boxes denote Port Phillip Heads MNP boundaries

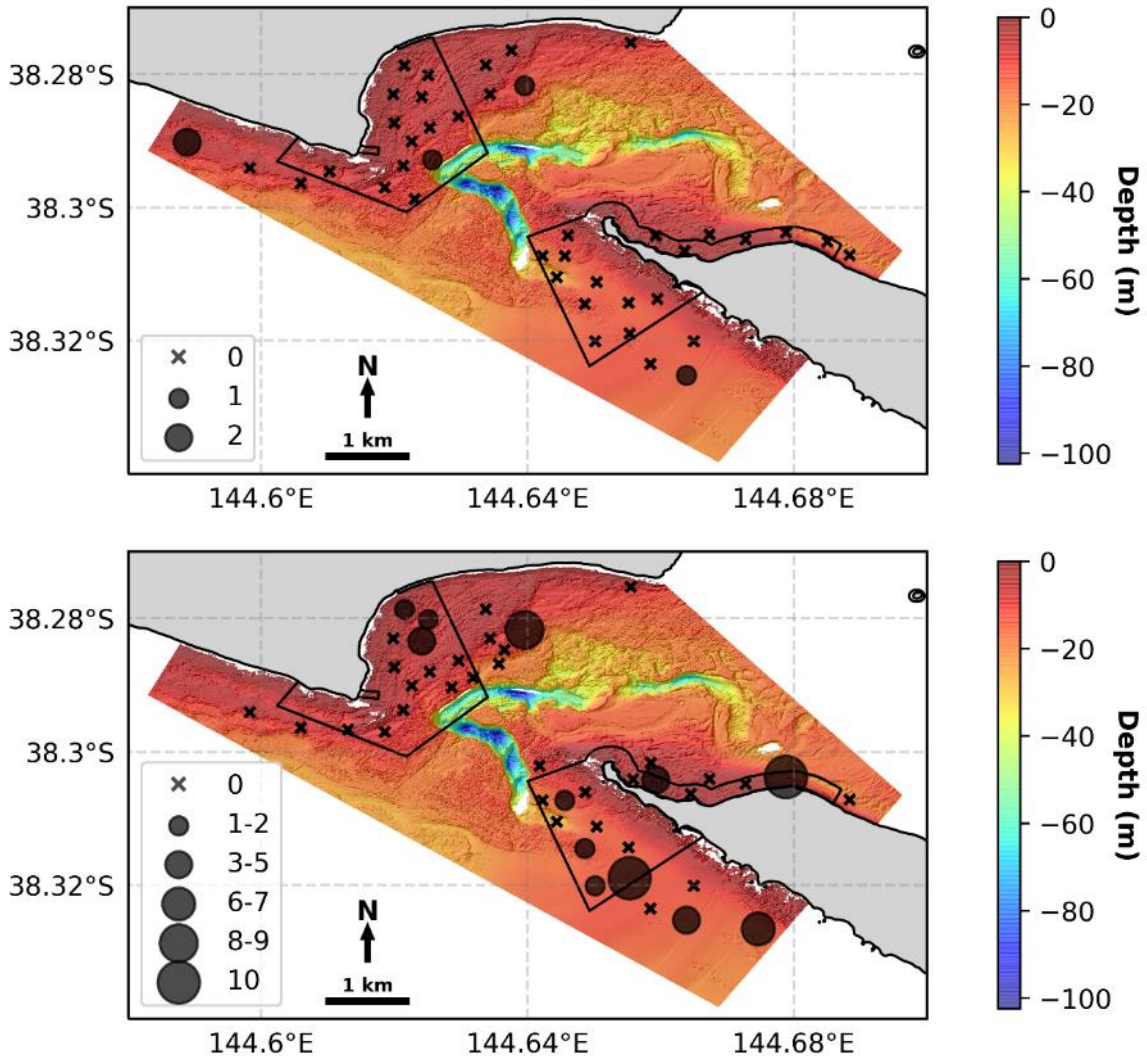

Figure 3.35: Relative abundance of *Chrysophrys auratus* for all BRUVS deployments from 2018 (top) and 2019 (bottom) sampling efforts. The size of each site marker corresponds to the relative abundance of *C.s auratus* observed at that site. These sites are overlaid on hillshaded bathymetry of the study area, coloured by depth. Black boxes denote Port Phillip Heads MNP boundaries

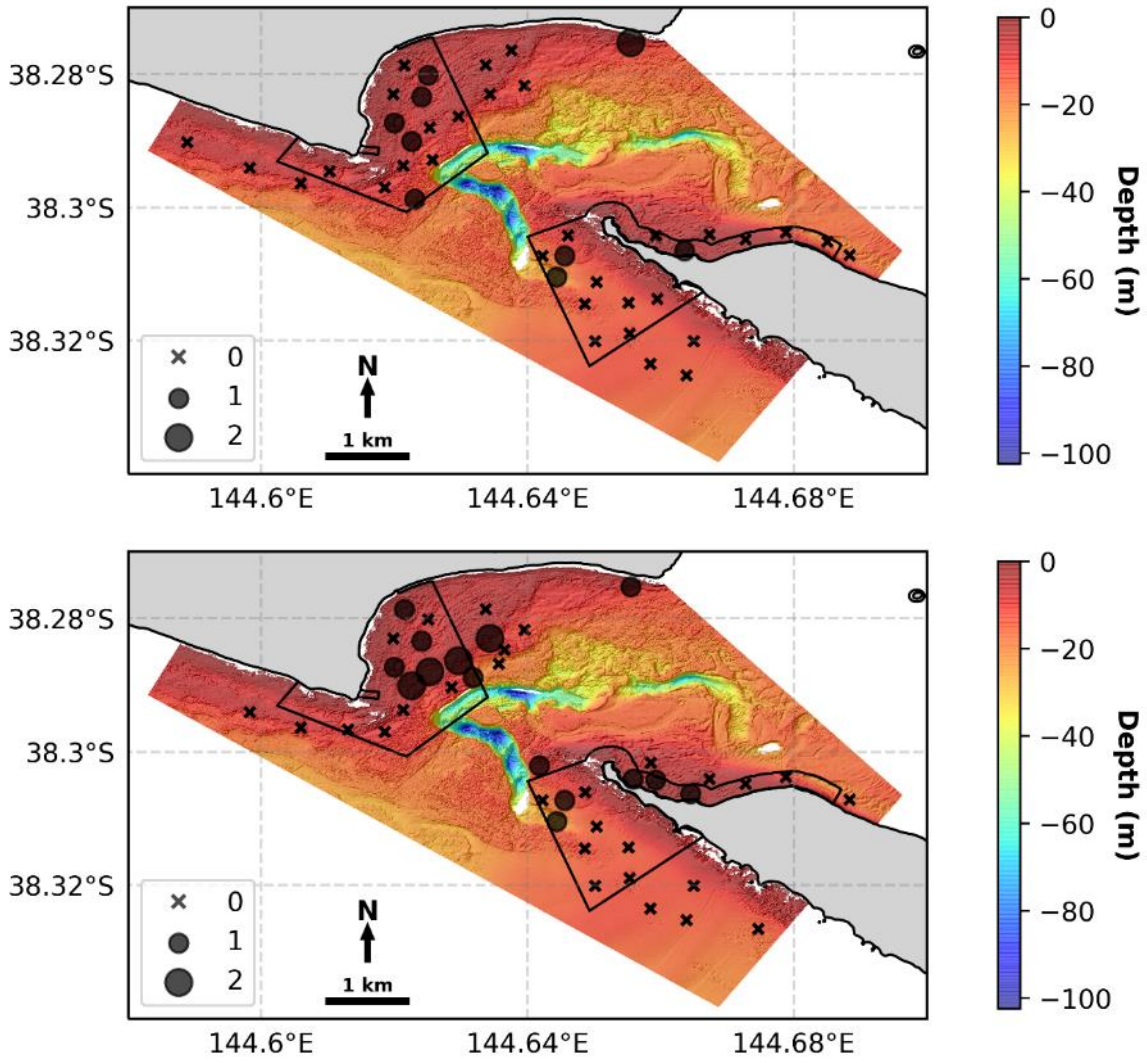

Figure 3.36: Relative abundance of *Dactylophora nigricans* for all BRUVS deployments from 2018 (top) and 2019 (bottom) sampling efforts. The size of each site marker corresponds to the relative abundance of *D. nigricans* observed at that site. These sites are overlaid on hillshaded bathymetry of the study area, coloured by depth. Black boxes denote Port Phillip Heads MNP boundaries

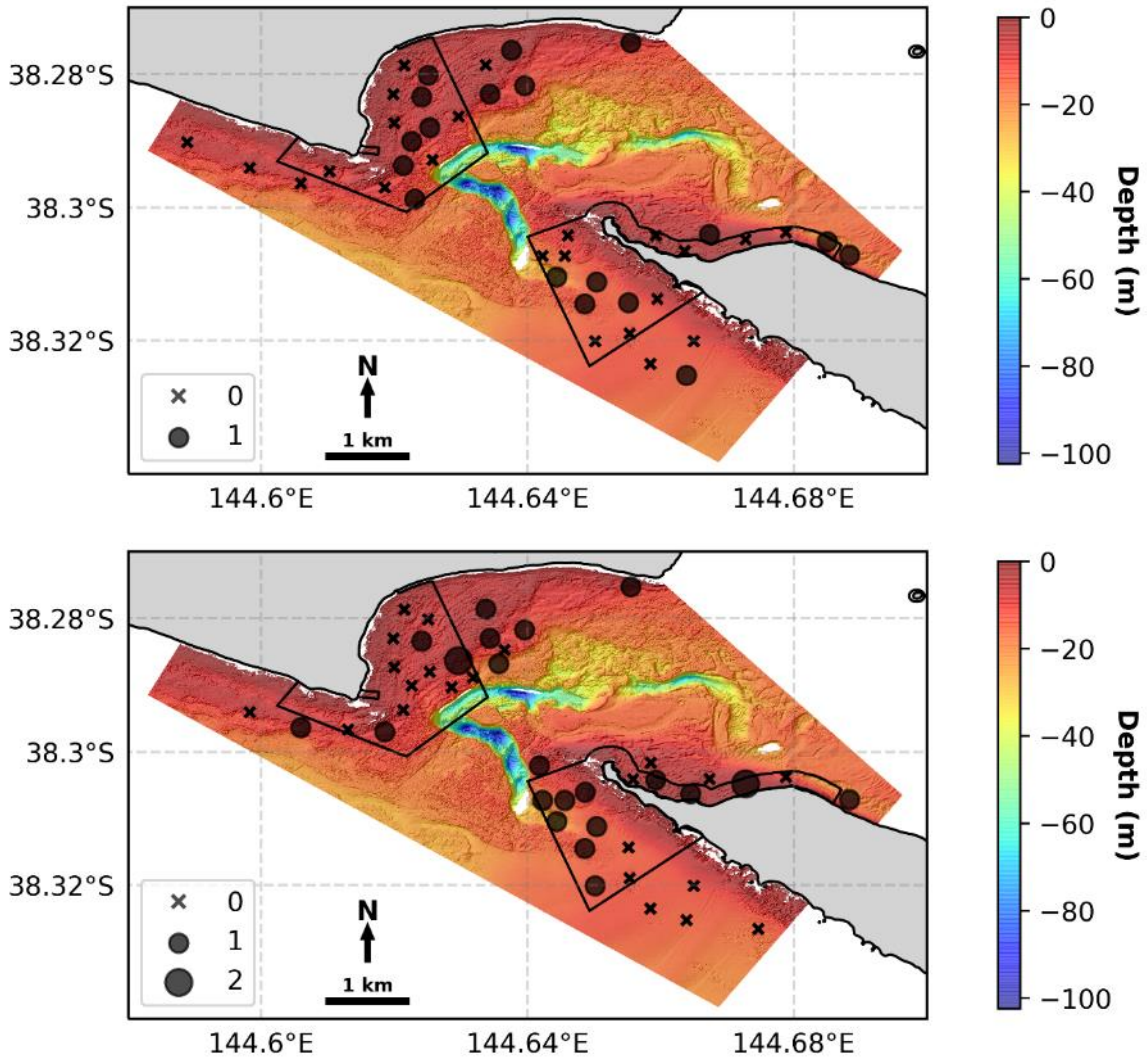

Figure 3.37: Relative abundance of *Bathytoshia brevicaudata* for all BRUVS deployments from 2018 (top) and 2019 (bottom) sampling efforts. The size of each site marker corresponds to the relative abundance of *B. brevicaudata* observed at that site. These sites are overlaid on hillshaded bathymetry of the study area, coloured by depth. Black boxes denote Port Phillip Heads MNP boundaries

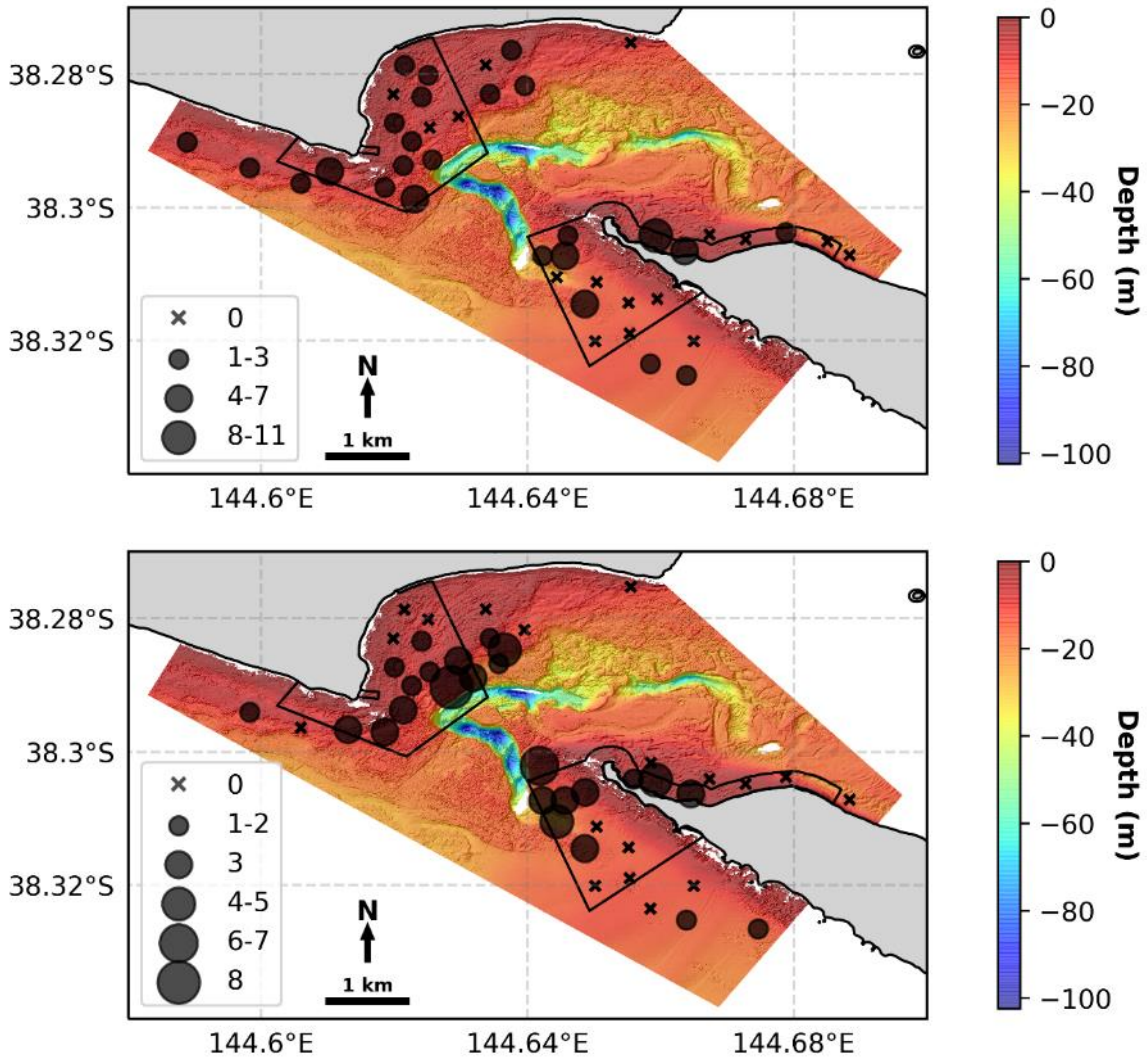

Figure 3.38: Relative abundance of *Meuschenia freycineti* for all BRUVS deployments from 2018 (top) and 2019 (bottom) sampling efforts. The size of each site marker corresponds to the relative abundance of *M. freycineti* observed at that site. These sites are overlaid on hillshaded bathymetry of the study area, coloured by depth. Black boxes denote Port Phillip Heads MNP boundaries.

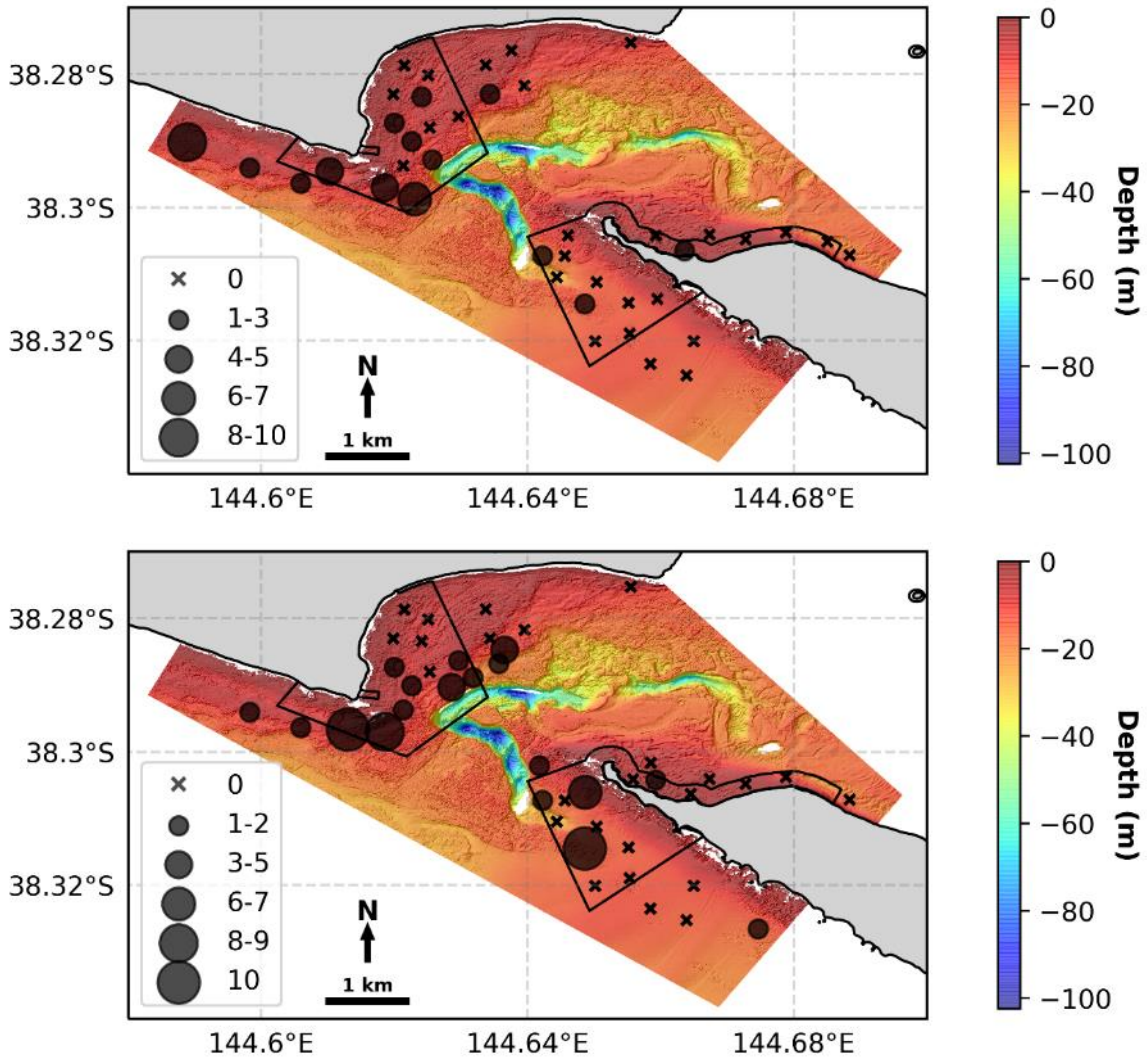

Figure 3.39: Relative abundance of *Meuschenia hippocrepis* for all BRUVS deployments from 2018 (top) and 2019 (bottom) sampling efforts. The size of each site marker corresponds to the relative abundance of *M. hippocrepis* observed at that site. These sites are overlaid on hillshaded bathymetry of the study area, coloured by depth. Black boxes denote Port Phillip Heads MNP boundaries

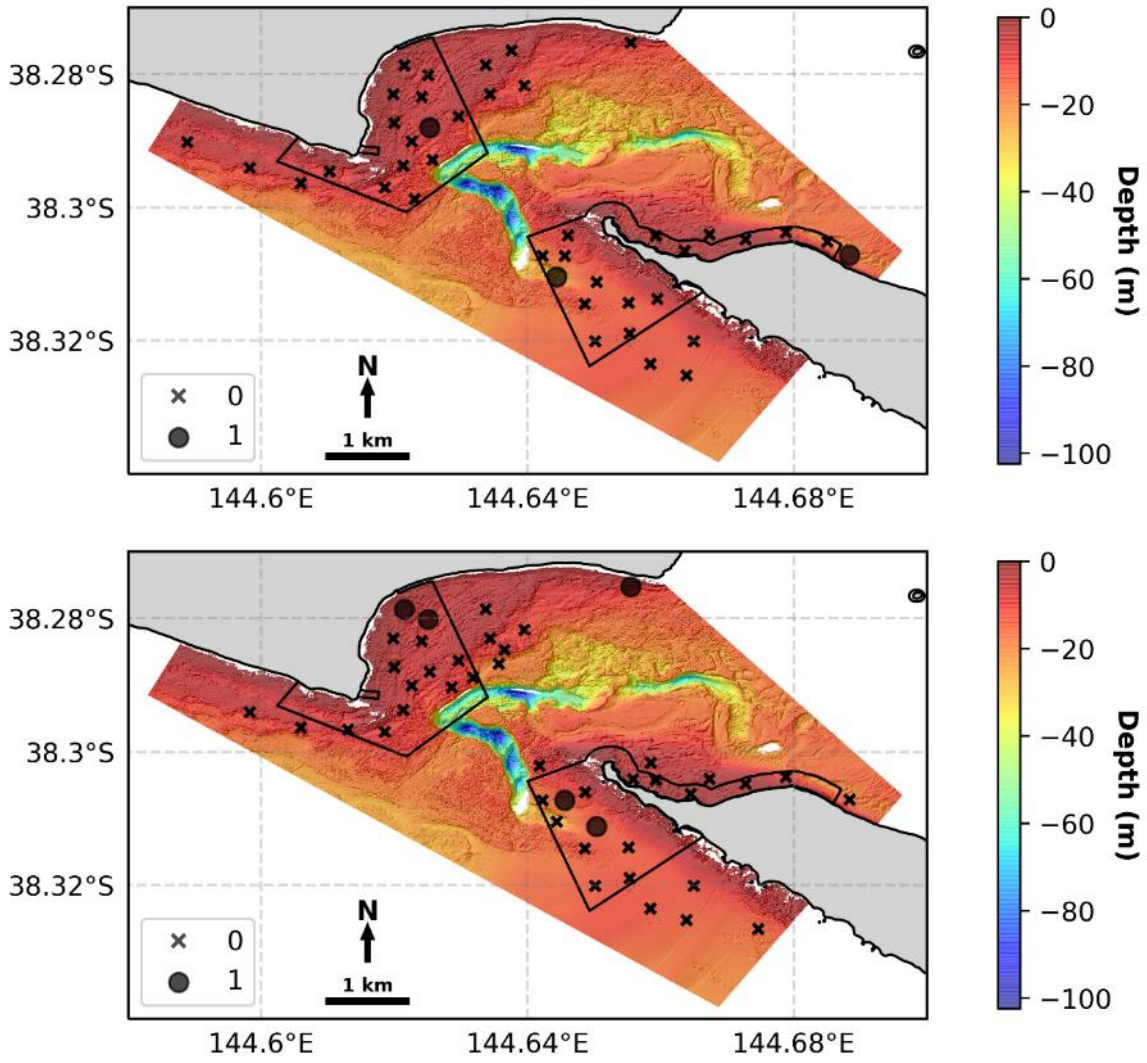

Figure 3.40: Relative abundance of *Myliobatis tenuicaudatus* for all BRUVS deployments from 2018 (top) and 2019 (bottom) sampling efforts. The size of each site marker corresponds to the relative abundance of *M. tenuicaudatus* observed at that site. These sites are overlaid on hillshaded bathymetry of the study area, coloured by depth. Black boxes denote Port Phillip Heads MNP boundaries

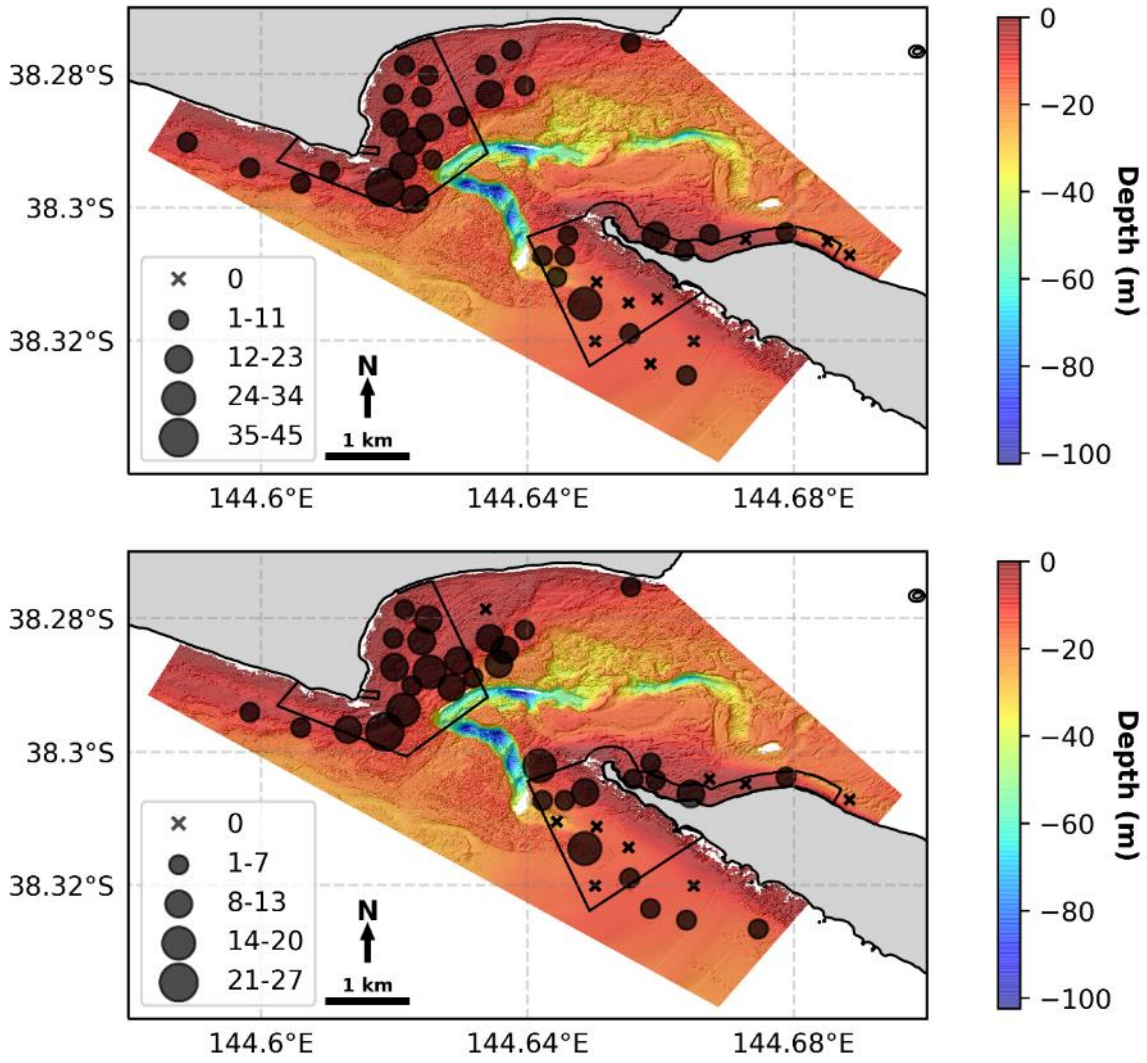

Figure 3.41: Relative abundance of *Notolabrus tetricus* for all BRUVS deployments from 2018 (top) and 2019 (bottom) sampling efforts. The size of each site marker corresponds to the relative abundance of *N. tetricus* observed at that site. These sites are overlaid on hillshaded bathymetry of the study area, coloured by depth. Black boxes denote Port Phillip Heads MNP boundaries

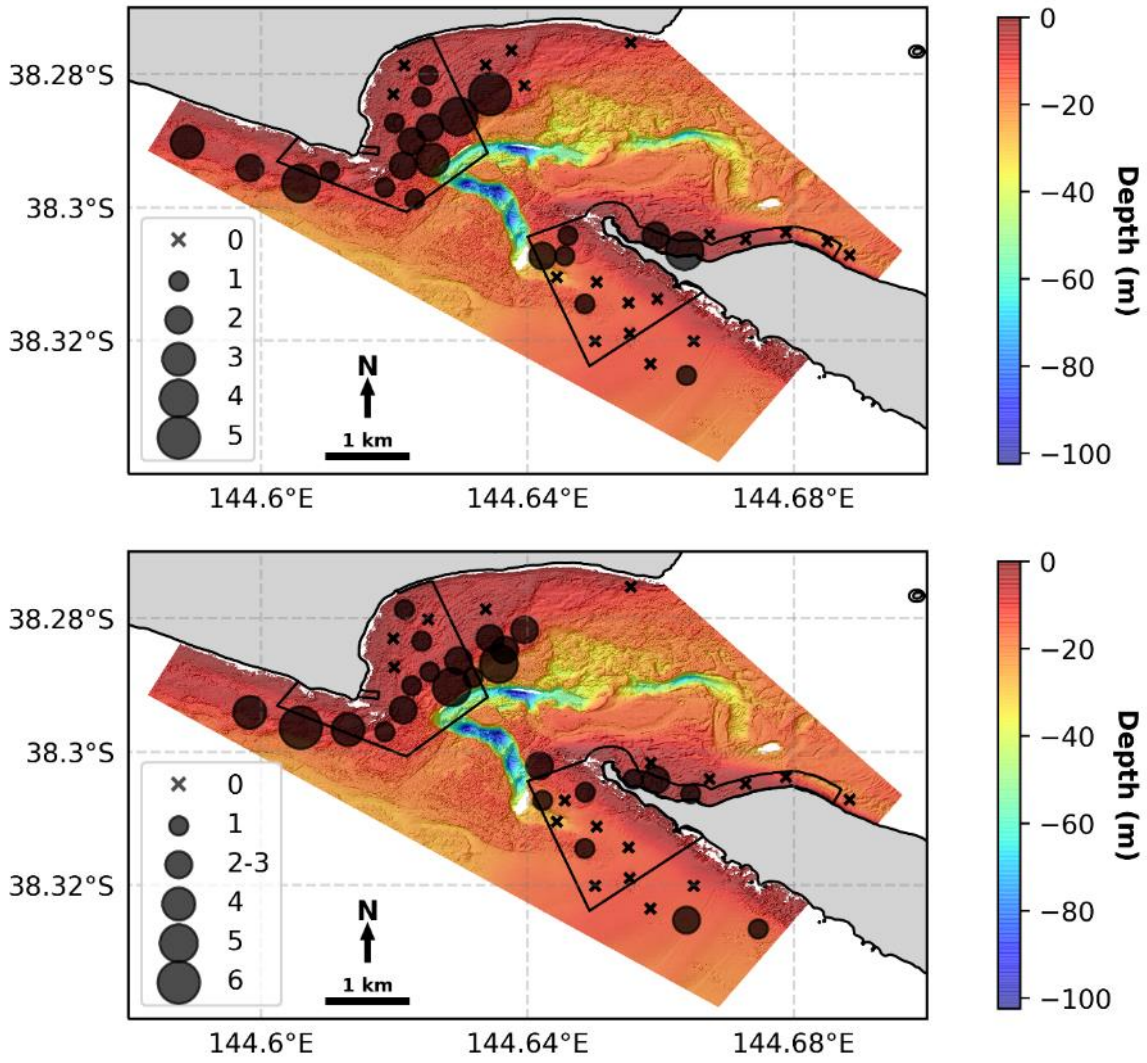

Figure 3.42: Relative abundance of *Pictilabrus laticlavius* for all BRUVS deployments from 2018 (top) and 2019 (bottom) sampling efforts. The size of each site marker corresponds to the relative abundance of *P. laticlavius* observed at that site. These sites are overlaid on hillshaded bathymetry of the study area, coloured by depth. Black boxes denote Port Phillip Heads MNP boundaries

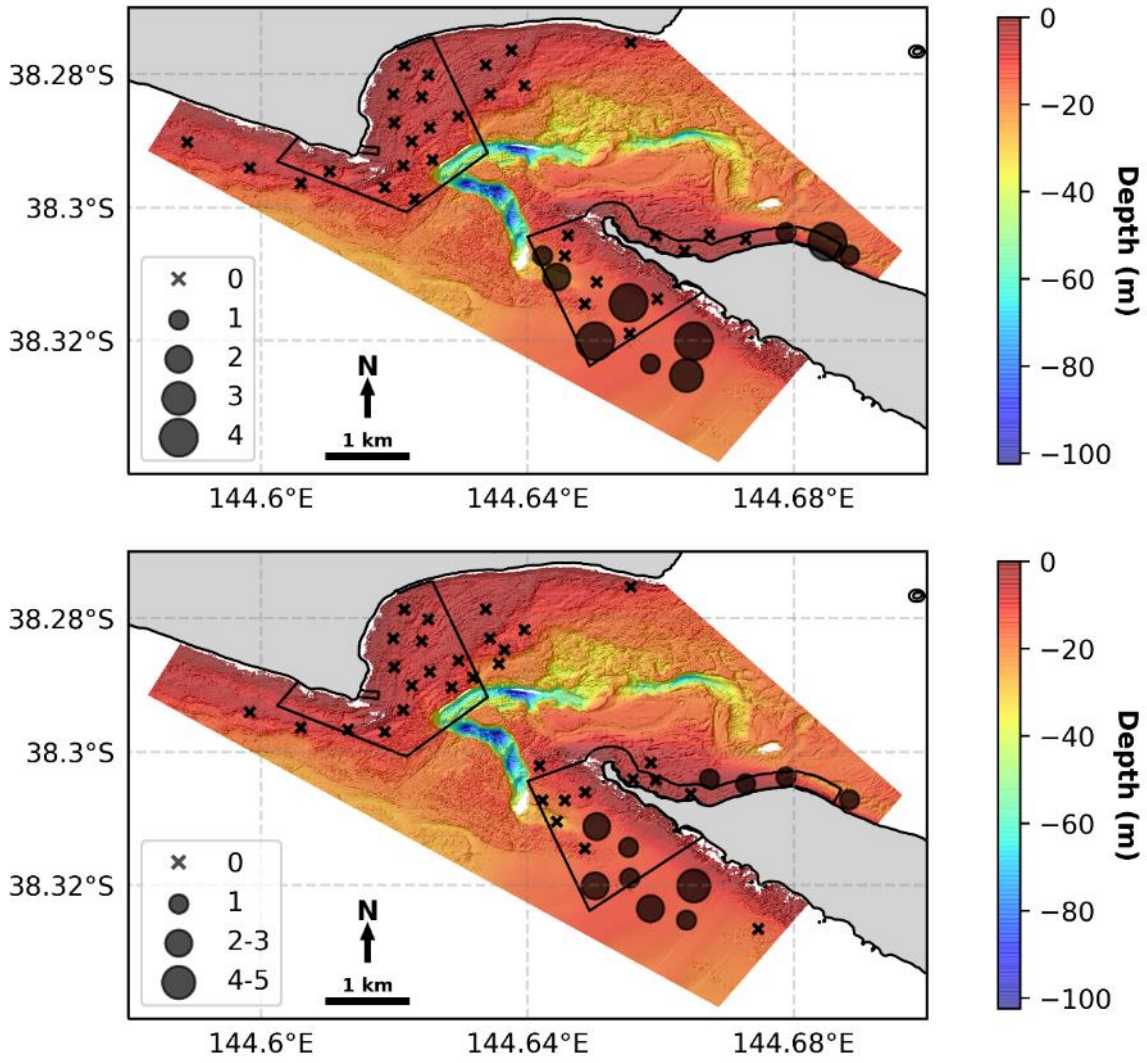

Figure 3.43: Relative abundance of *Platycephalus bassensis* for all BRUVS deployments from 2018 (top) and 2019 (bottom) sampling efforts. The size of each site marker corresponds to the relative abundance of *Platycephalus bassensis* observed at that site. These sites are overlaid on hillshaded bathymetry of the study area, coloured by depth. Black boxes denote Port Phillip Heads MNP boundaries

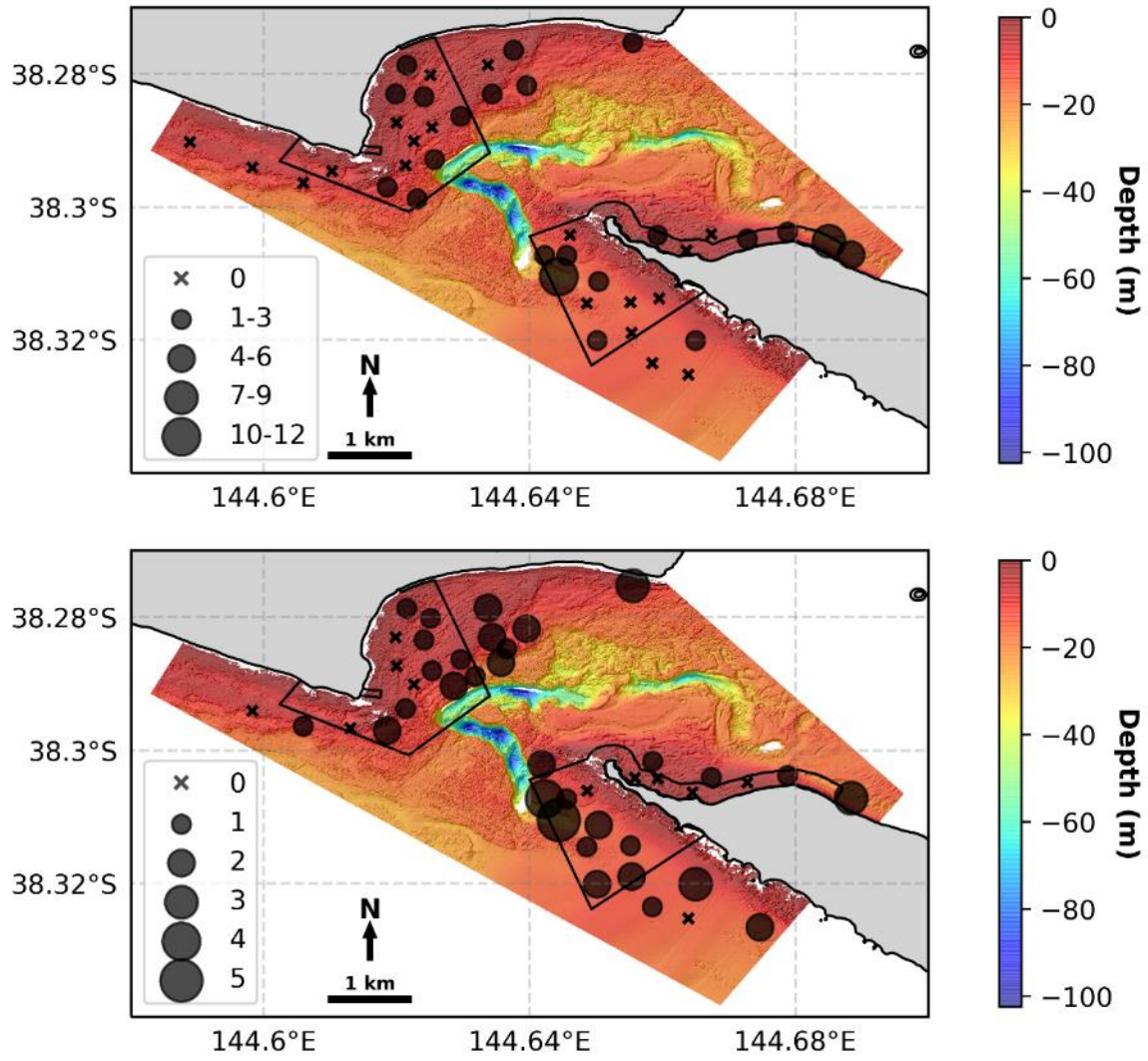

Figure 3.44: Relative abundance of *Trygonorrhina dumerilii* for all BRUVS deployments from 2018 (top) and 2019 (bottom) sampling efforts. The size of each site marker corresponds to the relative abundance of *T. dumerilii* observed at that site. These sites are overlaid on hillshaded bathymetry of the study area, coloured by depth. Black boxes denote Port Phillip Heads MNP boundaries

3.5.2 Comparison between baited remote underwater video stations and Reef Life Survey

In total, 97 species of fish from 51 families were detected using RLS and BRUVS surveys conducted as part of this study (Table 3.9). Of these, 48 species from 26 families were found in both RLS and BRUVS. The Reef Life Survey method detected twice as many unique species as the BRUVS method: 32 unique species and 14 unique families were detected in the Reef Life Survey alone compared with 14 unique species and 6 unique families detected only in the BRUVS surveys.

Table 3.9: Fish species observed in either Reef Life Survey (RLS) alone, baited remote underwater video stations (BRUVS) alone or both

Both	RLS alone	BRUVS alone
Acanthaluteres vittiger	*Acanthaluteres spilomelanurus*	*Aracana ornata*
Achoerodus spp.	*Aetapcus maculatus*	*Aracana* spp.
Aplodactylus arctidens	*Anoplocapros lenticularis*	*Cephaloscyllium laticeps*
Aracana aurita	*Aplodactylus lophodon*	*Contusus brevicaudus*
Arripis georgianus	*Arripis trutta*	*Kyphosus sydneyanus*
Atypichthys strigatus	*Bovichtus angustifrons*	*Neosebastes scorpaenoides*
Bathytoshia brevicaudata	*Brachaluteres jacksonianus*	*Notorynchus cepedianus*
Caesioperca rasor	*Chironemus georgianus*	*Platycephalus bassensis*
Chironemus maculosus	*Chironemus marmoratus*	*Platycephalus* spp.
Chrysophrys auratus	Gobiid spp.	*Pseudophycis* spp.
Dactylophora nigricans	*Heteroclinus kuiteri*	*Scorpis lineolata*
Dinolestes lewini	*Meuschenia australis*	*Sillaginodes punctatus*
Diodon nicthemerus	*Nesogobius* spp.	*Spiniraja whitleyi*
Dotalabrus aurantiacus	*Phycodurus eques*	*Thamnaconus degeni*
Enoplosus armatus	*Phyllopteryx taeniolatus*	
Eubalichthys mosaicus	*Platycephalus laevigatus*	
Eupetrichthys angustipes	*Pseudocaranx georgianus*	
Girella zebra	*Pseudolabrus luculentus*	
Haletta semifasciata	*Scolecenchelys breviceps*	
Heterodontus portusjacksoni	*Seriolella brama*	
Heteroscarus acroptilus	*Siphamia cephalotes*	
Hypoplectrodes nigroruber	*Siphonognathus beddomei*	
Meuschenia flavolineata	*Spratelloides* spp.	
Meuschenia freycineti	*Trachichthys australis*	
Meuschenia galii	*Trachinops caudimaculatus*	
Meuschenia hippocrepis	*Trinorfolkia clarkei*	
Meuschenia venusta	*Trygonoptera imitata*	
Myliobatis tenuicaudatus	*Trygonoptera mucosa*	
Neoodax balteatus	*Urolophus cruciatus*	
Notolabrus fucicola	*Urolophus gigas*	
Notolabrus tetricus	*Urolophus paucimaculatus*	
Olisthops cyanomelas	*Vincentia conspersa*	

Table 3.9 (continued): Fish species observed in either Reef Life Survey (RLS) alone, baited remote underwater video stations (BRUVS) alone or both

Both	RLS alone	BRUVS alone
Paraplesiops meleagris		
Parascyllium variolatum		
Parequula melbournensis		
Parma victoriae		
Pempheris multiradiata		
Pentaceropsis recurvirostris		
Pictilabrus laticlavius		
Platycephalus speculator		
Pseudogoniistius nigripes		
Pseudolabrus rubicundus		
Scobinichthys granulatus		
Scorpis aequipinnis		
Tetractenos glaber		
Tilodon sexfasciatus		
Trygonorrhina dumerilii		
Upeneichthys vlamingii		

3.6 Towed video

This study achieved extensive towed video coverage across the entire Port Phillip Heads MNP, including Popes Eye and Portsea Hole, in both 2018 and 2019 (Figure 2.6). A total of 42 transects were completed, totalling approximately 60 km of observations. Furthermore, within these transects, 5,893 downward-facing stills were successfully acquired (Table 3.10). From these data, 40 georeferenced still images (or the maximum number of images available) were extracted and classified for each 5 m depth stratum for the greater Port Phillip Heads MNP. A higher density of images was classified for the Popes Eye and Portsea Hole sites to ensure all habitat types were covered in habitat maps. This process was completed for both surveys resulting in the classification of 912 georeferenced stills.

In addition to observations made in the RLS method, the invasive Japanese Kelp (*Undaria pinnatifida*) was further observed in benthic photo quadrats at Portsea Hole towed video transects in 2018 surveys. Within the Portsea Hole site, these observations were made at a depth of 15 m, at the top of the reef wall (−38.31114, 144.71062), within the marine national park (Figure 3.45). There were no other observations of *U. pinnatifida* in photo quadrats in both towed video surveys (2018 and 2019).

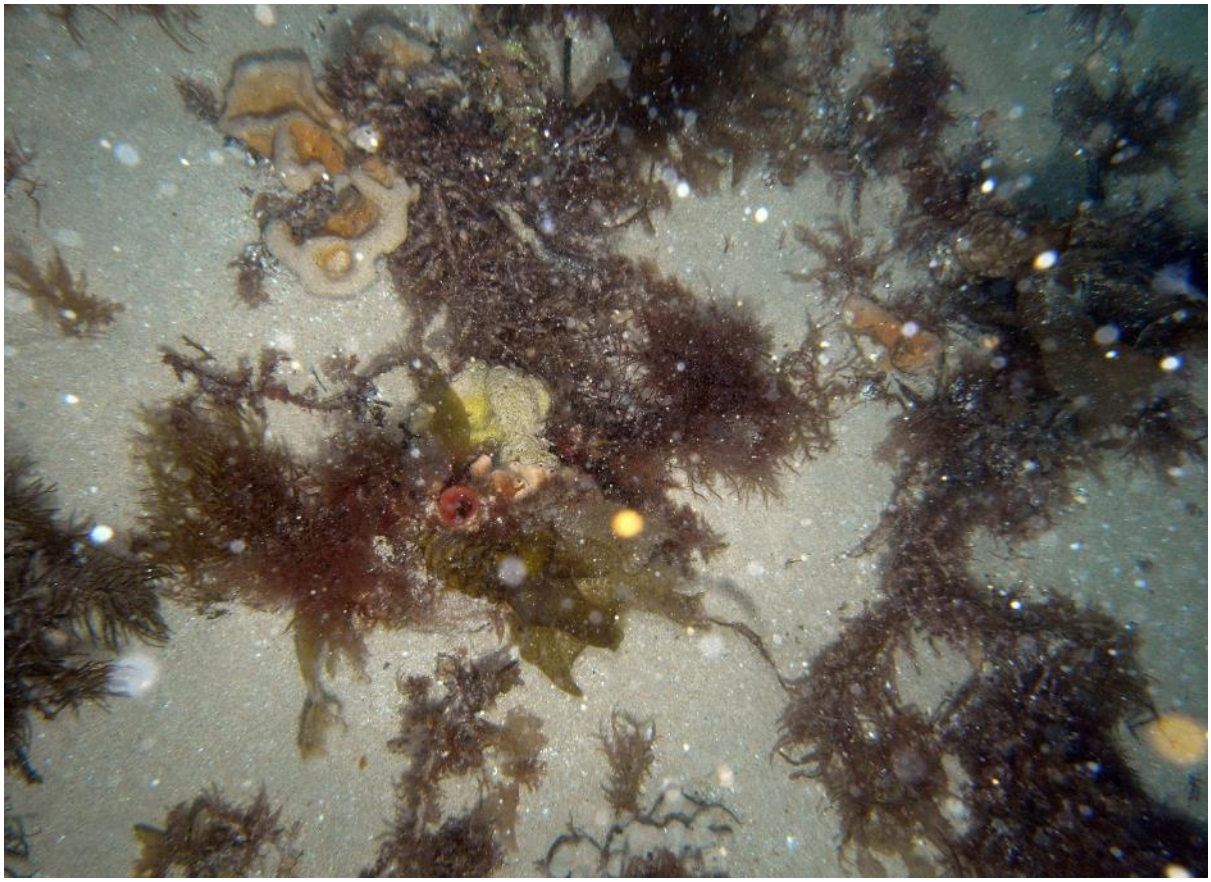

Figure 3.45: Photo quadrat collected from the 2018 towed video survey of Portsea Hole, containing instances of the invasive Japanese Kelp (*Undaria pinnatifida*)

Table 3.10: Summary of distances covered, number of transects completed and number of downward-facing stills successfully collected using towed video in this study

	2018	2019	Total
Distance towed (km)	28.14	32.77	60.91
No. of transects completed	20	22	42
No. of downward-facing stills acquired	3,320	2,573	5,893
No. of classified downward-facing stills	540	372	912

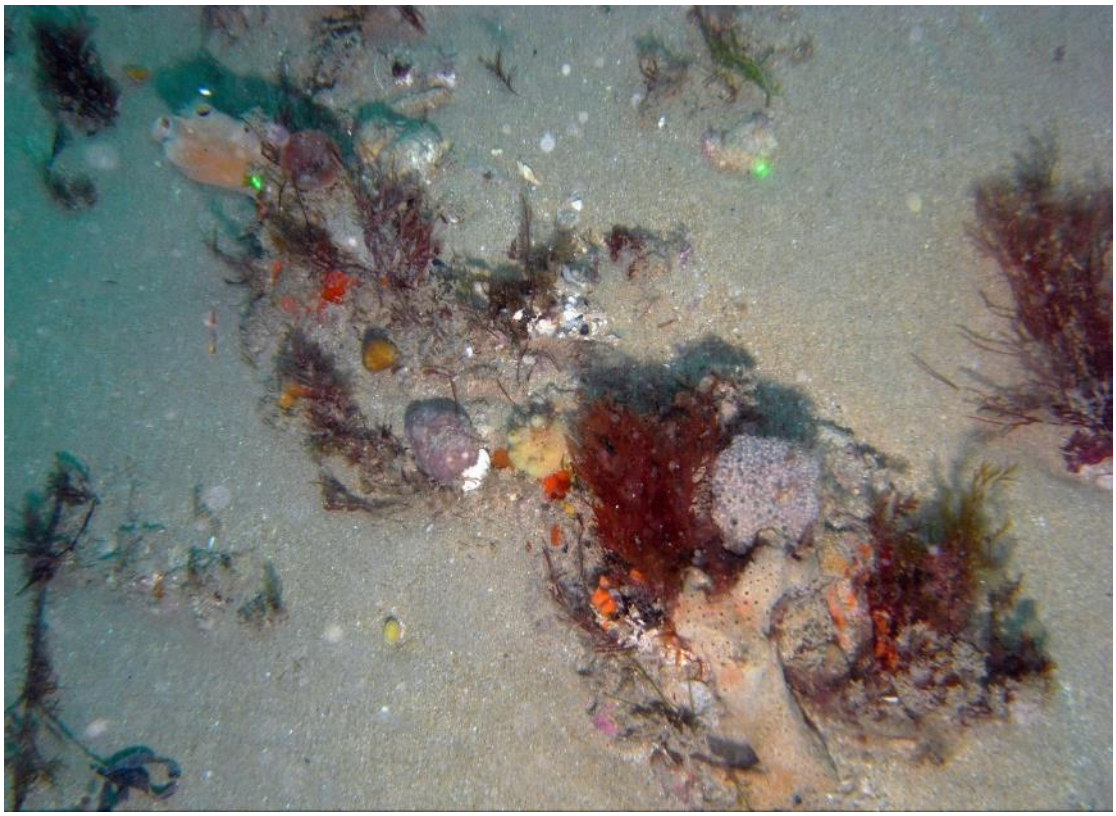

Figure 3.46: Examples of downward-facing georeferenced stills collected using towed video, showing various benthic habitat types found in Port Phillip Heads MNP. Photo quadrats were subsequently annotated using 25 random points, which results in detailed habitat classifications

3.6.1 Depth-related patterns of habitat composition

Classification of georeferenced downward-facing stills revealed slight variations in dominant cover types within the greater Port Phillips Head region between 2018 and 2019 (Figure 3.47); most likely the location of the towed area differed between years. The highest proportion of vegetation was observed between the 10 and 15 m depth contours. For both years, biota covered 69–76% of this depth, which was largely dominated by brown algae *Phyllospora comosa*, *Ecklonia radiata* and *Cystophora* spp. The dominance of these species varied between years: in 2018 *Cystophora* spp. was dominant while in 2019 *E. radiata* was dominant. However, this was likely a function of the position of the towed video transect rather than an actual change. The percentage cover of *P. comosa* stayed consistent between years. Apart from the 10 to 15 m contour, all other depths within the greater Port Phillip Heads MNP region were dominated by sediment (55–90%). Seagrasses (*Amphibolis antarctica*, *Halophila australis* and *Zostera* spp.) were present between 5 and 15 m in both years, making up approximately 5% of the area surveyed.

Proportions of habitat composition remained consistent between years at both Popes Eye and Portsea Hole (Figure 3.48). As with the greater Port Phillip Heads MNP region, these

sites were also dominated by sediment (51–60% for Popes Eye and 76–80% for Portsea Hole) in the towed video observed. The biota of Popes Eye was largely made up of algae (34–43%). The biota of Portsea Hole was dominated by red algae (8–10%), followed by approximately equal proportions of brown algae and sessile invertebrates (2.5–5%). Minor differences in cover were largely due to the inability to repeat transects over the exact same area. While transects were repeated as closely as possible, conditions such as visibility, swell and currents dictate the quality and location of successful imagery.

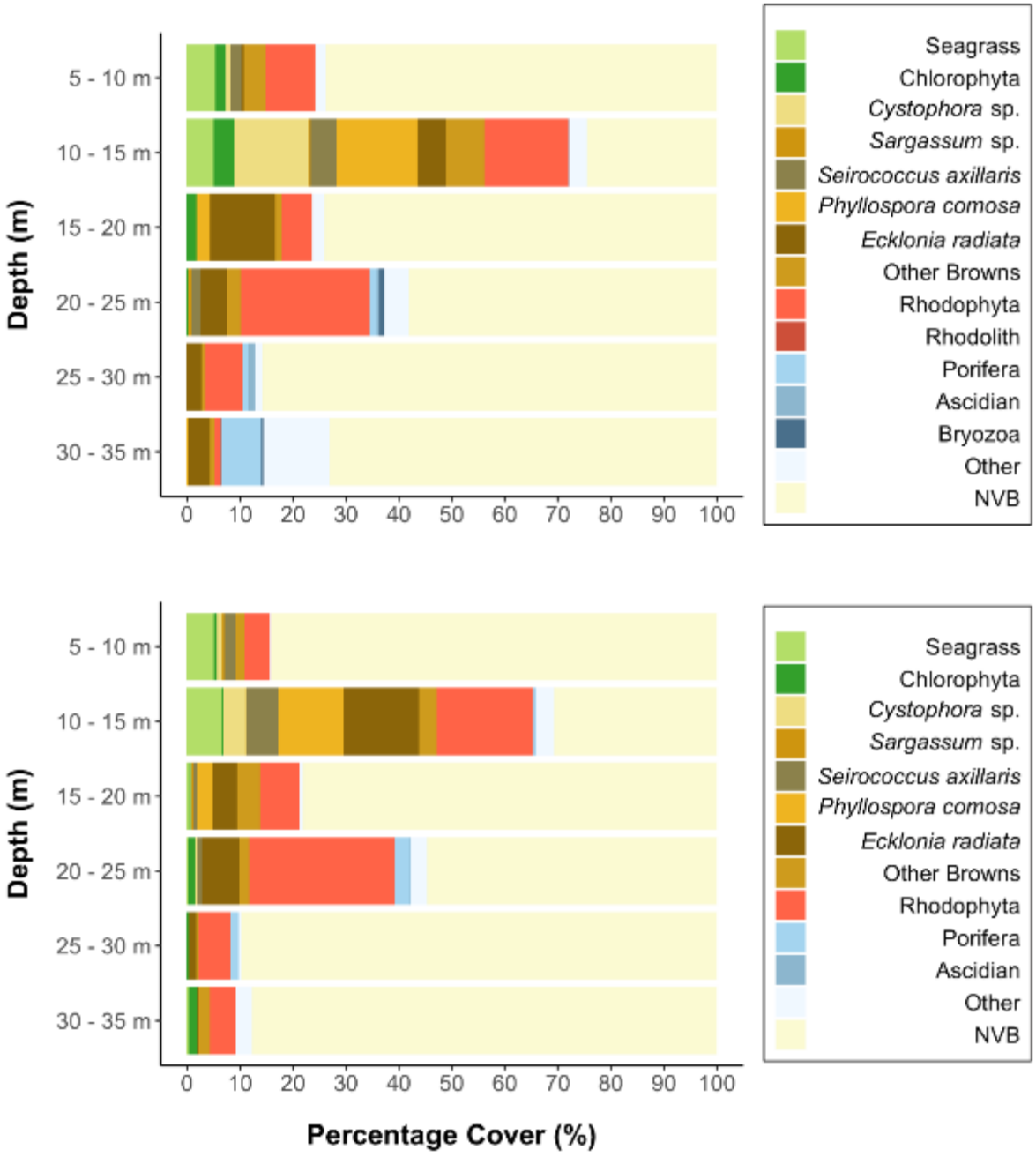

Figure 3.47: Depth zonation of broad habitat categories for 2018 (top) and 2019 (bottom) for the greater Port Phillip Heads MNP, observed by classifying downward-facing still images collected using towed video. NVB = no visible biota

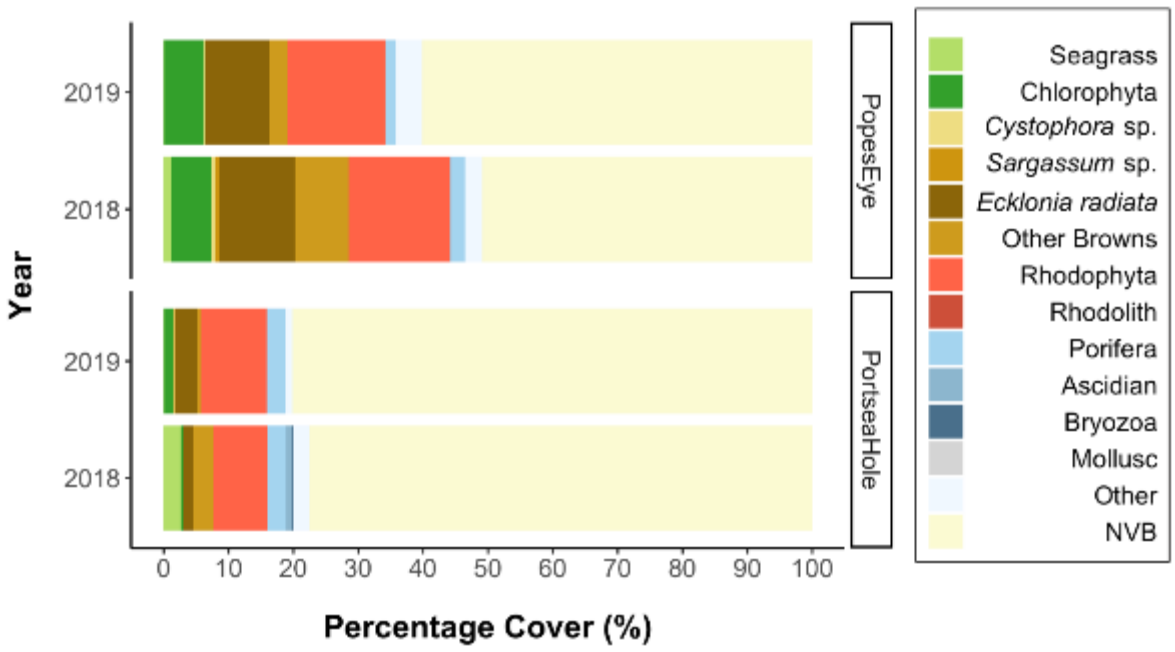

Figure 3.48: Depth zonation of broad habitat categories for 2018 (top) and 2019 (bottom) for Popes Eye and Portsea Hole, observed by classifying downward-facing still images collected using towed video. NVB = no visible biota

3.6.2 Habitat maps

Habitat classification maps for Popes Eye predicted 77% of the area to be sediment-dominated habitats (ba5.23 and ba5.73) (Table 3.11, Figure 3.49). Reefs of Popes Eye were largely limited to the man-made rock structure and were dominated by *Ecklonia radiata* (ba3.22). Maps show a trend of *E. radiata*–dominated habitat on shallower sections of reef, with sand-influenced sub-canopy brown algae on deeper sections.

Table 3.11: Predicted area (m^2) and predicted percentage cover (%) of habitat types at Popes Eye, using random forest models across a total area of 22,381.75 m^2

Biotic code	Biotic title	Predicted area (m^2)	Predicted percentage cover (%)
ba5.23	Infralittoral fine sand	7,224.17	32.23
ba3.22	*Ecklonia radiata* assemblages on moderate energy rock	4,116.53	18.39
ba3.23	Sub-canopy brown seaweed assemblages on moderate energy rock with sand influence	985.69	4.40
ba5.73	Mixture of brown, red and green algae with sponges	10,055.37	44.93

Sediment classes (ba5.2, ba5.7 and ba5.8) made up 97% of the predicted cover of the Portsea Hole site (Table 3.12, Figure 3.51). Of these sediment classes, ba5.2 (Sublittoral sand and muddy sand) was the most prolific with an estimated cover of 58.53%. Over one-third of the mapped area (38.26%) was classified as either ba5.7 (Sublittoral seaweed on sediment) or ba5.8 (Sublittoral seagrass beds). Areas of Sublittoral seaweed on sediment and Sublittoral seagrass on sediment were hard for the model to differentiate, so were grouped together as a single class. As the reef of Portsea Hole is such a vertical feature, it only makes up a small area within the park (3%). It contains a dense mix of multiple BC4 classes that make it impossible to classify this area beyond a single reef class; however, some classes identified in this area included *Ecklonia radiata* assemblages on moderate energy rock (ba3.22), Sub-canopy brown seaweed assemblages on moderate energy rock with sand influence (ba3.23), Moderate energy sandy veneer and scoured patch rock (ba3.2d), Lower infralittoral assemblages on moderate energy rock (ba3.2g) and Moderate energy tide-swept faunal communities (ba4.2b).

Table 3.12: Predicted area (m^2) and predicted percentage cover (%) of habitat types at Portsea Hole, using random forest models across a total area of 100,587.11 m^2

Biotic code	Biotic title	Predicted area (m^2)	Predicted percentage cover (%)
ba3.2	Moderate energy infralittoral rock	3,223.28	3.20
ba5.2	Sublittoral sand and muddy sand	58,878.56	58.53
ba5.7 and ba5.8	Sublittoral seaweed on sediment and Sublittoral seagrass beds	38,485.27	38.26

Table 3.13: Inventory of all BC4 classes (with number of observations) used to train models for Popes Eye and Portsea Hole

Site	Biotic code	Biotic title	Number of observations
Popes Eye	ba5.23	Infralittoral fine sand	53
	ba3.22	*Ecklonia radiata* assemblages on moderate energy rock	99
	ba3.23	Sub-canopy brown seaweed assemblages on moderate energy rock with sand influence	32
	ba5.73	Mixture of brown, red and green algae with sponges	88
	ba5.83	*Zostera* and *Ruppia* beds	1
	bz	Unassigned	6
Total no. of observations			279
Portsea Hole	ba3.22	*Ecklonia radiata* assemblages on moderate energy rock	13
	ba3.23	Sub-canopy brown seaweed assemblages on moderate energy rock with sand influence	10
	ba3.2d	Moderate energy sandy veneer and scoured patch rock	5
	ba3.2g	Lower infralittoral assemblages on moderate energy rock	25
	ba4.2b	Moderate energy tide-swept faunal communities	3
	ba5.23	Infralittoral fine sand	64
	ba5.25	Circalittoral fine sand	3
	ba5.73	Mixture of brown, red and green algae with sponges	39
	ba5.82	*Halophila* beds	3
	ba5.83	*Zostera* and *Ruppia* beds	3
	bz	Unassigned	1
Total no. of observations			169

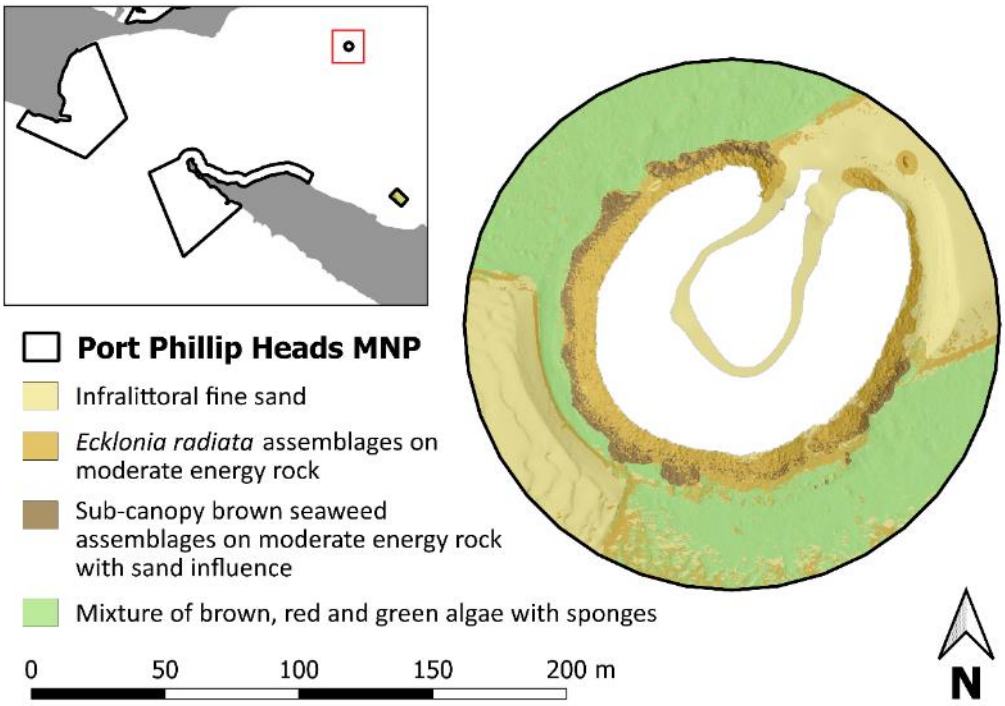

Figure 3.49: Predictive habitat map for Popes Eye using CBiCS classes. Created using ModelMap in R

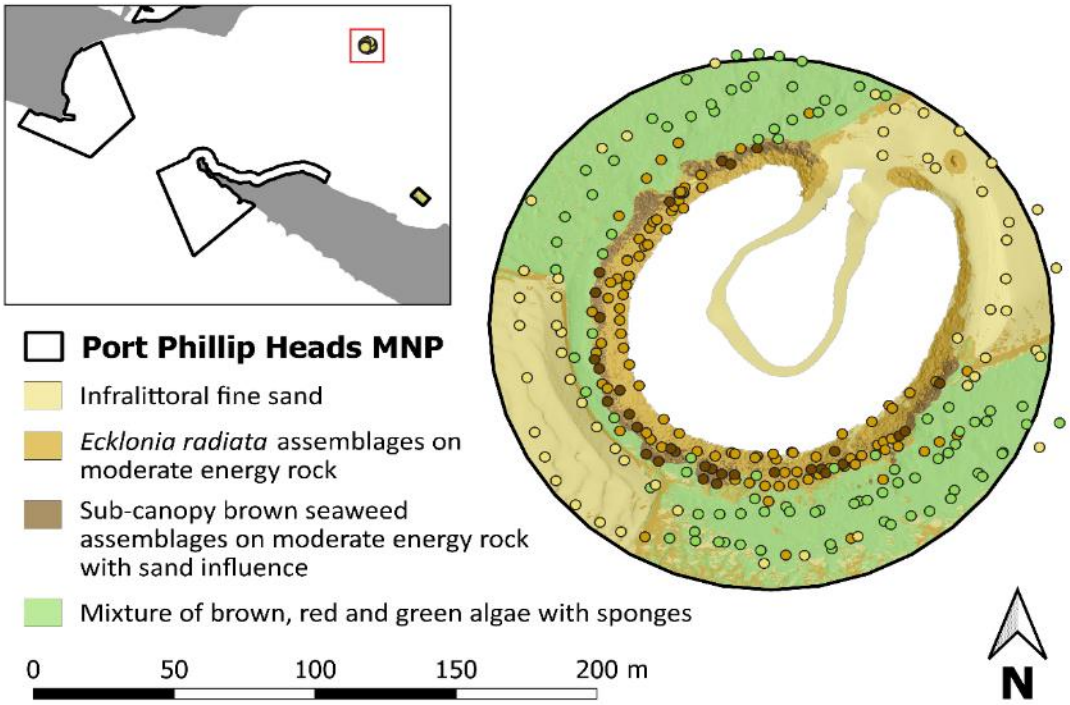

Figure 3.50: Predictive habitat map for Popes Eye using CBiCS classes showing classified ground truth images as coloured points. Created using ModelMap in R

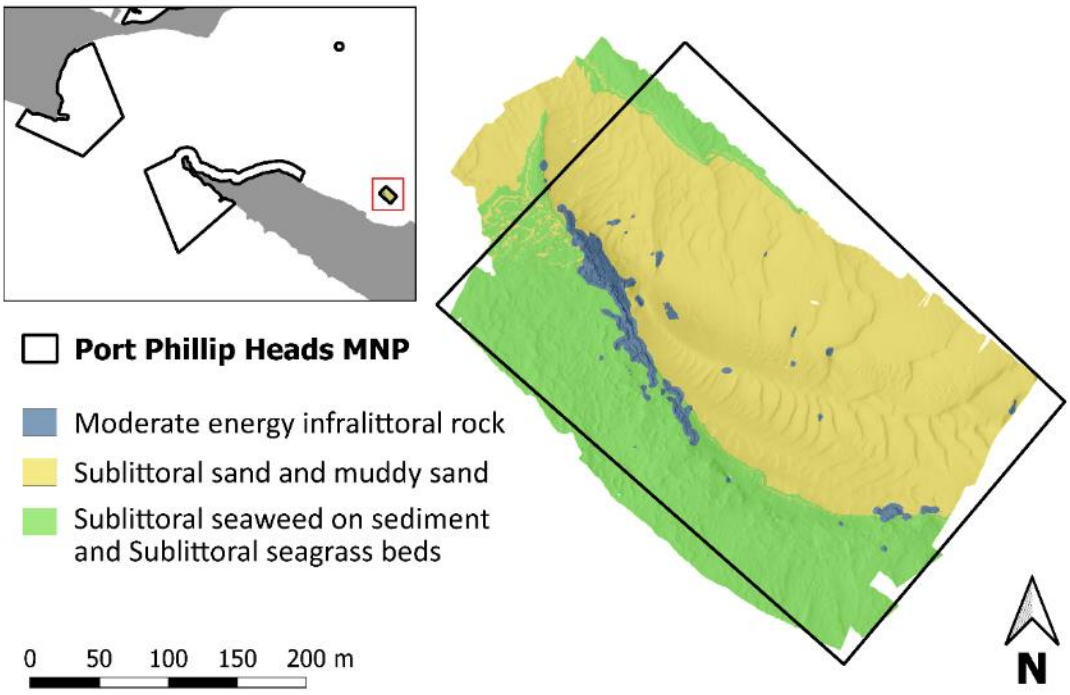

Figure 3.51: Predictive habitat map for Portsea Hole using CBiCS classes. Created using ModelMap in R

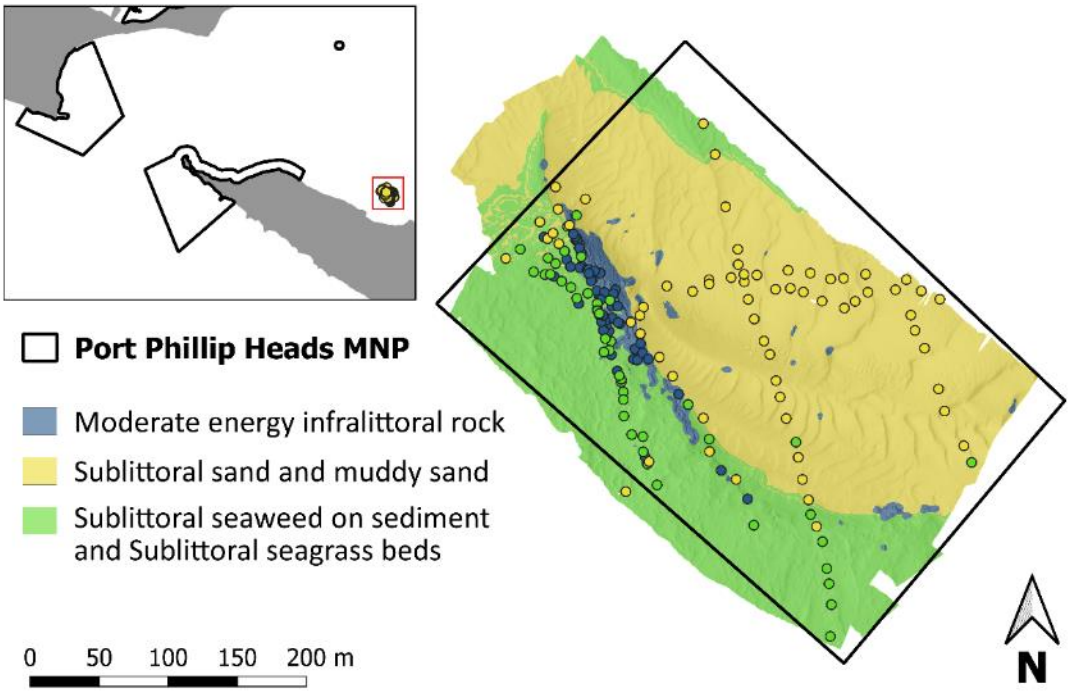

Figure 3.52: Predictive habitat map for Portsea Hole using CBiCS classes showing classified ground truth images as coloured points. Created using ModelMap in R

3.7 Fisheries-independent Southern Rock Lobster survey

A total of 115 spatially referenced lobster pots were placed inside and outside the marine national park between 2 and 6 April 2019 (Figure 2.6). Twenty-five Southern Rock Lobster (*Jasus edwardsii*) with an estimated total biomass of 47.4 kg were caught and examined during this study. While sampling effort was similar, with 60 pots within and 55 outside the MPA, 17 lobsters were caught within the protected waters compared with 8 in fished waters. Although more lobster were caught within the MPA, the low sample numbers preclude statistical analysis. No lobsters caught inside or outside the MPA were under legal size. Lobsters caught within the park were found to be on average slightly smaller than those caught in fished areas: a difference of 7 mm in carapace size and 240 g in weight was found between means inside and outside the MPA (Figures 3.53 and 3.54, Table 3.14).

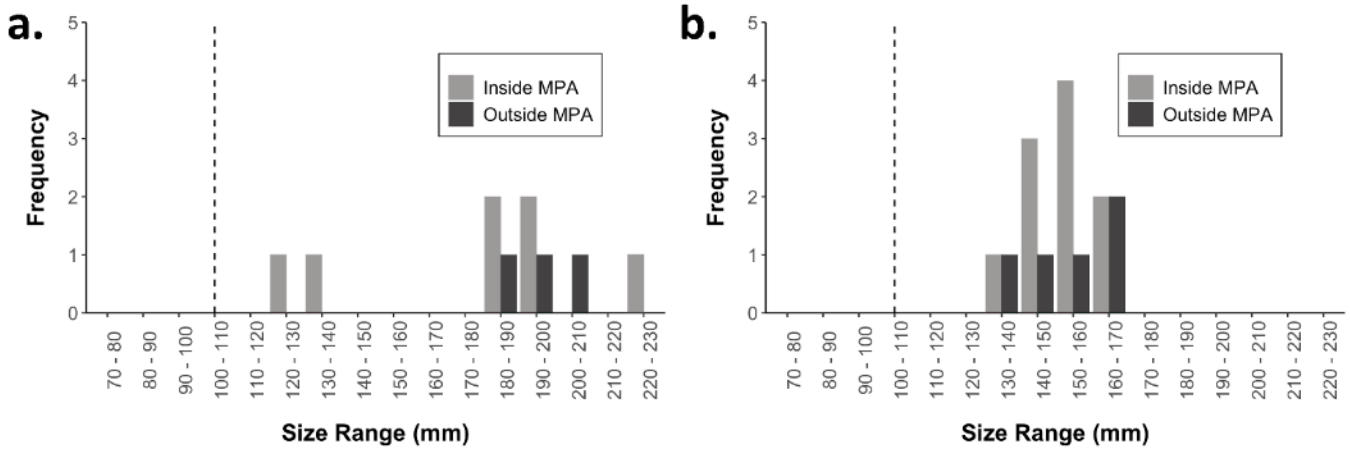

Figure 3.53: Southern Rock Lobster (*Jasus edwardsii*) male (a) and female (b) size distributions (carapace length in mm) inside and outside Port Phillip Heads MNP with the length of legal size displayed as a dashed grey line in each distribution plot

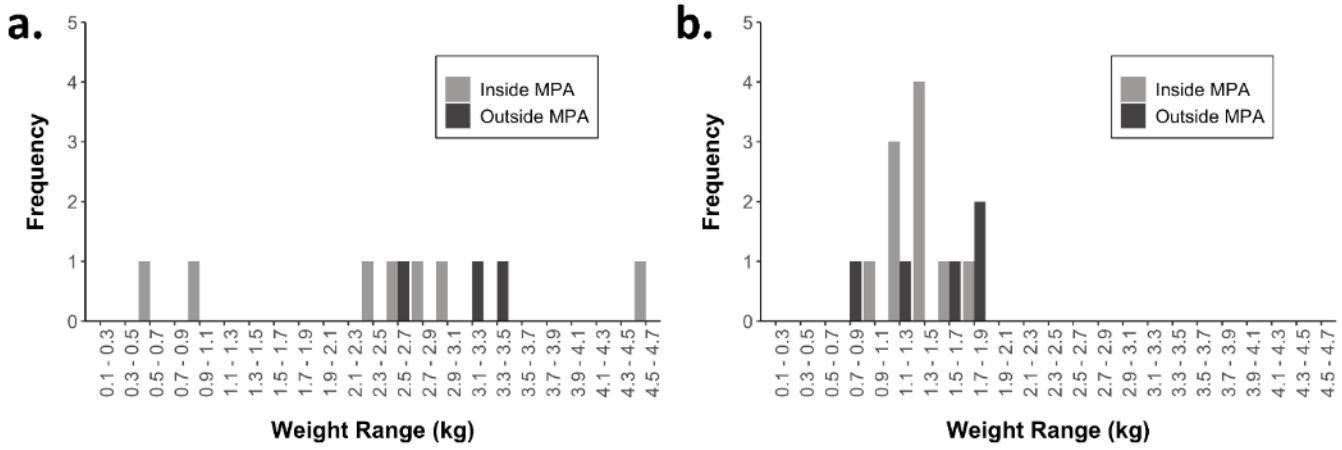

Figure 3.54: Southern Rock Lobster (*Jasus edwardsii*) male (a) and female (b) size distributions (total weight in kg) inside and outside the Port Phillip Heads MNP

Table 3.14: Southern Rock Lobster statistics inside (*n* = 60) and outside (*n* = 55) Port Phillip Heads MNP

Location	Sex	No. of individuals	No. of legal size individuals	Average carapace length (mm)	SD of average carapace length	Biomass (kg)	Average weight (kg)	SD of average weight	No. of reproductive females
Inside park	Male	7	7	177.1	35.3	17.1	2.4	1.3	
	Female	10	10	152.1	7.6	13.9	1.4	0.2	0
	Total	17	17	162.4	25.7	30.9	1.8	1.0	
Outside park	Male	3	3	197.3	8.3	9.3	3.1	0.4	
	Female	5	5	153.2	13.5	7.2	1.4	0.4	0
	Total	8	8	169.8	25.4	16.5	2.1	0.9	

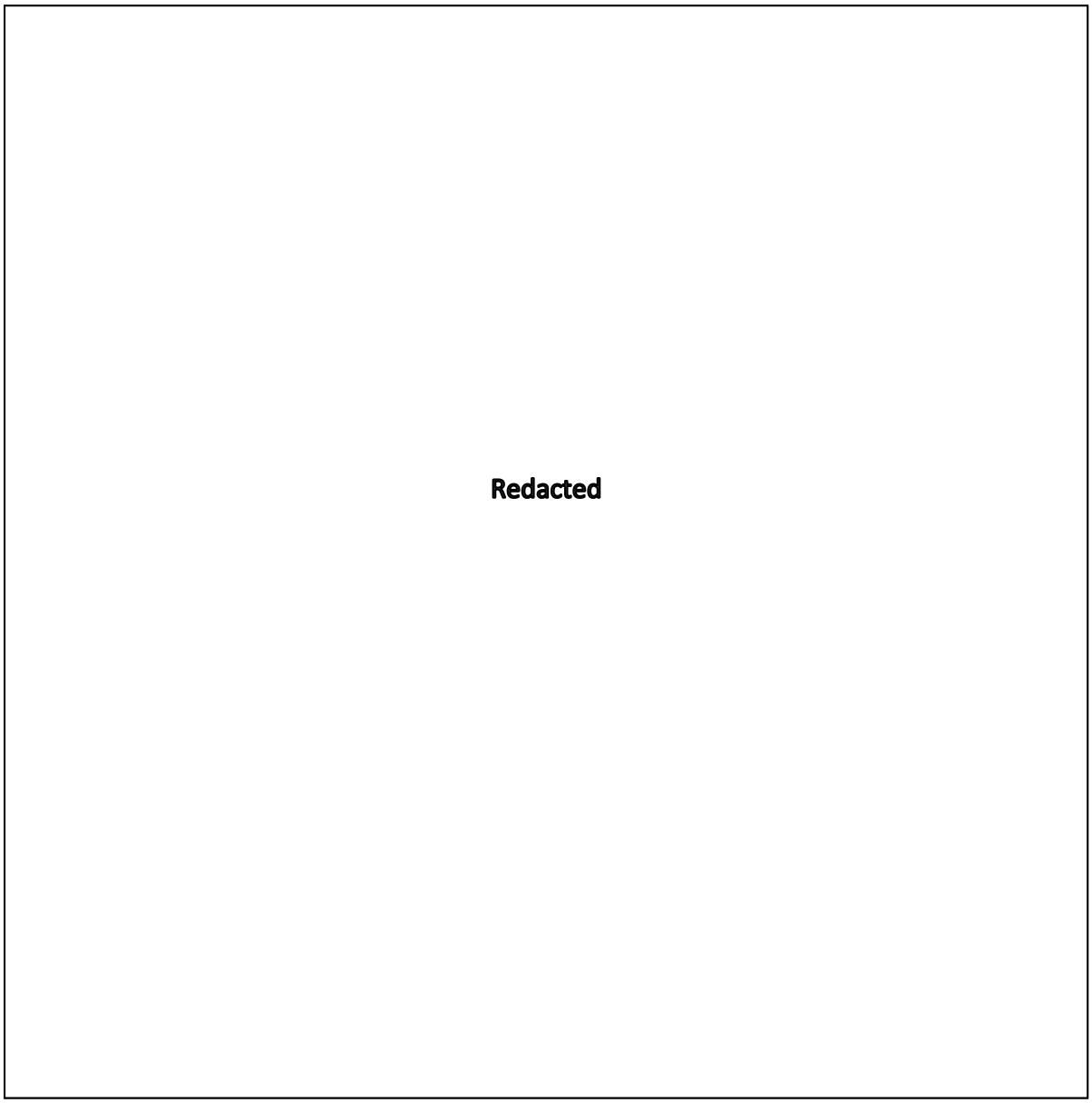

Figure 3.55: Total abundance of *Jasus edwardsii* for all lobster pot deployments. The size of each site marker corresponds to the total abundance of *J. edwardsii* observed at that site. These sites are overlaid on hillshaded bathymetry of the study area, coloured by depth. Black boxes denote Port Phillip Heads MNP boundaries. The dotted square in the top plot indicates the area of the bottom plot

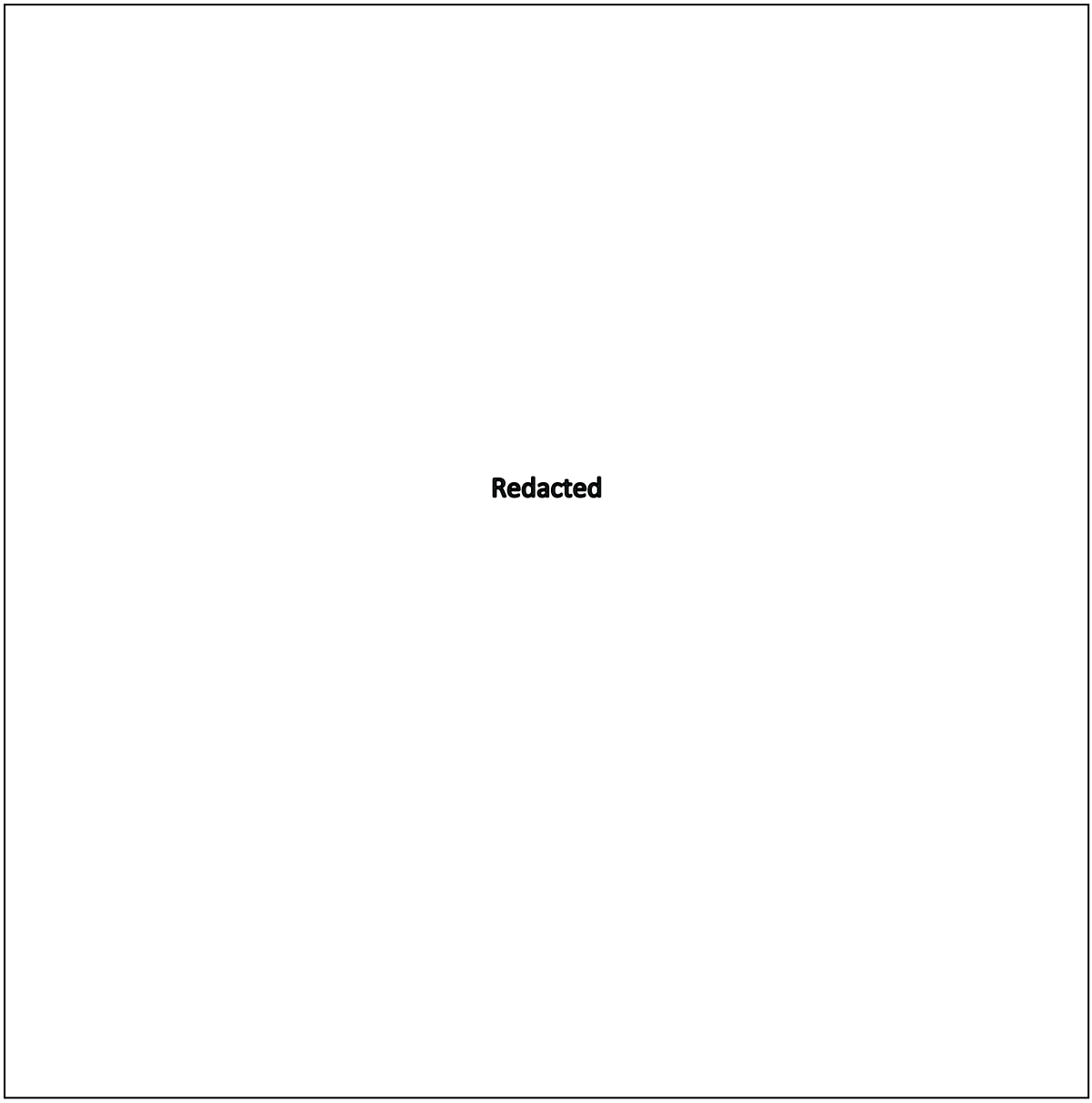

Figure 3.56: Abundance of female *Jasus edwardsii* for all lobster pot deployments. The size of each site marker corresponds to the abundance of female *J. edwardsii* observed at that site. These sites are overlaid on hillshaded bathymetry of the study area, coloured by depth. Black boxes denote Port Phillip Heads MNP boundaries. The dotted square in the top plot indicates the area of the bottom plot

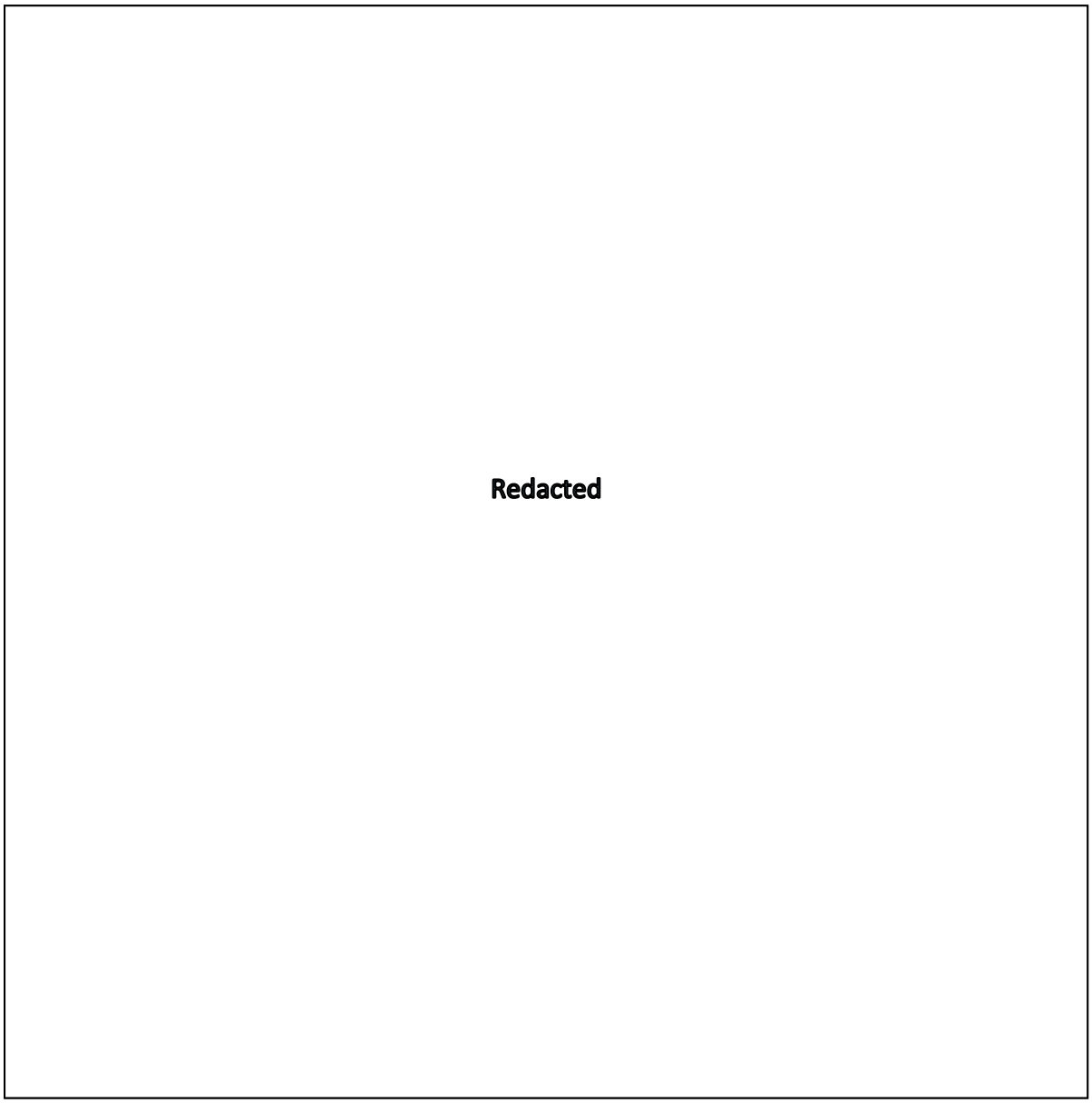

Figure 3.57: Abundance of male *Jasus edwardsii* for all lobster pot deployments. The size of each site marker corresponds to the male abundance of *J. edwardsii* observed at that site. These sites are overlaid on hillshaded bathymetry of the study area, coloured by depth. Black boxes denote Port Phillip Heads MNP boundaries. The dotted square in the top plot indicates the area of the bottom plot

Figure 3.58: Total abundance (kg) of *Jasus edwardsii* for all lobster pot deployments. The size of each site marker corresponds to the total abundance (kg) of *Jasus edwardsii* observed at that site. These sites are overlaid on hillshaded bathymetry of the study area, coloured by depth. Black boxes denote Port Phillip Heads MNP boundaries. The dotted square in the top plot indicates the area of the bottom plot

Table 3.15: Bycatch observed from lobster potting using research pots with no escape gaps in the Port Phillip Heads MNP and adjacent fished reference locations. All bycatch observed was identified, measured and promptly return to the water

Bycatch species	Inside park	Outside park
***Cephaloscyllium laticeps* (Draughtboard Shark)**	4	0
***Heterodontus portusjacksoni* (Port Jackson Shark)**	2	0
Octopodidae spp. (octopus)	3	0
Echinodermata spp. (starfish)	0	1
***Nectocarcinus tuberculosus* (Velvet Crab)**	20	7
***Meuschenia hippocrepis* (Horseshoe Leatherjacket)**	9	2
***Meuschenia freycineti* (Six-Spine Leatherjacket)**	10	4
Moridae spp. (morid cod)	0	1
***Chironemus maculosus* (Silver Spot)**	1	1
***Plagusia chabrus* (Chabrus Crab)**	4	0
Diogenidae spp. (hermit crabs)	1	0

4 Discussion

4.1 Subtidal reefs

4.1.1 Benthic communities

Subtidal demersal vegetation was observed using a range of data sources throughout this study. An underwater visual census (UVC) approach was previously implemented as part of the Subtidal Reef Monitoring Program (SRMP) across 7 time series from 1998 to 2015 (Woods et al., 2014), allowing an understanding of trends through time. While this study also used a UVC approach and completed surveys at the same sites, it implemented Reef Life Survey (RLS) methodology rather than SRMP methods. The main differences in the new approach were the replacement of in situ quadrat surveys with photo quadrats and a reduced survey effort from a total transect distance of 200 m to 100 m at each site, except that the 2019 RLS survey effort was doubled at each site to cover the same area as the SRMP methodology for fishes (Figure 2.4). Data were normalised to account for differences in sampling effort between the 2 techniques. In relation to collecting habitat data, while a major advantage of using photo quadrats is that divers do not require high-level algal taxonomic identification skills, that approach does limit the data that can be acquired. For example, we were only able to compare canopy-forming species identified using RLS methods to previous SRMP observations, as understorey communities are often obscured in the photo quadrats. Since the SRMP program began, RLS has become a common method for completing UVC surveys of shallow subtidal reefs. Globally, the RLS technique has allowed approximately 2,000 sites to be surveyed using a standard set of survey methods. Adopting such a common and widespread program allows many opportunities for comparing the condition of the Port Phillip Heads MNP with other areas around the globe. Locally, the RLS approach provides opportunities to increase survey effort across the network. However, continued reporting for time series analyses depends on the experience and quality of data provided by RLS divers.

While overall control charts showed that macroalgal indicators are in either fair or good condition, coverage of *Ecklonia radiata* has declined since its high in 2002. *E. radiata* has consistently had a lower percentage cover inside the park than in the reference sites. Its percentage cover within the park declined dramatically to around 5% in 2016–17, but this decline was not seen in the reference areas. However, in recent years percentage cover of *E. radiata* within the park has increased. Percentage cover of *Phyllospora comosa*, another important canopy-forming species, has also gradually decreased over time, but it has seen a recent uptick in 2019 within the park. Outside the park, *P. comosa* has followed the same trends but with much lower overall percentage cover across the entire time series, indicating that the reference sites generally experience lower *P. comosa* coverage. Despite the recent recovery of *E. radiata* and *P. comosa*, which are the most important canopy-

forming species on rocky reefs in the region, it is important to monitor their future trajectory closely. The remaining algal species or assemblages observed from 2002 to 2019 show a general negative trend through time without a recent increase. The lack of increase in the last couple of years could be due to the increase in *E. radiata* or *P. comosa* coverage, either because they are outcompeting the other algal species or because it is difficult to observe the sub-canopy species in the photo quadrats.

This project also implemented towed video surveys of subtidal reefs within the Port Phillip Heads MNP. This methodology allowed broadscale forward-facing video footage to be collected at the same time as highly detailed downward-facing still images. The downward-facing still imagery was used to understand community structure throughout the park because it provided high taxonomic resolution and extensive spatial coverage across the MPA. The georeferenced images from this method also allowed for the creation of spatially explicit habitat maps by associating the observations with characteristics of the seafloor. Habitat maps, therefore, allowed us to estimate coverage of the different habitat-forming species. At Popes Eye, reefs are dominated by *E. radiata* while the sediment areas contain a sparse mix of sponges and algal species. In contrast, Portsea Hole is mainly made up of either bare sediment or sediment covered in seagrass or macroalgae. Reef within Portsea Hole is predominantly in the form of a vertical wall, which means it only takes up a small horizontal area of the park (3%) and is hard to classify beyond a single reef class. The RLS surveys showed this region to contain diverse habitat classes spread vertically up and down the wall, such as *Ecklonia radiata* assemblages on moderate energy rock (ba3.22), Sub-canopy brown seaweed assemblages on moderate energy rock with sand influence (ba3.23), Moderate energy sandy veneer and scoured patch rock (ba3.2d), Lower infralittoral assemblages on moderate energy rock (ba3.2g) and Moderate energy tide-swept faunal communities (ba4.2b). Differentiating this area further would require higher density imagery. As it is a relatively small area, autonomous underwater vehicles capable of creating a mosaic of the seabed from high-resolution imagery may provide an ideal solution. However, the deployment would require a vehicle capable of navigating across steep slopes and vertical walls and operating in a high-current environment. These types of habitat maps are useful for planning further monitoring of the marine national park, as each habitat is likely to support different communities, and can aid in designing surveys. In addition, they can be used to assess areal coverage change through time.

Each of the imaging methods implemented here played a different role in gaining an understanding of the distribution and change in benthic communities within the Port Phillip Heads MNP. Photo quadrats captured during UVC helped to achieve the highest image clarity of all methods; however, the constraints of diving limited the spatial extent and depth of these surveys. The UVC approach also had the least spatially explicit position information, positions being identified by a centroid of the site locality rather than individual referenced images. In the context of this study, however, UVC provided an

important link to extend SRMP monitoring within the park and the ability to extend key time series in data collection. Towed video-derived downward-facing stills achieved similar taxonomic resolution to UVC photo quadrats. This method can be extended across the entire park and had the advantage of precise geolocation provide by the ultra-short baseline (USBL) system. Towed video also allowed the capture of orders of magnitude more images than UVC; it provides a cost-effective solution for sampling communities in deeper sections of the park (excluding the canyon system due to strong currents and shipping hazards). An added advantage of the towed video methodology is that multiple streams of data can be obtained at once, dramatically increasing the efficiency of this method.

4.1.2 Large mobile fish (including sharks and rays)

Fish assemblages within and adjacent to the Port Phillip Heads MNP were observed using a range of methods throughout this study. Results showed the current status of all key mobile fish species to be healthy as all species analysed fell within the zone of good condition.

This study let us use baited remote underwater video stations (BRUVS) to establish time series monitoring of fish assemblages over the entire depth range of the Port Phillip Heads MNP (excluding the canyon system). While UVC techniques are known to sample a different set of species to those sampled by BRUVS, and in particular to sample cryptic species (Colton and Swearer, 2010; Lowry et al., 2012), using BRUVS in this study greatly increased the depth range of observations. This greater depth range increases the number of species that can be observed by including 14 species only found beyond depths surveyed by UVC divers. The continued use of BRUVS for monitoring MPAs through time will allow similar time series analyses as those performed for diver surveys, including creating control charts. While there are not currently enough data to complete those types of analysis, this sampling will serve as baseline information for future exploration.

Including BRUVS in monitoring also allowed the creation of spatially explicit models for various diversity metrics and abundance of key groups and species throughout the park, aided by the distribution of sample locations across observed environmental gradients (Figure 2.6). Reaching the same density of field locations using UVC methods would not be feasible. Our approach, driven by a solid foundation understanding of the seabed structure provided by sonar and LiDAR technologies, allows for a spatially balanced design across the environmental variability of the site. An advantage of distribution modelling approaches, such as those used in this study, is the ability to predict patterns in abundance and biodiversity beyond sampled locations if relationships with environmental drivers can be inferred (Araújo and Guisan, 2006; Sequeira et al., 2016). Distribution modelling can be relevant for a range of applications such as tracking invasive species and researching effects of climate change (Elith and Graham, 2009). This study, for example, predicted hotspots of species richness and abundance across an area of over 15 km^2, including across the entire extent of the Port Phillip Heads MNP (except for the canyons, which are difficult to sample

due to traffic hazards). Our findings identified strong relationships with environmental drivers for some species and community groups, but not for all groups. For example, the models for *Meuschenia freycineti* and *Trygonorrhina dumerilii* explained a significant amount of the variance in the relative abundance of these species and predicted their distribution with fairly good accuracy. On the other hand, models for *Bathytoshia brevicaudata* and total biomass, among others, did not explain much of the variation and were not able to create high confidence predictions. These differences in results could relate to the habitat affinities of the different species, the prevalence of the species, the size of the samples and/or the representativeness of the samples. Despite the shortcomings of some of these models, they can be used to help plan sampling in the future to target areas that are likely to improve the modelling capacity for the different species and/or groups. Baseline knowledge obtained from BRUVS surveys in this study can now be used by park authorities to target diversity assessments and to identify sites of high biodiversity or public interest not previously visited.

4.1.3 Mobile macroinvertebrates

***Jasus edwardsii* (Southern Rock Lobster)**

Fisheries-independent surveys of Southern Rock Lobster (*Jasus edwardsii*) populations within and adjacent to Port Phillip Heads MNP showed no statistically significant trends with respect to protection, and only a limited number of SRL were captured during this study. These low numbers could be due to a number of circumstances related to the Port Phillip Heads MNP. First, the park is close to the heavily populated Melbourne area, and there is likely to be greater recreational fishing of SRL in the areas of Port Phillip Bay surrounding the park than in more isolated locations along the coast. Poaching within the marine national park could also be occurring, reducing numbers. Anecdotal observations show the potential of drift dives occurring through the park and potentially exiting the park boundary with catch. Previous studies on other species (e.g. abalone (Miller et al., 2019)) have shown highly structured marine populations within Port Phillip Bay, indicating a lack of connectivity with open coast systems. If the population of SRL is not sufficient within the bay to provide an adequate supply of larvae, these numbers may stay low. The lack of juveniles observed also suggests that recruitment to this area is low.

Despite the low numbers of SRL caught in this study, these results will act as an appropriate baseline for future studies documenting changes in this marine national park to assess how the population responds to protection, recruitment and a changing climate through time. Continued sampling of this and other MPAs will provide a more conclusive understanding of how *J. edwardsii* are responding to complete removal of fishing pressure within MPA boundaries across the state.

Other key macroinvertebrates

Port Phillip Heads MNP also provides refuge for key macroinvertebrates such as the commercially important *Haliotis laevigata* (Greenlip Abalone) and *Haliotis rubra* (Blacklip Abalone) as well as *Cenolia trichoptera* (Orange Feather Star), *Heliocidaris erythrogramma (*Purple Sea Urchin*), Meridiastra gunnii* (Gunns Six-Armed star) and *Tosia australis* (Southern Biscuit Star). Control charts from this study found that *H. laevigata* are responding to protection with increases in biomass through time and a current standing of 'good'. Unfortunately, *H. rubra* has seen a steady decrease through time and its biomass has been below the lower control limit since 2015. Previous work on *H. rubra* has shown that it is susceptible to increasing temperatures, and the warming trend during summer in the bay could potentially be increasing its mortality during spawning periods (Raimondi et al., 2002; Rosenblum et al., 2005). Also, recruitment in this region is likely dependent on spawning populations within the bay (Miller et al., 2019), which may also be decreasing with increasing temperatures.

H. erythrogramma has maintained a relatively low population in the Port Phillip Heads MNP since 1998, but there have been increases in populations in other parts of the bay. Previous work has shown that *H. erythrogramma* can have strong effects on the entire ecosystem (Carnell and Keough, 2016), so it is important to monitor this population through time. Large increases in abundance have the potential to create urchin barrens, resulting in drastic changes to the ecosystems inside the marine national park.

4.2 Intertidal reefs

4.2.1 *Hormosira banksii*–dominated communities

As a canopy-forming fucoid, *Hormosira banskii* is a keystone species on intertidal platforms within Port Phillip Heads MNP (Pocklington et al., 2019). It is therefore imperative that its future trajectory is closely monitored to prevent the potential cascading effects of a decline. Cover of *H. banksii* has been monitored on the Port Phillip Heads intertidal platform since 2004, where it has been studied using individual quadrats as part of the IRMP program. Deakin University researchers have developed methods of completing unmanned aerial vehicle (UAV) surveys of intertidal platforms that have been shown to produce comparable results to IRMP or Parks Victoria's citizen science intertidal monitoring program Sea Search (Murfitt et al., 2017). To continue the previous time series, for 2018 and 2019 surveys, 'virtual quadrats' were placed on UAV images of the intertidal platform and IRMP methodologies were followed. Results showed that *H. banksii* cover was maintained well above the LLAC of 48% (minimum value from reference site). Cover increased from 62% in 2013, to an all-time high of 87% in 2018 and 2019. No surveys were conducted at the reference site (Cheviot Beach) in 2018 or 2019, so it is difficult to know if this is

representative of a broader pattern (e.g. relating to environmental conditions) or a result of park management.

New UAV approaches to intertidal reef community assessments provided in this report allow the opportunity to move beyond spot count assessment to develop time series observations across the full platform. Use of UAVs reveals the potential for high-resolution remote sensing to be introduced into current intertidal monitoring efforts through the automated quantification of dominant, habitat-forming macroalgae from the UAV imagery, and the ability to capture fine (centimetre) scale geomorphological variables over the whole platform. Numerous studies have observed intertidal biota and assemblages from the ground (O'Hara et al., 2010; Schiel, 2004; Underwood and Jernakoff, 1981), providing detailed information on fine-scale influences and interactions of the intertidal biota. These include the importance of spatial scales and patches (e.g. Archambault and Bourget, 1996; Airoldi 2003), interactions and competition between biota (e.g. Dayton, 1971); Borell et al. 2004) and susceptibility to environmental and anthropogenic impacts (e.g. Airoldi, 1998; Jackson and McIlvenny, 2011). In situ observations, however, are generally labour intensive and only able to measure a subset of the platform in each survey. Through the use of autonomous UAV flight, developments in photogrammetry software such as Pix4D with specialist apps (PIX4DCapture) that allow for cloud-based upload, data processing and storage, and machine learning algorithms developed in this study, much of the process of quantifying the entire platform extent of the habitat-forming algae *H. banksii* has been automated. These advances greatly increase the efficiency and cost-effectiveness of surveying intertidal platforms, while also significantly increasing the sampling area.

UAVs are becoming increasingly efficient to deploy in the field due to decreasing costs and increased performance and ease of use. Despite the benefits of cost savings in image acquisition, there are challenges in detecting objects by their spectral properties from aerial imagery. Data resolution, image clarity, flying height, timing of image capture, camera angle, and flight direction are just some of the considerations (Joyce et al., 2018). In intertidal environments, these considerations are further compounded by the need to consider tidal conditions, sun glint and shadows on imagery. We found that imagery obtained in bright sunlight at low tide was better suited to object-based approaches. Excessive image blur in low-light data capture or moving water on the platform led to poor classifications. Bright sunny conditions decrease image blur in final orthomosaics but are problematic as they increase the incidence of sun glint from standing water on the platform and deepen areas of shadow. Additionally, there is significant effort and cost involved in processing and automated interpretation of large sets of high-resolution imagery (Joyce et al., 2018).

5 References

Airoldi, L. (1998). Roles of disturbance, sediment stress, and substratum retention on spatial dominance in algal turf. *Ecology*, 79(8), 2759-2770.

Airoldi, L. (2003). The effects of sedimentation on rocky coast assemblages. In R. N. Gibson and R. J. A. Atkinson (eds), *Oceanography and marine biology, an annual review, Volume 41* (pp. 169-171): CRC Press, London.

Allemand, J., Keysers, J., Quadros, N. and Deen, R. (2017). *2017 Victorian Coastal DEM report*.

Althaus, F., Hill, N., Ferrari, R. et al. (2015). A standardised vocabulary for identifying benthic biota and substrata from underwater imagery: the CATAMI classification scheme. *PLOS ONE, 10*(10), e0141039.

Anderson, D. R., Burnham, K. P. and Thompson, W. L. (2000). Null hypothesis testing: problems, prevalence, and an alternative. *The Journal of Wildlife Management*, *64*(4), 912-923.

Araújo, M. B. and Guisan, A. (2006). Five (or so) challenges for species distribution modelling. *Journal of Biogeography, 33*(10), 1677-1688. doi:10.1111/j.1365-2699.2006.01584.x

Archambault, P. and Bourget, E. (1996). Scales of coastal heterogeneity and benthic intertidal species richness, diversity and abundance. *Marine Ecology Progress Series, 136*, 111-121.

Austin, M. P. (1998). An ecological perspective on biodiversity investigations: examples from Australian eucalypt forests. *Annals of the Missouri Botanical Garden*, *85*(1), 2-17.

Barton (2018). MuMIn: Multi-Model Inference. R package version 1.43.17. https://cran.r-project.org/web/packages/MuMIn/

Bjørnstad, O. (2009). ncf: spatial nonparametric covariance functions. R package ver. 1.1. https://cran.r-project.org/web/packages/ncf/

Bolker, B. M., Brooks, M. E., Clark, C. J., Geange, S. W., Poulsen, J. R., Stevens, M. H. H. and White, J.-S. S. (2009). Generalized linear mixed models: a practical guide for ecology and evolution. *Trends in Ecology and Evolution, 24*(3), 127-135.

Borell, E. M., Foggo, A. and Coleman, R. A. (2004). Induced resistance in intertidal macroalgae modifies feeding behaviour of herbivorous snails. *Oecologia, 140*(2), 328-334.

Cappo, M., Speare, P. and De'ath, G. (2004). Comparison of baited remote underwater video stations (BRUVS) and prawn (shrimp) trawls for assessments of fish biodiversity in inter-reefal areas of the Great Barrier Reef Marine Park. *Journal of Experimental Marine Biology and Ecology, 302*(2), 123-152. doi:10.1016/j.jembe.2003.10.006

Carnell, P. E. and Keough, M. J. (2016). The influence of herbivores on primary producers can vary spatially and interact with disturbance. *Oikos, 125*(9), 1273-1283. doi:10.1111/oik.02502

Carnell, P. E. and Keough, M. J. (2019). Reconstructing historical marine populations reveals major decline of a kelp forest ecosystem in Australia. *Estuaries and Coasts, 42*(3), 765-778.

Colton, M. A. and Swearer, S. E. (2010). A comparison of two survey methods: differences between underwater visual census and baited remote underwater video. *Marine Ecology Progress Series, 400*, 19-36.

Dayton, P. K. (1971). Competition, disturbance, and community organization: the provision and subsequent utilization of space in a rocky intertidal community. *Ecological Monographs, 41*(4), 351-389.

Devillers, R., Pressey, R. L., Grech, A., Kittinger, J. N., Edgar, G. J., Ward, T. and Watson, R. (2015). Reinventing residual reserves in the sea: are we favouring ease of establishment over need for protection? *Aquatic Conservation: Marine and Freshwater Ecosystems, 25*(4), 480-504.

DHI (Danish Hydraulic Institute). (2016). MIKE 21. DHI. https://www.mikepoweredbydhi.com/

Dormann, C. F., Elith, J., Bacher, S. et al. (2013). Collinearity: a review of methods to deal with it and a simulation study evaluating their performance. *Ecography, 36*(1), 27-46.

Edmunds, M. and Flynn, A. (2015). *A Victorian marine biotope classification scheme*. Report to Deakin University and Parks Victoria. Australian Marine Ecology Report No. 545.

Eigenraam, M., McCormick, F. and Contreras, Z. (2016). *Marine and coastal ecosystem accounting: Port Phillip Bay*. State of Victoria, Department of Environment, Land, Water and Planning.

Elith, J. and Graham, C. H. (2009). Do they? How do they? WHY do they differ? On finding reasons for differing performances of species distribution models. *Ecography, 32*(1), 66-77. doi:10.1111/j.1600-0587.2008.05505.x

Exelis Visual Information Solutions (n.d.). ENVI, Exelis Visual Information Solutions, Boulder, Colorado. https://www.l3harrisgeospatial.com/Software-Technology/ENVI

Freeman, E. A., Frescino, T. S. and Moisen, G. G. (2018). ModelMap: an R package for model creation and map production. https://cran. r-project.org/web/packages/ModelMap/vignettes/VModelMap. pdf

Galaiduk, R., Radford, B. T., Wilson, S. K. and Harvey, E. S. (2017). Comparing two remote video survey methods for spatial predictions of the distribution and environmental niche suitability of demersal fishes. *Scientific Reports*, *7*, 17633.

Hart, S. P. and Edmunds, M. J. (2005). *Parks Victoria standard operating procedure: biological monitoring of intertidal reefs*: Parks Victoria Technical Series No. 21, Parks Victoria.

Hijmans, R. J. and van Etten, J. (2014). raster: Geographic data analysis and modeling. R package version, 2 (8). https://cran.r-project.org/web/packages/raster/

Ierodiaconou, D., Young, M., Miller, A. et al. (2018). *Patterns of interaction between habitat and oceanographic variables affecting the connectivity and productivity of invertebrate fisheries*. Fisheries Research and Development Corporation.

IMOS (Integrated Marine Observing System) (2018). AVHRR L3S SST. Retrieved from http://rs-data1-mel.csiro.au/imos-srs/sst/ghrsst/L3S-1m/

Jackson, A. C. and McIlvenny, J. (2011). Coastal squeeze on rocky shores in northern Scotland and some possible ecological impacts. *Journal of Experimental Marine Biology and Ecology, 400*(1-2), 314-321.

James, G., Witten, D., Hastie, T. and Tibshirani, R. (2013). *An introduction to statistical learning.* Springer.

Joyce, K. E., Duce, S., Leahy, S. M., Leon, J. and Maier, S. W. (2018). Principles and practice of acquiring drone-based image data in marine environments. *Marine and Freshwater Research*, *70*(7), 952-963.

Jung, C. A., Swearer, S. E. and Jenkins, G. P. (2010). Changes in diversity in the fish assemblage of a southern Australian embayment: consistent spatial structuring at decadal scales. *Marine and Freshwater Research, 61*(12), 1425-1434.

Keough, M. J. and Quinn, G. P. (1998). Effects of periodic disturbances from trampling on rocky intertidal algal beds. *Ecological Applications, 8*(1), 141-161.

Kuhn, M. (2008). Building predictive models in R using the caret package. *Journal of Statistical Software, 28*(5), 1-26.

Langlois, T., Williams, J., Monk, J. et al. (2018). Marine sampling field manual for benthic stereo BRUVS (baited remote underwater videos). In: R. Przeslawski and S. Foster (eds), *Field manuals for marine sampling to monitor Australian waters*, National Environmental Science Programme (NESP), pp. 82-104.

Liaw, A. and Wiener, M. (2002). Classification and regression by randomForest. *R News, 2*(3), 18-22.

Lowry, M., Folpp, H., Gregson, M. and Suthers, I. (2012). Comparison of baited remote underwater video (BRUV) and underwater visual census (UVC) for assessment of artificial reefs in estuaries. *Journal of Experimental Marine Biology and Ecology, 416-417*, 243-253.

Miller, A. D., Hoffmann, A. A., Tan, M. H. et al. (2019). Local and regional scale habitat heterogeneity contribute to genetic adaptation in a commercially important marine mollusc (*Haliotis rubra*) from southeastern Australia. *Molecular Ecology, 28*(12), 3053-3072.

Montgomery, D. C. (2007). *Introduction to statistical quality control,* 6th ed., John Wiley & Sons.

Murfitt, S. L., Allan, B. M., Bellgrove, A., Rattray, A., Young, M. A. and Ierodiaconou, D. (2017). Applications of unmanned aerial vehicles in intertidal reef monitoring. *Scientific Reports*, *7*, 10259.

O'Hara, T. D., Addison, P. F. E., Gazzard, R., Costa, T. L. and Pocklington, J. B. (2010). A rapid biodiversity assessment methodology tested on intertidal rocky shores. *Aquatic Conservation: Marine and Freshwater Ecosystems, 20*(4), 452-463.

Plummer, A., Morris, L., Blake, S. and Ball, D. (2003). *Marine natural values study, Victorian marine national parks and sanctuaries*. Parks Victoria Technical Series No. 1, Parks Victoria.

Pocklington, J. B., Jenkins, S. R., Bellgrove, A., Keough, M. J., O'Hara, T. D., Masterson-Algar, P. E. and Hawkins, S. J. (2018). Disturbance alters ecosystem engineering by a canopy-forming alga. *Journal of the Marine Biological Association of the United Kingdom, 98*(4), 687-698. doi:10.1017/S0025315416002009

Pocklington, J. B., Keough, M. J., O'Hara, T. D. and Bellgrove, A. (2019). The influence of canopy cover on the ecological function of a key autogenic ecosystem engineer. *Diversity, 11*(5), 79.

Povey, A. and Keough, M. J. (1991). Effects of trampling on plant and animal populations on rocky shores. *Oikos*, *61*(3), 355-368.

Power, B. and Boxshall, A. (2007). Marine national park and sanctuary monitoring plan 2007-2012. Parks Victoria Technical Series No 54, Parks Victoria.

Punt, A. E. (2003). The performance of a size-structured stock assessment method in the face of spatial heterogeneity in growth. *Fisheries Research, 65*(1-3), 391-409.

QGIS.org (2019). QGIS Geographic Information System. QGIS Association. http://www.qgis.org

Raimondi, P. T., Wilson, C. M., Ambrose, R. F., Engle, J. M. and Minchinton, T. E. (2002). Continued declines of black abalone along the coast of California: are mass mortalities related to El Niño events? *Marine Ecology Progress Series, 242*, 143-152.

Reef Life Survey. (2015). *Standardised survey procedures for monitoring rocky and coral reef ecological communities*. Reef Life Survey, Hobart, Tasmania, http://dx.doi.org/10.25607/OBP-33

Rosenblum, E. S., Viant, M. R., Braid, B. M., Moore, J. D., Friedman, C. S. and Tjeerdema, R. S. (2005). Characterizing the metabolic actions of natural stresses in the California red abalone, *Haliotis rufescens* using ^{1}H NMR metabolomics. *Metabolomics, 1*(2), 199-209.

Royall, R. (1997). *Statistical evidence: a likelihood paradigm*. Chapman and Hall.

Sappington, J. M., Longshore, K. M. and Thompson, D. B. (2007). Quantifying landscape ruggedness for animal habitat analysis: a case study using bighorn sheep in the Mojave Desert. *The Journal of Wildlife Management, 71*(5), 1419-1426.

Schiel, D. R. (2004). The structure and replenishment of rocky shore intertidal communities and biogeographic comparisons. *Journal of Experimental Marine Biology and Ecology, 300*(1-2), 309-342.

Schiel, D. R. and Taylor, D. I. (1999). Effects of trampling on a rocky intertidal algal assemblage in southern New Zealand. *Journal of Experimental Marine Biology and Ecology, 235*(2), 213-235.

Sequeira, A. M. M., Mellin, C., Lozano-Montes, H. M., Vanderklift, M. A., Babcock, R. C., Haywood, M. D. E., Meeuwig, J. J. and Caley, M. J. (2016). Transferability of predictive models of coral reef fish species richness. *Journal of Applied Ecology, 53*(1), 64-72.

Spencer, M. L., Stoner, A. W., Ryer, C. H. and Munk, J. E. (2005). A towed camera sled for estimating abundance of juvenile flatfishes and habitat characteristics: comparison with beam trawls and divers. *Estuarine, Coastal and Shelf Science, 64*(2-3), 497-503.

Thompson, W. L. and Lee, D. C. (2000). Modeling relationships between landscape-level attributes and snorkel counts of chinook salmon and steelhead parr in Idaho. *Canadian Journal of Fisheries and Aquatic Sciences, 57*(9), 1834-1842.

Underwood, A. J. and Jernakoff, P. (1981). Effects of interactions between algae and grazing gastropods on the structure of a low-shore intertidal algal community. *Oecologia, 48*(2), 221-233.

Valavanis, V. D., Pierce, G. J., Zuur, A. F., Palialexis, A., Saveliev, A., Katara, I. and Wang, J. (2008). Modelling of essential fish habitat based on remote sensing, spatial analysis and GIS. *Hydrobiologia*, *612*, 5-20.

Victorian Environmental Assessment Council. (2014). *Marine investigation – final report*. Victorian Environmental Assessment Council.

Wood, S. (2015). Package 'mgcv'. R package version, 1, 29.

Woods, B. and Edmunds, M. (2013). *Victorian Subtidal Reef Monitoring Program: the reef biota at Merri Marine Sanctuary, February 2013*. Parks Victoria Technical Series No. 87.

Woods, B., Edmunds, M. and Brown, H. (2014). *Victorian Subtidal Reef Monitoring Program: the reef biota at Point Addis Marine National Park, June 2013*. Parks Victoria Technical Series No. 94.

Yee, T. W. and Mitchell, N. D. (1991). Generalized additive models in plant ecology. *Journal of Vegetation Science, 2*(5), 587-602.

Young, M. A., Ierodiaconou, D., Edmunds, M., Hulands, L. and Schimel, A. C. G. (2016). Accounting for habitat and seafloor structure characteristics on southern rock lobster (*Jasus edwardsii*) assessment in a small marine reserve. *Marine Biology, 163*(6), 141. doi:10.1007/s00227-016-2914-y

6 Appendices

Appendix 1. Relative abundances (mean ± SE) of all fish species observed in method 1 of Reef Life Surveys, for each year sampled (2016, 2017, 2018 and 2019)

Family	Taxon	Common name	2016	2017	2018	2019
Aplodactylidae	*Aplodactylus arctidens*	Marblefish	0.31 ± 0.16	0.55 ± 0.26	0.19 ± 0.08	0.19 ± 0.06
Aplodactylidae	*Aplodactylus lophodon*	Rock Cale	0 ± 0	0 ± 0	0 ± 0	0.03 ± 0.02
Apogonidae	*Siphamia cephalotes*	Little Siphonfish	5.15 ± 2.81	0 ± 0	0 ± 0	0.21 ± 0.21
Apogonidae	*Vincentia conspersa*	Southern Cardinalfish	0 ± 0	0 ± 0	0 ± 0	0.01 ± 0.01
Aracanidae	*Anoplocapros lenticularis*	White-Barred Boxfish	0 ± 0	0.03 ± 0.03	0.03 ± 0.03	0 ± 0
Aracanidae	*Aracana aurita*	Shaw's Cowfish	0 ± 0	0.17 ± 0.07	0.03 ± 0.03	0 ± 0
Arripidae	*Arripis georgianus*	Tommy Rough	2.65 ± 2.65	0 ± 0	0 ± 0	0 ± 0
Arripidae	*Arripis trutta*	Australian Salmon	1.12 ± 0.77	17.28 ± 17.28	0 ± 0	0 ± 0
Bovichtidae	*Bovichtus angustifrons*	Dragonet	0 ± 0	0.03 ± 0.03	0.06 ± 0.04	0.01 ± 0.01
Carangidae	*Pseudocaranx georgianus*	Silver Trevally	0.12 ± 0.12	0.59 ± 0.55	0 ± 0	0 ± 0
Centrolophidae	*Seriolella brama*	Snottynose Trevalla	0 ± 0	2.93 ± 2.93	0 ± 0	0 ± 0
Cheilodactylidae	*Dactylophora nigricans*	Dusky Morwong	0.46 ± 0.15	0.28 ± 0.12	0.56 ± 0.18	0.53 ± 0.12
Chironemidae	*Chironemus georgianus*	Western Kelpfish	0 ± 0	0.03 ± 0.03	0 ± 0	0 ± 0
Chironemidae	*Chironemus maculosus*	Silver Spot	0.04 ± 0.04	0 ± 0	0 ± 0	0 ± 0
Chironemidae	*Chironemus marmoratus*	Kelpfish	0.04 ± 0.04	0 ± 0	0 ± 0	0.03 ± 0.02
Clinidae	*Heteroclinus kuiteri*	Kuiters Weedfish	0 ± 0	0.03 ± 0.03	0 ± 0	0 ± 0
Clupeidae	*Spratelloides* spp.	Unidentified herring	115 ± 81.41	27.59 ± 15.41	9.38 ± 9.38	0 ± 0
Dasyatidae	*Bathytoshia brevicaudata*	Smooth Stingray	0.04 ± 0.04	0.1 ± 0.08	0.12 ± 0.06	0.03 ± 0.03
Dinolestidae	*Dinolestes lewini*	Longfin Pike	0.54 ± 0.54	0.07 ± 0.07	0.31 ± 0.28	0.43 ± 0.34
Diodontidae	*Diodon nicthemerus*	Globe Fish	0.42 ± 0.28	0.28 ± 0.12	0.47 ± 0.2	0.24 ± 0.09
Enoplosidae	*Enoplosus armatus*	Old Wife	1.31 ± 0.49	1.38 ± 0.46	3.47 ± 0.89	2.25 ± 0.91
Gerreidae	*Parequula melbournensis*	Silverbelly	0.08 ± 0.08	0 ± 0	0 ± 0	0 ± 0
Gobiidae	Gobiid spp.	Unidentified goby	0 ± 0	0 ± 0	0.22 ± 0.17	0 ± 0
Gobiidae	*Nesogobius* spp.	Goby	0.19 ± 0.16	0.69 ± 0.69	0 ± 0	0 ± 0
Heterodontidae	*Heterodontus portusjacksoni*	Port Jackson Shark	0 ± 0	0 ± 0	0.38 ± 0.38	0.01 ± 0.01
Kyphosidae	*Atypichthys strigatus*	Mado Sweep	0.04 ± 0.04	0.07 ± 0.05	0 ± 0	0 ± 0
Kyphosidae	*Girella zebra*	Zebra Fish	0.96 ± 0.58	2.45 ± 0.97	1.5 ± 0.56	2.4 ± 0.74

Kyphosidae	*Scorpis aequipinnis*	Sea Sweep	3.31 ± 1.94	2.14 ± 1.28	4.03 ± 2.44	1.65 ± 0.91
Kyphosidae	*Tilodon sexfasciatus*	Moonlighter	0.23 ± 0.13	0.17 ± 0.11	1.78 ± 0.55	0.79 ± 0.26
Labridae	*Achoerodus gouldii*	Western Blue Groper	0.08 ± 0.05	0.03 ± 0.03	0.06 ± 0.04	0.01 ± 0.01
Labridae	*Dotalabrus aurantiacus*	Castelnau's Wrasse	0.12 ± 0.06	0.45 ± 0.21	0.56 ± 0.22	0.24 ± 0.07
Labridae	*Eupetrichthys angustipes*	Snake-Skin Wrasse	0 ± 0	0 ± 0	0.06 ± 0.06	0.04 ± 0.03
Labridae	*Notolabrus fucicola*	Purple Wrasse	0 ± 0	0 ± 0	0.06 ± 0.04	0.01 ± 0.01
Labridae	*Notolabrus tetricus*	Blue-Throat Wrasse	23.31 ± 4.03	17.72 ± 2.25	23.72 ± 3.11	19.13 ± 1.44
Labridae	*Pictilabrus laticlavius*	Senator Wrasse	3.69 ± 1.2	5 ± 1.08	7.06 ± 1.44	4.6 ± 0.49
Labridae	*Pseudolabrus luculentus*	Luculentus Wrasse	0.38 ± 0.25	0 ± 0	0 ± 0	0 ± 0
Labridae	*Pseudolabrus rubicundus*	Rosy Wrasse	0.15 ± 0.15	0.1 ± 0.08	0.03 ± 0.03	0.13 ± 0.06
Latridae	*Pseudogoniistius nigripes*	Magpie Perch	1.73 ± 0.52	1.45 ± 0.3	3.31 ± 0.73	1.66 ± 0.23
Monacanthidae	*Acanthaluteres spilomelanurus*	Bridled Leatherjacket	0.77 ± 0.69	0.48 ± 0.42	0.62 ± 0.38	0.01 ± 0.01
Monacanthidae	*Acanthaluteres vittiger*	Toothbrush Leatherjacket	2 ± 1.03	1.03 ± 0.47	3.91 ± 2.96	0.29 ± 0.12
Monacanthidae	*Brachaluteres jacksonianus*	Pygmy Leatherjacket	0.04 ± 0.04	0.07 ± 0.05	0 ± 0	0.01 ± 0.01
Monacanthidae	*Eubalichthys mosaicus*	Mosaic Leatherjacket	0 ± 0	0.03 ± 0.03	0 ± 0	0 ± 0
Monacanthidae	*Meuschenia australis*	Brown-Striped Leatherjacket	0 ± 0	0.72 ± 0.37	0.03 ± 0.03	0.04 ± 0.03
Monacanthidae	*Meuschenia flavolineata*	Yellow-Stripe Leatherjacket	2.27 ± 0.85	2.21 ± 0.66	3.44 ± 0.86	2.62 ± 0.56
Monacanthidae	*Meuschenia freycineti*	Six-Spine Leatherjacket	2.04 ± 1.43	2.86 ± 1.33	2.41 ± 1.01	0.88 ± 0.41
Monacanthidae	*Meuschenia galii*	Blue-Lined Leatherjacket	0.12 ± 0.08	0.21 ± 0.08	0.34 ± 0.13	0.31 ± 0.09
Monacanthidae	*Meuschenia hippocrepis*	Horseshoe Leatherjacket	1.46 ± 0.47	3.97 ± 1.4	3.81 ± 0.99	4.85 ± 0.96
Monacanthidae	*Meuschenia venusta*	Stars and Stripes Leatherjacket	0 ± 0	0 ± 0	0 ± 0	0.01 ± 0.01
Monacanthidae	*Scobinichthys granulatus*	Rough Leatherjacket	0.69 ± 0.3	0.93 ± 0.62	0.72 ± 0.32	0.29 ± 0.08
Mullidae	*Upeneichthys vlamingii*	Southern Goatfish	1.77 ± 0.44	0.9 ± 0.22	1.12 ± 0.34	0.49 ± 0.11
Myliobatidae	*Myliobatis tenuicaudatus*	Eagle Ray	0 ± 0	0 ± 0	0.09 ± 0.09	0 ± 0
Odacidae	*Haletta semifasciata*	Blue Rock Whiting	0.08 ± 0.05	0.1 ± 0.06	0.53 ± 0.17	0.51 ± 0.35
Odacidae	*Heteroscarus acroptilus*	Rainbow Cale	0.31 ± 0.12	0.28 ± 0.16	0.34 ± 0.12	0.15 ± 0.07
Odacidae	*Neoodax balteatus*	Little Rock Whiting	0.46 ± 0.27	0.31 ± 0.19	0.56 ± 0.3	0.12 ± 0.07
Odacidae	*Olisthops cyanomelas*	Herring Cale	4.27 ± 1.24	3.76 ± 1.03	3.34 ± 0.64	5.25 ± 0.73
Odacidae	*Siphonognathus beddomei*	Pencil Weed Whiting	0.04 ± 0.04	0.07 ± 0.05	0.06 ± 0.04	0.06 ± 0.03

Ophichthidae	*Scolecenchelys breviceps*	Shorthead Worm Eel	0 ± 0	0 ± 0	0 ± 0	0.01 ± 0.01
Parascylliidae	*Parascyllium variolatum*	Varied Catshark	0 ± 0	0 ± 0	0 ± 0	0.01 ± 0.01
Pataecidae	*Aetapcus maculatus*	Warty Prowfish	0.08 ± 0.05	0 ± 0	0 ± 0	0 ± 0
Pempheridae	*Pempheris multiradiata*	Common Bullseye	4.15 ± 3.84	0.52 ± 0.29	4.19 ± 1.85	2.13 ± 1.05
Pentacerotidae	*Pentaceropsis recurvirostris*	Long-Snouted Boarfish	0.04 ± 0.04	0.03 ± 0.03	0.09 ± 0.07	0.15 ± 0.06
Platycephalidae	*Platycephalus laevigatus*	Rock Flathead	0 ± 0	0.03 ± 0.03	0 ± 0	0 ± 0
Platycephalidae	*Platycephalus speculator*	Yank Flathead	0 ± 0	0 ± 0	0.03 ± 0.03	0 ± 0
Plesiopidae	*Paraplesiops meleagris*	Western Blue Devil	0.12 ± 0.08	0 ± 0	0.06 ± 0.04	0.01 ± 0.01
Plesiopidae	*Trachinops caudimaculatus*	Southern Hulafish	4.85 ± 2.35	3.07 ± 2.12	0.94 ± 0.85	0.69 ± 0.45
Pomacentridae	*Parma victoriae*	Victorian Scalyfin	8.65 ± 2.5	6.24 ± 1.8	8.91 ± 1.52	3.76 ± 0.61
Rhinobatidae	*Trygonorrhina dumerilii*	Southern Fiddler Ray	0 ± 0	0 ± 0	0.03 ± 0.03	0 ± 0
Rhinobatidae	*Trygonorrhina fasciata*	Eastern Fiddler Ray	0 ± 0	0.03 ± 0.03	0 ± 0	0.01 ± 0.01
Serranidae	*Caesioperca rasor*	Barber Perch	5.12 ± 3.05	3.45 ± 1.91	4.69 ± 2.59	1.04 ± 0.68
Serranidae	*Hypoplectrodes nigroruber*	Banded Seaperch	0 ± 0	0 ± 0	0.06 ± 0.06	0.01 ± 0.01
Sparidae	*Chrysophrys auratus*	Snapper	0.04 ± 0.04	0.03 ± 0.03	0 ± 0	0.01 ± 0.01
Sphyraenidae	*Sphyraena novaehollandiae*	Snook	0 ± 0	0.03 ± 0.03	0 ± 0	0 ± 0
Syngnathidae	*Phycodurus eques*	Leafy Seadragon	0.04 ± 0.04	0 ± 0	0 ± 0	0 ± 0
Syngnathidae	*Phyllopteryx taeniolatus*	Weedy Seadragon	0 ± 0	0.07 ± 0.07	0 ± 0	0 ± 0
Tetraodontidae	*Tetractenos glaber*	Smooth Toadfish	0.62 ± 0.46	0 ± 0	0.91 ± 0.76	0 ± 0
Trachichthyidae	*Trachichthys australis*	Roughy	0.04 ± 0.04	0 ± 0	0 ± 0	0 ± 0
Tripterygiidae	*Trinorfolkia clarkei*	Common Threefin	0.04 ± 0.04	0 ± 0	0 ± 0	0 ± 0
Urolophidae	*Trygonoptera imitata*	Eastern Shovelnose Stingaree	0 ± 0	0 ± 0	0.16 ± 0.13	0.01 ± 0.01
Urolophidae	*Trygonoptera mucosa*	Western Stingaree	0.15 ± 0.09	0.07 ± 0.07	0.09 ± 0.05	0 ± 0
Urolophidae	*Urolophus cruciatus*	Banded Stingaree	0.04 ± 0.04	0 ± 0	0 ± 0	0 ± 0
Urolophidae	*Urolophus gigas*	Spotted Stingaree	0.04 ± 0.04	0.07 ± 0.05	0.06 ± 0.04	0 ± 0
Urolophidae	*Urolophus paucimaculatus*	Sparsely Spotted Stingaree	0.04 ± 0.04	0.1 ± 0.1	0.03 ± 0.03	0.04 ± 0.03

Appendix 2. Relative abundances (mean ± SE) of all macroinvertebrate and cryptic fish species observed in method 2 of Reef Life Surveys, for each year sampled (2016, 2017, 2018 and 2019)

Family	Taxon	Common name	2016	2017	2018	2019
Alpheidae	*Alpheus* spp.	Pistol prawns	0.08 ± 0.05	0 ± 0	0 ± 0	0 ± 0
Antedonidae	*Antedon loveni*	Loven's Feather Star	0.42 ± 0.22	0.25 ± 0.13	0.09 ± 0.09	0.97 ± 0.94
Aplysiidae	*Aplysia dactylomela*	Spotted Sea Hare	0 ± 0	0 ± 0	0.09 ± 0.09	0 ± 0
Asteriidae	*Asterias amurensis*	Northern Pacific Seastar	0 ± 0	0 ± 0	0.16 ± 0.11	0 ± 0
Asteriidae	*Coscinasterias muricata*	Eleven-Arm Star	0 ± 0	0.04 ± 0.04	0.47 ± 0.38	0.04 ± 0.03
Asteriidae	*Uniophora granifera*	Granular Seastar	0.58 ± 0.36	0.25 ± 0.12	0.25 ± 0.17	0.27 ± 0.13
Asterinidae	*Meridiastra gunnii*	Gunns Six-Armed Star	3.85 ± 1.53	2.46 ± 1.08	1.75 ± 0.74	1.43 ± 0.59
Asterinidae	*Pseudonepanthia troughtoni*	Troughton's Seastar	0.15 ± 0.09	0 ± 0	0.31 ± 0.13	0.18 ± 0.09
Asteropseidae	*Petricia vernicina*	Velvet Star	0.15 ± 0.09	0.21 ± 0.12	0.12 ± 0.06	0.13 ± 0.05
Buccinidae	*Cominella eburnea*	Ribbed Cominella	0.04 ± 0.04	0 ± 0	0 ± 0	0 ± 0
Buccinidae	*Cominella lineolata*	Lined Whelk	0 ± 0	0 ± 0	0 ± 0	0.01 ± 0.01
Buccinidae	*Penion mandarinus*	Mandarin Whelk	0.04 ± 0.04	0.14 ± 0.08	0.03 ± 0.03	0.03 ± 0.02
Calliostomatidae	*Astele armillata*	Top Shell	0 ± 0	0 ± 0	0.03 ± 0.03	0 ± 0
Carcinidae	*Carcinus maenas*	Green Crab	0 ± 0	0.04 ± 0.04	0 ± 0	0 ± 0
Chromodorididae	*Ceratosoma amoenum*	Nudibranch	0 ± 0	0.04 ± 0.04	0.12 ± 0.09	0 ± 0
Chromodorididae	*Ceratosoma brevicaudatum*	Short Tailed Nudibranch	0.08 ± 0.05	0.04 ± 0.04	0.09 ± 0.05	0.04 ± 0.03
Chromodorididae	*Goniobranchus tinctorius*	Red Netted Goniobranchus	0.04 ± 0.04	0 ± 0	0.09 ± 0.09	0.04 ± 0.03
Chromodorididae	*Mexichromis macropus*	Nudibranch	0.04 ± 0.04	0 ± 0	0 ± 0	0 ± 0
Chromodorididae	*Verconia haliclona*	Nudibranch	0.04 ± 0.04	0 ± 0	0 ± 0	0 ± 0
Chromodorididae	*Verconia verconis*	Verco's Chromodorid	0.04 ± 0.04	0.04 ± 0.04	0.03 ± 0.03	0 ± 0
Cidaridae	*Goniocidaris impressa*	Pencil Urchin	0 ± 0	0.04 ± 0.04	0 ± 0	0 ± 0
Comatulidae	*Cenolia tasmaniae*	Tasmanian Feather Star	0.08 ± 0.05	0 ± 0	0 ± 0	0.07 ± 0.06
Comatulidae	*Cenolia trichoptera*	Orange Feather Star	13.81 ± 5.21	13.93 ± 5.17	18.03 ± 5.09	14.67 ± 3.28
Conidae	*Conus anemone*	Anemone Cone	0.27 ± 0.1	0.04 ± 0.04	0.25 ± 0.1	0.09 ± 0.04
Cymatiidae	*Argobuccinum pustulosum*	Triton Shell	0.04 ± 0.04	0 ± 0	0 ± 0	0 ± 0
Cymatiidae	*Austrosassia parkinsonia*	Trumpet Shell	0.04 ± 0.04	0.04 ± 0.04	0 ± 0	0 ± 0
Cymatiidae	*Cabestana spengleri*	Triton Shell	0.23 ± 0.14	0 ± 0	0.09 ± 0.05	0.15 ± 0.05
Cymatiidae	*Monoplex parthenopeus*	Hairy Triton	0 ± 0	0 ± 0	0.03 ± 0.03	0 ± 0
Cymatiidae	*Sassia* spp.	Triton shells	0 ± 0	0.04 ± 0.04	0 ± 0	0 ± 0
Cymatiidae	*Cymatiella verrucosa*	Verrucose Triton	0.08 ± 0.05	0 ± 0	0 ± 0	0 ± 0
Cypraeidae	*Notocypraea declivis*	Speckled Cowrie	0.04 ± 0.04	0 ± 0	0 ± 0	0 ± 0
Diogenidae	*Cancellus typus*	Miner Hermit Crab	0.04 ± 0.04	0 ± 0	0 ± 0	0 ± 0
Diogenidae	*Paguristes frontalis*	Southern Hermit Crab	1.19 ± 0.53	0.82 ± 0.33	0.69 ± 0.27	0.9 ± 0.25
Discodoridae	*Jorunna* spp.	Nudibranchs	0.04 ± 0.04	0 ± 0	0 ± 0	0 ± 0
Doridiidae	*Doris chrysoderma*	Chrysanthemum Nudibranch	0 ± 0	0 ± 0	0 ± 0	0.01 ± 0.01
Echinasteridae	*Echinaster arcystatus*	Pale Mosaic Seastar	0 ± 0	0 ± 0	0 ± 0	0.01 ± 0.01
Echinasteridae	*Plectaster decanus*	Mosaic Seastar	0.04 ± 0.04	0.04 ± 0.04	0.09 ± 0.09	0 ± 0
Echinometridae	*Heliocidaris erythrogramma*	Purple Sea Urchin	12.85 ± 5.06	8.14 ± 3.3	5.5 ± 2.24	9.27 ± 2.88
Facelinidae	*Phyllodesmium serratum*	Serrated Phyllodesmium	2.04 ± 1.77	0 ± 0	0 ± 0	0.04 ± 0.04
Facelinidae	*Pteraeolidia ianthina*	Blue Dragon	0.04 ± 0.04	0 ± 0	0 ± 0	0 ± 0

Fasciolariidae	*Australaria australasia*	Tulip Shell	0.27 ± 0.16	0.07 ± 0.07	0.19 ± 0.1	0.16 ± 0.05
Fissurellidae	*Scutus antipodes*	Elephant Snail	0.08 ± 0.05	0.04 ± 0.04	0.09 ± 0.07	0.04 ± 0.03
Flabellinidae	*Coryphellina rubrolineata*	Red-Lined Flabellina	0 ± 0	0 ± 0	0.03 ± 0.03	0 ± 0
Gastropteridae	*Sagaminopteron ornatum*	Bat-Wing Seaslug	0.08 ± 0.05	0 ± 0	0.06 ± 0.04	0.06 ± 0.04
Goniasteridae	*Fromia polypora*	Many-Spotted Seastar	0.12 ± 0.08	0.11 ± 0.08	0.38 ± 0.13	0.12 ± 0.05
Goniasteridae	*Pentagonaster duebeni*	Fire-Brick Star	0.77 ± 0.38	0.86 ± 0.75	0.44 ± 0.31	0.21 ± 0.08
Goniasteridae	*Tosia australis*	Southern Biscuit Star	3.23 ± 1.05	0.64 ± 0.21	1.38 ± 0.66	1.48 ± 0.35
Goniasteridae	*Tosia magnifica*	Magnificent Biscuit Star	0.04 ± 0.04	0 ± 0	0.06 ± 0.04	0.01 ± 0.01
Goniasteridae	*Nectria macrobrachia*	Large-Plated Seastar	0 ± 0	0 ± 0	0 ± 0	0.01 ± 0.01
Goniasteridae	*Nectria multispina*	Multi-Spined Seastar	0.12 ± 0.06	0.11 ± 0.08	0.09 ± 0.05	0.6 ± 0.11
Goniasteridae	*Nectria ocellata*	Ocellate Seastar	0.69 ± 0.23	0.61 ± 0.18	0.59 ± 0.23	0.12 ± 0.05
Goniasteridae	*Nectria pedicelligera*	Seastar	0.04 ± 0.04	0 ± 0	0 ± 0	0 ± 0
Goniasteridae	*Nectria* spp.	Seastars	0 ± 0	0 ± 0	0.09 ± 0.09	0 ± 0
Haliotidae	*Haliotis elegans*	Elegant Abalone	0 ± 0	0.04 ± 0.04	0 ± 0	0 ± 0
Haliotidae	*Haliotis laevigata*	Greenlip Abalone	10.85 ± 4.43	7.5 ± 3.2	4.09 ± 1.03	4.99 ± 1.22
Haliotidae	*Haliotis rubra*	Blacklip Abalone	3.38 ± 1.09	4.11 ± 1.42	1.16 ± 0.62	4.21 ± 0.92
Haliotidae	*Haliotis scalaris*	Grooved Abalone	0 ± 0	0.04 ± 0.04	0 ± 0	0.04 ± 0.03
Loliginidae	*Sepioteuthis australis*	Southern Calamary	0.27 ± 0.27	0 ± 0	0.03 ± 0.03	0 ± 0
Madrellidae	*Madrella sanguinea*	Blood Red Sea Slug	0.04 ± 0.04	0 ± 0	0 ± 0	0 ± 0
Majidae	*Leptomithrax gaimardii*	Spider Crab	0 ± 0	0 ± 0	0.03 ± 0.03	0 ± 0
Mitridae	*Isara glabra*	Black Mitre	0.04 ± 0.04	0 ± 0	0.03 ± 0.03	0.03 ± 0.02
Muricidae	*Bedeva baileyana*	Bailey's Rock Shell	0 ± 0	0.04 ± 0.04	0 ± 0	0.06 ± 0.05
Muricidae	*Dicathais orbita*	Dog Whelk	0.58 ± 0.19	0.43 ± 0.23	0.78 ± 0.36	0.94 ± 0.35
Muricidae	Muricid spp.	Unidentified murex or rock shell	0 ± 0	0.04 ± 0.04	0 ± 0	0 ± 0
Muricidae	*Pterochelus triformis*	Murex Shell	0 ± 0	0.11 ± 0.06	0.03 ± 0.03	0 ± 0
Ovalipidae	*Nectocarcinus integrifrons*	Red Swimmer Crab	0.12 ± 0.08	0 ± 0	0 ± 0	0.04 ± 0.03
Ovalipidae	*Nectocarcinus tuberculosus*	Velvet Crab	0.04 ± 0.04	0.04 ± 0.04	0.12 ± 0.06	0.25 ± 0.12
Palinuridae	*Jasus edwardsii*	Southern Rock Lobster	0.04 ± 0.04	0 ± 0	0.12 ± 0.07	0.01 ± 0.01
Phasianellidae	*Phasianella australis*	Pheasant Shell	0.42 ± 0.19	0.04 ± 0.04	0.09 ± 0.07	0.3 ± 0.08
Phasianellidae	*Phasianella ventricosa*	Pheasant Shell	0.15 ± 0.09	0.04 ± 0.04	0.03 ± 0.03	0.06 ± 0.03
Pilumnidae	*Heteropilumnus fimbriatus*	Bearded Crab	0.04 ± 0.04	0 ± 0	0 ± 0	0 ± 0
Plagusiidae	*Guinusia chabrus*	Red Bait Crab	0.19 ± 0.1	0.07 ± 0.05	0.38 ± 0.22	0.06 ± 0.03
Plakobranchidae	*Elysia expansa*	Black-Margined Sea Slug	0 ± 0	0.04 ± 0.04	0 ± 0	0 ± 0
Polyceridae	*Tambja verconis*	Verco's Nudibranch	0 ± 0	0 ± 0	0 ± 0	0.03 ± 0.03
Ranellidae	*Ranella australasia*	Australian Rock Whelk	0 ± 0	0 ± 0	0.03 ± 0.03	0.03 ± 0.03
Sepiidae	*Sepia apama*	Giant Cuttlefish	0.23 ± 0.1	0.04 ± 0.04	0.12 ± 0.06	0.03 ± 0.02
Temnopleuridae	*Amblypneustes ovum*	Short-Spined Urchin	0 ± 0	0.11 ± 0.06	0 ± 0	0.01 ± 0.01
Temnopleuridae	*Holopneustes inflatus*	Inflated Egg Urchin	0 ± 0	0 ± 0	0.09 ± 0.07	0.04 ± 0.03
Temnopleuridae	*Holopneustes porosissimus*	Short-Spined Urchin	0.12 ± 0.08	0 ± 0	0.06 ± 0.06	0.01 ± 0.01
Temnopleuridae	*Holopneustes purpurascens*	Short-Spine Urchin	0 ± 0	0 ± 0	2.5 ± 2.5	0.01 ± 0.01
Trochidae	*Chlorodiloma odontis*	Chequered Winkle	0 ± 0	0.04 ± 0.04	0 ± 0	0 ± 0
Trochidae	*Clanculus undatus*	Wavy Top Shell	0 ± 0	0.04 ± 0.04	0 ± 0	0 ± 0
Trochidae	*Phasianotrochus eximius*	Giant Kelp Shell	0.31 ± 0.16	0.14 ± 0.08	0.47 ± 0.17	0.39 ± 0.09

Trochidae	*Phasianotrochus rutilus*	Wavy Kelp Shell	0 ± 0	0.14 ± 0.11	0 ± 0	0 ± 0
Trochidae	*Prothalotia lehmanni*	Lehmann's Top Shell	0.65 ± 0.46	0.61 ± 0.31	0.44 ± 0.24	0.33 ± 0.13
Trochidae	*Thalotia conica*	Conical Top Shell	0.35 ± 0.25	1.21 ± 0.48	0.31 ± 0.23	0.09 ± 0.06
Turbinidae	*Astralium tentoriiforme*	Tent Turban	0.12 ± 0.12	0 ± 0	0.06 ± 0.04	0.1 ± 0.05
Turbinidae	*Bellastraea aurea*	Star Shell	0 ± 0	0 ± 0	0 ± 0	0.25 ± 0.14
Turbinidae	*Bellastraea squamifera*	Star Shell	1.08 ± 0.53	0.79 ± 0.29	1.03 ± 0.32	0.01 ± 0.01
Turbinidae	*Lunella undulata*	Turban Shell	0.08 ± 0.08	0.11 ± 0.06	0.41 ± 0.25	0.24 ± 0.08

Appendix 3. Relative abundances (mean ± SE) of all fish species observed by BRUVS for each year sampled (2018 and 2019)

Family	Taxon	Common name	2018	2019
Aplodactylidae	*Aplodactylus arctidens*	Marblefish	0 ± 0	0.08 ± 0.04
Aracanidae	*Aracana aurita*	Shaw's Cowfish	0.05 ± 0.03	0 ± 0
Aracanidae	*Aracana ornata*	Ornate Cowfish	0 ± 0	0.02 ± 0.02
Aracanidae	*Aracana* sp.	Cowfish	0.02 ± 0.02	0.02 ± 0.02
Arripidae	*Arripis georgianus*	Tommy Rough	0 ± 0	0.5 ± 0.39
Cheilodactylidae	*Dactylophora nigricans*	Dusky Morwong	0.23 ± 0.07	0.44 ± 0.09
Chironemidae	*Chironemus maculosus*	Silver Spot	0 ± 0	0.04 ± 0.03
Dasyatidae	*Bathytoshia brevicaudata*	Smooth Stingray	0.42 ± 0.08	0.48 ± 0.08
Dinolestidae	*Dinolestes lewini*	Longfin Pike	0.09 ± 0.09	1.35 ± 0.81
Diodontidae	*Diodon nicthemerus*	Globe Fish	0.05 ± 0.03	0.12 ± 0.05
Enoplosidae	*Enoplosus armatus*	Old Wife	0.23 ± 0.09	0.42 ± 0.11
Gerreidae	*Parequula melbournensis*	Silverbelly	0.19 ± 0.08	0.04 ± 0.03
Heterodontidae	*Heterodontus portusjacksoni*	Port Jackson Shark	0.33 ± 0.09	0.5 ± 0.12
Hexanchidae	*Notorynchus cepedianus*	Broadnose Sevengill Shark	0.02 ± 0.02	0 ± 0
Kyphosidae	*Atypichthys strigatus*	Mado Sweep	0 ± 0	0.02 ± 0.02
Kyphosidae	*Girella zebra*	Zebra Fish	1.23 ± 0.51	1.65 ± 0.52
Kyphosidae	*Kyphosus sydneyanus*	Silver Drummer	0 ± 0	0.02 ± 0.02
Kyphosidae	*Scorpis aequipinnis*	Sea Sweep	0.12 ± 0.06	0.81 ± 0.55
Kyphosidae	*Scorpis lineolata*	Silver Sweep	0.02 ± 0.02	0.02 ± 0.02
Kyphosidae	*Tilodon sexfasciatus*	Moonlighter	0.02 ± 0.02	0.25 ± 0.12
Labridae	*Achoerodus* spp.	Blue Groper	0.05 ± 0.03	0 ± 0
Labridae	*Dotalabrus aurantiacus*	Castelnau's Wrasse	0 ± 0	0.02 ± 0.02
Labridae	*Eupetrichthys angustipes*	Snake-Skin Wrasse	0.02 ± 0.02	0.06 ± 0.04
Labridae	*Notolabrus fucicola*	Purple Wrasse	0.49 ± 0.4	0.19 ± 0.08
Labridae	*Notolabrus tetricus*	Blue-Throat Wrasse	8.02 ± 1.4	7.15 ± 1.04
Labridae	*Pictilabrus laticlavius*	Senator Wrasse	1.07 ± 0.21	1.52 ± 0.24
Labridae	*Pseudolabrus rubicundus*	Rosy Wrasse	0.02 ± 0.02	0.25 ± 0.12
Latridae	*Pseudogoniistius nigripes*	Magpie Perch	0.4 ± 0.1	0.52 ± 0.1
Majidae	*Leptomithrax gaimardii*	Spider Crab	0 ± 0	0.02 ± 0.02
Monacanthidae	*Acanthaluteres vittiger*	Toothbrush Leatherjacket	0.37 ± 0.26	0.27 ± 0.16
Monacanthidae	*Eubalichthys mosaicus*	Mosaic Leatherjacket	0.05 ± 0.03	0.02 ± 0.02
Monacanthidae	*Meuschenia flavolineata*	Yellow-Stripe Leatherjacket	0.49 ± 0.13	0.54 ± 0.12
Monacanthidae	*Meuschenia freycineti*	Six-Spine Leatherjacket	1.91 ± 0.42	1.83 ± 0.32
Monacanthidae	*Meuschenia galii*	Blue-Lined Leatherjacket	0.16 ± 0.06	0.23 ± 0.06
Monacanthidae	*Meuschenia hippocrepis*	Horseshoe Leatherjacket	1.26 ± 0.36	1.48 ± 0.37
Monacanthidae	*Meuschenia venusta*	Stars and Stripes Leatherjacket	0.05 ± 0.05	0 ± 0
Monacanthidae	*Scobinichthys granulatus*	Rough Leatherjacket	0.51 ± 0.15	0.23 ± 0.07
Monacanthidae	*Thamnaconus degeni*	Degen's Leatherjacket	0.05 ± 0.03	0 ± 0
Moridae	*Pseudophycis* spp.	Cod	0 ± 0	0.04 ± 0.03
Mullidae	*Upeneichthys vlamingii*	Southern Goatfish	0.79 ± 0.2	0.58 ± 0.17
Myliobatidae	*Myliobatis tenuicaudatus*	Eagle Ray	0.07 ± 0.04	0.1 ± 0.04
Neosebastidae	*Neosebastes scorpaenoides*	Common Gurnard Perch	0.14 ± 0.06	0.15 ± 0.06
Odacidae	*Haletta semifasciata*	Blue Rock Whiting	0.05 ± 0.03	0.08 ± 0.05

Odacidae	*Heteroscarus acroptilus*	Rainbow Cale	0.05 ± 0.03	0.08 ± 0.04
Odacidae	*Neoodax balteatus*	Little Rock Whiting	0.07 ± 0.05	0 ± 0
Odacidae	*Olisthops cyanomelas*	Herring Cale	0.56 ± 0.12	0.71 ± 0.15
Ovalipidae	*Ovalipes australiensis*	Common Sand Crab	0.26 ± 0.11	0.02 ± 0.02
Parascylliidae	*Parascyllium variolatum*	Varied Catshark	0.02 ± 0.02	0.02 ± 0.02
Pempheridae	*Pempheris multiradiata*	Common Bullseye	0 ± 0	0.08 ± 0.06
Pentacerotidae	*Pentaceropsis recurvirostris*	Long-Snouted Boarfish	0.02 ± 0.02	0.06 ± 0.05
Platycephalidae	*Platycephalus bassensis*	Sand Flathead	0.6 ± 0.19	0.56 ± 0.19
Platycephalidae	*Platycephalus* sp.	Flathead	0.09 ± 0.04	0 ± 0
Platycephalidae	*Platycephalus speculator*	Yank Flathead	0.07 ± 0.04	0.19 ± 0.08
Plesiopidae	*Paraplesiops meleagris*	Western Blue Devil	0 ± 0	0.02 ± 0.02
Pomacentridae	*Parma victoriae*	Victorian Scalyfin	0.35 ± 0.08	0.52 ± 0.12
Rajidae	*Spiniraja whitleyi*	Whitley's Skate	0 ± 0	0.02 ± 0.02
Rhinobatidae	*Trygonorrhina fasciata*	Fiddler Ray	1.19 ± 0.35	1.25 ± 0.16
Scyliorhinidae	*Cephaloscyllium laticeps*	Draughtboard Shark	0.12 ± 0.06	0.08 ± 0.05
Serranidae	*Caesioperca rasor*	Barber Perch	0 ± 0	1.06 ± 0.64
Serranidae	*Hypoplectrodes nigroruber*	Banded Seaperch	0 ± 0	0.02 ± 0.02
Sillaginidae	*Sillaginodes punctatus*	King George Whiting	0.12 ± 0.05	0.46 ± 0.14
Sparidae	*Chrysophrys auratus*	Snapper	0.26 ± 0.14	2.25 ± 0.86
Tetraodontidae	*Contusus brevicaudus*	Prickly Toadfish	0.12 ± 0.05	0.4 ± 0.1
Tetraodontidae	*Tetractenos glaber*	Smooth Toadfish	0.05 ± 0.05	0.06 ± 0.05

Back cover: Jewel Anemone (*Corynactis australis*). Photo: Parks Victoria